

*Doctoral Thesis*

**Příprava a vlastnosti materiálů pro inteligentní  
systémy**

**Preparation and properties of materials for intelligent systems**

**Ing. Tomáš Plachý**

Studijní program: Chemie a technologie materiálů

Studijní obor: Technologie makromolekulárních látek

Školitel: doc. Dr. Ing. Vladimír Pavlínek

Konzultant: Ing. Michal Sedlačík, Ph.D.

Zlín, 2016

On this place I would like thanks to my supervisor assoc. prof. Vladimír Pavlínek for his help, patient, and personal values which were beyond of the frame of this thesis, and to my consultant Michal Sedláčik, Ph.D. for the same. I would like to further thank to all colleagues, friends, and people that I met and who taught me many new things and gave me important paradigmas. Especially, assoc. prof. Tomáš Sedláček, assoc. prof. Ivo Kuřitka, assoc. prof. Anežka Lengálová, Miroslav Mrlík, Ph.D., Pavel Bažant, Ph.D., Jakub Kadlčák Ph.D., and MSc. Michal Cvek. Last but not least many thanks go to my family. Thank you.

## Content

1. THEORETICAL BACKGROUND .....	6
1.1 General overview of smart fluids .....	6
1.2 Rheological behaviour of smart fluids .....	6
1.3 Physical background of the electrorheological effect .....	9
1.4 Composition of electrorheological fluids .....	13
1.4.1 Liquid medium .....	13
1.4.2 Dispersed phase.....	14
1.5 Factors influencing electrorheological effect .....	17
1.5.1 Electric field strength .....	17
1.5.2 Particles size and morphology .....	18
1.5.3 Temperature .....	19
1.5.4 Particle concentration.....	20
1.6 Requirements on electrorheological fluids.....	22
1.7 Shortcomings of electrorheological fluids .....	23
1.8 Application of smart fluids .....	23
2. MOTIVATION AND AIMS OF THE DOCTORAL STUDY .....	25
2.1 Motivation .....	25
2.2 Aims of the Doctoral Study .....	25
3. EXPERIMENTAL PART .....	26
4. THE THESIS CONTRIBUTION TO THE SCIENCE.....	37
5. LIST OF PAPERS .....	47

## **ABSTRACT**

Stimulus-responsive materials, often referred as intelligent systems, are of high interest for their unique controllable properties. As an external stimulus mainly pH, UV light, electric or magnetic fields are involved. A branch of intelligent systems which change their physical properties upon an application of external electric or magnetic fields are called smart fluids. Firstly, the electrorheological fluids were discovered by Winslow [1], who observed the formation of fibrous structures formed from electrically polarizable particles within the liquid medium in 1948. In the same year, Rabinow has observed the same phenomenon with magnetic particles in the liquid medium, and invented the magnetic fluid clutch [2]. Since their discovery the smart fluids have been a matter of an intensive research in many research groups. In the case of electrorheological fluids, their rheological parameters can easily be controlled through an application of an external electric field. Such ability comes from a creation of internal chain-like structures within them due to dipole-dipole interactions of the dispersed particles leading to a change from nearly Newtonian to Bingham-like behaviour. Thus, the electrorheological fluids can undergo a transition from liquid-like to a solid-like state changing their viscosity significantly. After a removal of an external electric field, the internal structures can be easily destroyed, which causes suspension viscosity reduction again and thus allows external control of rheological parameters. Such behaviour is highly demanding in many industrial fields, such as hydraulics and robotics, where these fluids are used as dampers, vibration controllers, or a medium for various clutches and valves.

Electrorheological fluids are generally two phase systems consisting of electrically polarizable particles dispersed in a non-conducting liquid carrier. The particles can be divided into two groups – organic and inorganic. Recently, attention has been concentrated on the carbonized materials. Materials containing carbon are exposed to high temperatures in an inert atmosphere, which leads to their transition to carbonaceous structure containing some heteroatoms (mostly nitrogen). Such particles exhibit considerable electric and dielectric properties and are therefore a promising material for the use in electrorheological fluids. Other recently introduced materials in electrorheology are oligomers of conducting polymers. Through doping process, which ensures their conductivity, it is possible to prepare particles with the demanding properties for electrorheological fluids.

## ABSTRAKT

Materiály schopné reagovat na vnější stimul, které se někdy nazývají jako inteligentní systémy, vzbuzují velký zájem díky svým unikátním a říditelným vlastnostem. Jako vnější stimul slouží zejména pH, světlo, elektrické či magnetické pole. Inteligentní systémy, které mění své fyzikální vlastnosti v reakci na aplikování vnějšího elektrického či magnetického pole se nazývají inteligentní kapaliny. Nejdříve byly roku 1948 objeveny elektoreologické kapaliny, kdy Winslow pozoroval formování fibrilárních struktur elektricky polarizovaných částic v kapalném médiu [1]. Ve stejném roce Rabinow pozoroval obdobný fenomén s magnetickými částicemi, na jehož základě vynalezl magnetickou spojku [2], kde jako médium byla používána právě magnetoreologická suspenze. Od svého objevu jsou inteligentní kapaliny předmětem intenzivního výzkumu v mnoha výzkumných skupinách. V případě elektoreologických kapalin je možné kontrolovat jejich reologické parametry pomocí aplikování externího fyzikálního pole. Tato schopnost vychází z vytváření vnitřních řetízkovitých struktur v těchto kapalinách díky interakci mezi dipóly dispergovaných částic, čímž se kapaliny přestávají chovat jako newtonské, a začnou naopak vykazovat binghamské tokové vlastnosti. Tyto kapaliny tedy mohou přecházet mezi kapalným a „pseudopevným“ stavem. Po odstranění vnějšího fyzikálního pole lze vnitřní vytvořené struktury lehce rozbít, což podmiňuje možnost řízení reologických parametrů celého systému. Takové chování je žádoucí v řadě průmyslových odvětví, zejména v hydraulice a robotice, kde jsou tyto kapaliny využívány jako tlumiče, regulátory vibrací nebo jako kapalně médium ve spojkách a ventilech.

Elektoreologické kapaliny jsou většinou dvousložkové systémy sestávající z elektricky polarizovatelných částic dispergovaných v nevodivém kapalném médiu. Používané částice lze rozdělit do dvou základních skupin – organické a anorganické. V poslední době je pozornost upínána k částicím karbonizovaných materiálů. Materiály obsahující uhlík jsou vystaveny vysokým teplotám v inertní atmosféře, čímž jsou převedeny na částice s uhlíkovou strukturou obsahující heteroatomy (nejčastěji dusík). Tyto částice poté vykazují výhodné elektrické a dielektrické vlastnosti a jeví se proto jako vhodný materiál pro elektoreologické kapaliny. Jinými nedávno představenými materiály v oblasti elektoreologie jsou oligomery vodivých polymerů. Pomocí dopování, které určuje jejich vodivost, je možné připravit materiály s přesně požadovanými vlastnostmi pro elektoreologické kapaliny.

# 1. THEORETICAL BACKGROUND

## 1.1 General overview of smart fluids

Smart fluids (SF) are liquids whose rheological parameters (viscosity, yield stress, viscoelastic moduli) can be controlled via an external physical field. Smart fluids are generally suspensions, where the dispersed phase is composed of electric or magnetic field-responsive particles. In the case of electrically polarizable particles, their suspensions are called as electrorheological (ER) fluids, while in the case of the magnetically polarizable particles their suspensions are called magnetorheological (MR) suspensions. Both of them can undergo controlled transition from liquid to a solid-like state. The transition occurs rapidly within milliseconds and, moreover, it is completely reversible. Such behaviour is highly demanded in some industrial fields and many applications [3-13] have been therefore proposed for these unique systems.

This change occurs due to an orientation of dispersed particles along with the streamlines of an applied electric field spanning the electrodes or the magnet poles inducing a magnetic field. While in the absence of the physical field, the distribution of the particles is completely random (Fig. 1a) [14], after its application the particles create highly organized chain-like structures (Fig. 1b) [14], controlling then the rheological properties of the whole system and leading to an abrupt increase in a viscosity and viscoelastic moduli. The formation of internal structures is called ER or MR effect, respectively, matter the applied physical field. The rheological behaviour of SFs, thus, covers broad spectrum of various responses to the applied deformation, *i.e.* their behaviour can be described from Newton's law in the absence of an external physical field to the models including the yield stress,  $\tau_y^1$ , such as Bingham model [15, 16].

## 1.2 Rheological behaviour of smart fluids

As it relies from above mentioned text, the main interest of researchers in these SFs is due to their controllable behaviour in the presence of an external physical field. In its absence the distribution of the particles within the SFs is random and the SFs then behave as Newtonian or slightly pseudoplastic fluids, and obey the Newton's (eq. 1) or the Krieger-Dougherty's formula [17] for the suspensions (eq. 2) [18].

---

<sup>1</sup> The yield stress,  $\tau_y$ , represents the stress that can system withstand before it starts to flow.

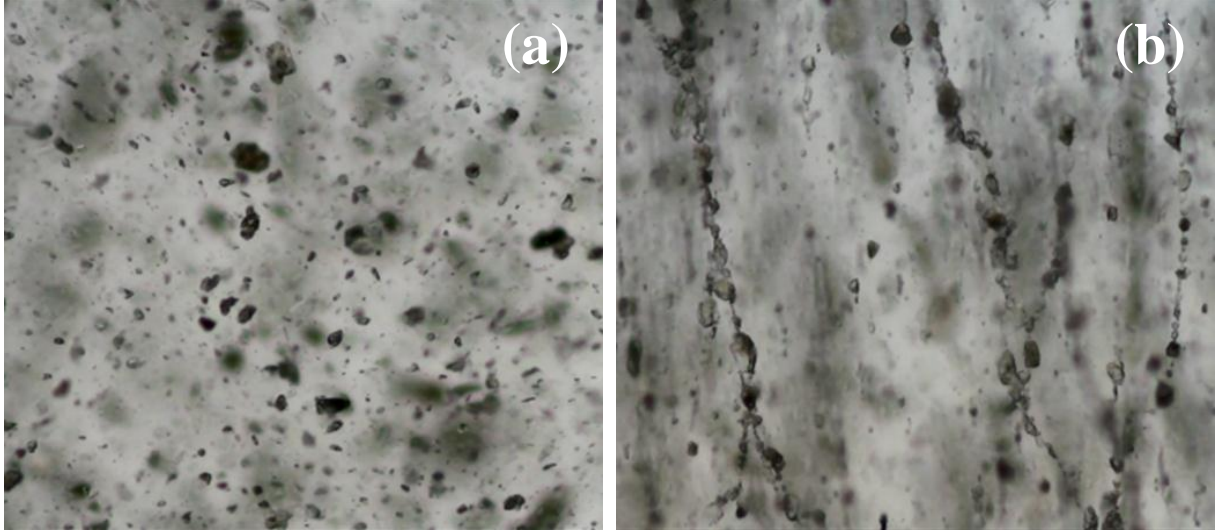


Fig. 1. An ER fluid (a) in the absence and (b) in the presence of an external electric field of strength  $0.3 \text{ kV mm}^{-1}$ .

$$\tau = \eta \times \dot{\gamma} \quad (1)$$

$$\eta = \eta_s \left(1 - \frac{\varphi}{\varphi_m}\right)^{-[\eta]\varphi_m} \quad (2)$$

In the eq. 1,  $\tau$  is shear stress,  $\eta$  and  $\dot{\gamma}$  are shear viscosity and shear rate, respectively. In eq. 2 the symbol  $\eta_s$  represents viscosity of the suspending fluid,  $\varphi$  and  $\varphi_m$  are the particle volume fraction and maximum-packing volume fraction, respectively. After an application of the external field, these fluids start to behave as viscoplastic fluids exhibiting yield stress and their rheological parameters can be then described in the simplest way by the Bingham equation (eq. 3) [19].

$$\tau = \tau_y + \eta_{pl} \times \dot{\gamma}; |\tau| \geq \tau_y \quad (3)$$

$$\dot{\gamma} = 0; |\tau| < \tau_y$$

The  $\tau_y$  describes the yield stress and  $\eta_{pl}$  is a plastic viscosity.

The Bingham model describes  $\tau_y$ , however, it is not well accurate in the flow prediction of pseudoplastic fluids, since it omits the pseudoplastic behaviour at low shear rates that leads to inaccurate values of the yield stress. In the prediction of the yield stress the Herschel-Bulkley model (eq. 4) is much more accurate [20] and it is also possible to use it for modelling of flow behaviour of SFs.

$$\tau = \tau_y + \eta_{pl} \times \dot{\gamma}^n \quad (4)$$

The exponent  $n$  here represents flow behaviour index. When  $n = 1$ , the equation is simplified to Bingham equation. If the exponent is  $n < 1$  the fluid behaves as the pseudoplastic fluid, which is the case of ER fluids and MR suspensions.

In the case of ER fluids, the special Cho-Choi-Jhon [21] model (eq. 5) has been proposed and it fits the flow curves of ER fluids very well. Unfortunately, it is not generally possible to use it for MR suspensions due to their slightly different shape upon an application of an external magnetic field.

$$\tau = \frac{\tau_y}{1+(t_1\dot{\gamma})^\alpha} + \eta_\infty \cdot \left(1 + \frac{1}{(t_2\dot{\gamma})^\beta}\right) \times \dot{\gamma} \quad (5)$$

In the Cho-Choi-Jhon model the  $t_1$  and  $t_2$  are time constants inverse of the shear rate representing the region where the shear stress exhibits a minimum at a low shear rate and inverse to a shear rate at which a pseudo-Newtonian behaviour starts, respectively. The exponent  $\alpha$  is related to the decrease in the shear stress and the values of  $\beta$  are between 0–1, since  $d\tau/d\dot{\gamma} > 0$ , and the  $\eta_\infty$  represents shear viscosity at high shear rates [21].

The advantage of using Cho-Choi-Jhon model over the Bingham one is clearly seen from Fig 2. The flow curves of SFs in the presence of an external physical field are determined by the collision between electrostatic resp. magnetic forces against hydrodynamic ones. Fig. 2 depicts the flow curve for ER fluid based on dodecylbenzene-sulfonic acid doped polyaniline (PANI) particles in silicone oil. At stresses lower than  $\tau_y$ , the electrostatic forces dominate over hydrodynamic ones. With increasing stress the ER fluid starts to flow and the values of shear stress start to decrease due to increasing hydrodynamic forces connected with the destruction and restoration of the internal structures. The dashed lines in Fig. 2 then represent the critical shear rate values at which the hydrodynamic forces start to dominate over electrostatic ones. It can be seen that with increasing electric field strength the values of critical shear rate increase, which represents the stiffer internal structures at stronger electric fields. The Cho-Choi-Jhon model is represented in Fig. 2 by solid lines and it is evident that this model can also describe the decrease in the shear stress before the hydrodynamic forces start to dominate. This model can thus much better fit the ER flow curves and also predict  $\tau_y$  more accurate than the Bingham model (dotted line).



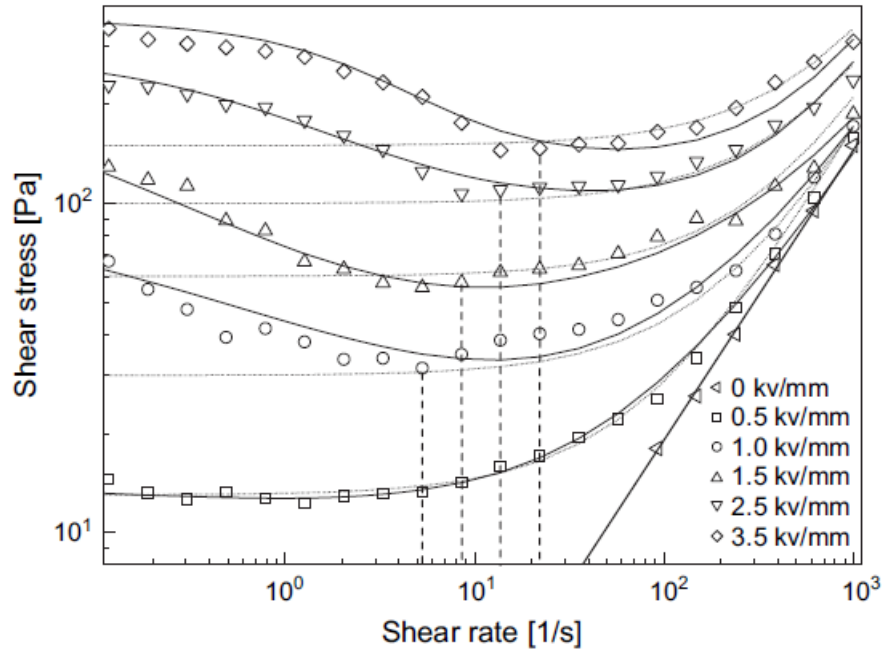


Fig. 2. ER flow curves for the ER fluid composed of dodecylbenzene-sulfonic acid doped PANI particles in silicone oil at various electric field strengths. The solid lines represent a fit according to Cho-Choi-Jhon model and the dotted lines represent the Bingham model. The dashed lines represent the critical shear rate. Reprinted from Kim et al. [22].

### 1.3 Physical background of the electrorheological effect

The ability of electrically polarizable particles to create organized chain-like structures upon an application of an external electric field arises from electrically induced dipole-dipole interactions [23]. When the electric field is applied the particles and their dipoles become polarized and then they orient themselves along the electric field direction and the structures hold together due to the mentioned dipole-dipole interactions (Fig. 3). Among the various types of polarizations, it is assumed that the interfacial Maxwell-Wagner [24] polarization is mainly responsible for the ER effect and it has been demonstrated that the higher dipole-dipole interactions the higher ER effect is observed. Beside the dielectric properties, the conductivity of the particles plays also the major role on the rate of the ER effect [24-26]. It not only contributes to the electrostatic forces between the particles determining the stiffness of the created structures, it also determines the response time of the particles [25]; it means, the higher conductivity of the particles the faster their polarization occurs.

Besides the intrinsic properties of the dispersed particles and liquid medium, the electric field strength also directs the rate of ER effect (*see chapter 1.5.1 Electric field strength*). In ER fluids in which the ER effect is directed

dominantly by polar molecules, the polar groups attract each other after an application of an electric field,  $E$ , and it has been demonstrated that the local electric field,  $E_L$ , between two aligned polar particles is much higher than the overall applied electric field [23, 27]. The high ratio  $\varepsilon_p/\varepsilon_{lm}$ , where  $\varepsilon_p$  represents the relative permittivity of dispersed particles and  $\varepsilon_{lm}$  is the relative permittivity of a liquid medium, is crucial for obtaining a strong  $E_L$  ( $E_L \gg E$ ) [23, 27], that further leads to high ER effects due to formation of stiffer chain-like structures. The mismatch between  $\varepsilon_p$  and  $\varepsilon_{lm}$  can be increased by introducing polar groups into the particles resulting in increased ER effects [28].

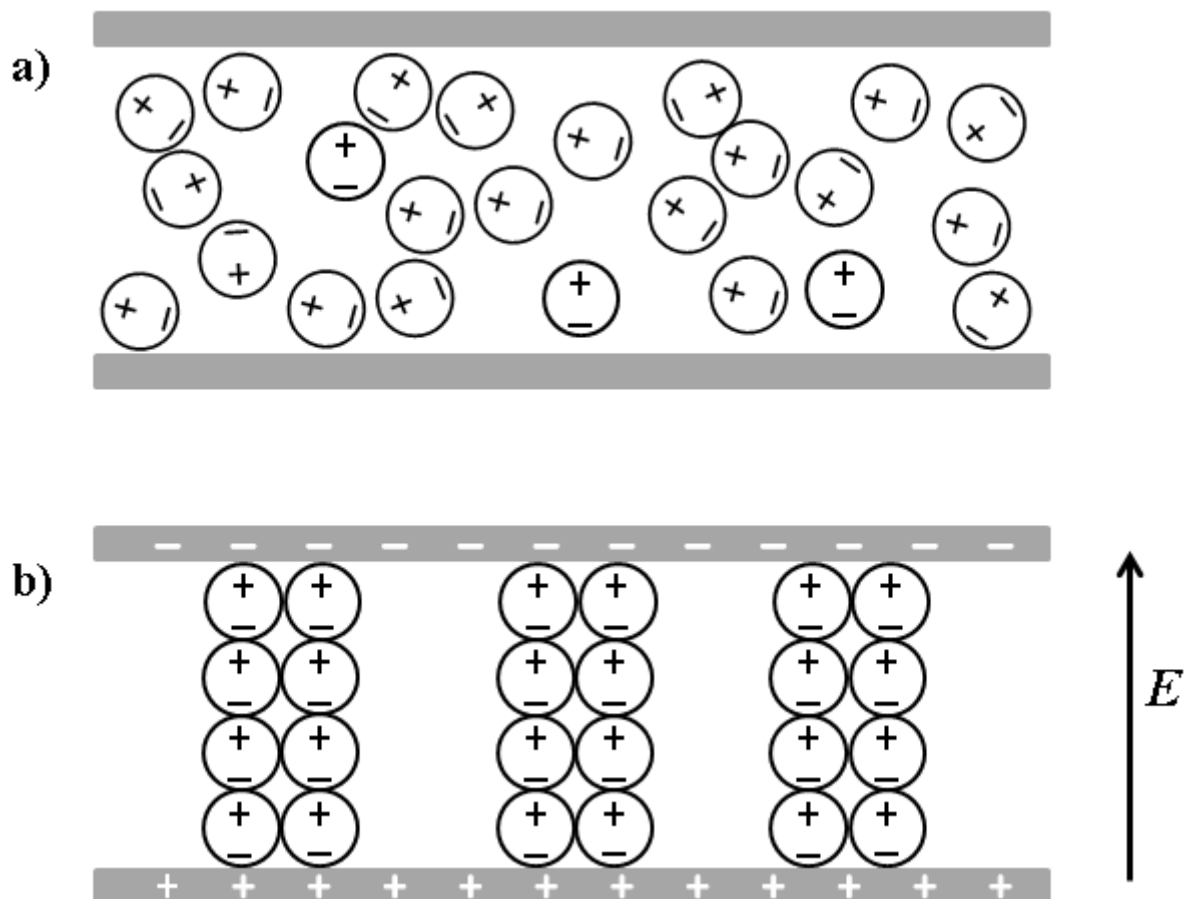


*Fig. 3. Electrically polarizable particles dispersed in an ER fluid and their formation into the internal chain-like structures. (a) In the absence of an external electric field the particles are randomly distributed within the ER fluid; (b) after an application of an external electric field,  $E$ , the particles create oriented chain-like structures spanning the electrodes.*

In addition to conductivity and relative permittivity, recently, the role of the position of the relaxation peak of dielectric losses of the ER fluids, which refers to the relaxation time,  $t_{rel}$  (eq. 6), on the ER effect has been a matter of investigation in some recent papers [29-31].

$$t_{\text{rel}} = \frac{1}{2\pi f} \quad (6)$$

In order to obtain exact values of  $t_{\text{rel}}$  and real permittivity part at zero,  $\varepsilon'_s$ , and infinite,  $\varepsilon'_\infty$ , frequency, and thus to be able to predict the ER properties of prepared ER fluids the Havriliak-Negami model (eq. 7) is frequently applied to the obtained data from the dielectric spectroscopy measurements of the ER fluids (Fig. 4; Tab. 1) [32].

$$\varepsilon^* = \varepsilon'_\infty + \frac{(\varepsilon'_s - \varepsilon'_\infty)}{(1 + (i\omega \cdot t_{\text{rel}})^a)^b} \quad (7)$$

The  $\varepsilon^*$  stays here for complex permittivity and  $\omega$  is the angular frequency. The parameters  $a$  and  $b$  represent the breadth and skewness of the distribution of relaxation times, respectively. The algebraic difference  $(\varepsilon'_s - \varepsilon'_\infty)$  is called the dielectric relaxation strength,  $\Delta\varepsilon'$  [32]. It has been also proposed that for high ER effects,  $t_{\text{rel}}$  should lay within  $1.6 \times 10^{-3}$  and  $1.6 \times 10^{-6}$  s (in the frequency range  $10^2 - 10^5$  Hz), and the dielectric loss tangent,  $\tan \delta$ , should be higher than 0.1 [25, 33].

The influence of the  $t_{\text{rel}}$  of ER fluids on their ER effect has been recently described by Wang et al. [30]. His work has shown that there is a certain threshold in relaxation times that is approximately  $t_{\text{rel}} = 10^{-2}$  s, and under this limit the stiffness of the internal structures in the ER fluids depends mainly on the electric and flow fields; thus, with variations in relaxation time under  $t_{\text{rel}} = 10^{-2}$  s, the shear rate at which the break of the internal structures occurs is nearly independent on  $t_{\text{rel}}$ . On the other hand, when  $t_{\text{rel}} > 10^{-2}$  s the shear rate at which the internal structures break down is more influenced by the  $t_{\text{rel}}$  of ER fluids instead of  $E$  [30].

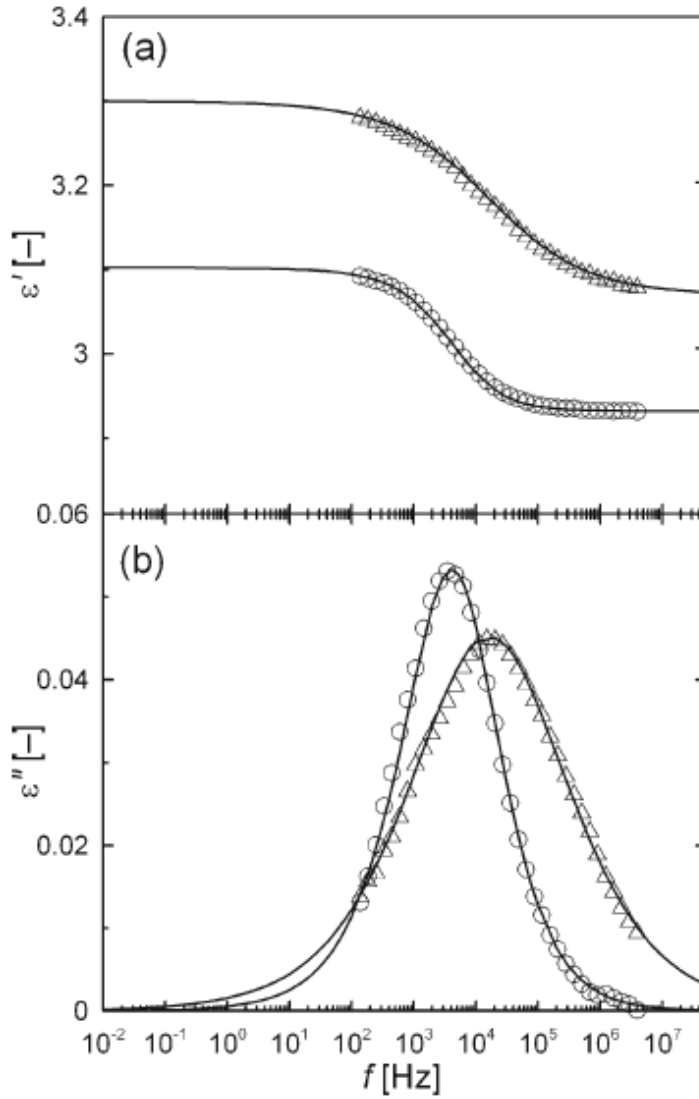


Fig. 4. (a) Real part,  $\varepsilon'$ , and (b) imaginary part,  $\varepsilon''$ , of complex permittivity dependence on frequency,  $f$ , for ER fluids of 5 wt% concentration based on  $\text{TiO}_2$  anatase ( $\circ$ ), and  $\text{TiO}_2$  rutile ( $\Delta$ ) particles. Reprinted from Sedlacik et al. [34].

Table 1 – Dielectric parameters of ER fluids of 5 wt% concentration based on  $\text{TiO}_2$  anatase and  $\text{TiO}_2$  rutile particles obtained from Havriliak-Negami model. Reprinted from Sedlacik et al. [34].

Parameter	$\text{TiO}_2$ anatase	$\text{TiO}_2$ rutile
$\varepsilon'_s$	3.10	3.30
$\varepsilon'_\infty$	2.93	3.07
$\Delta\varepsilon'$	0.17	0.23
$t_{\text{rel}}$ [s]	$3 \times 10^{-5}$	$9.06 \times 10^{-6}$

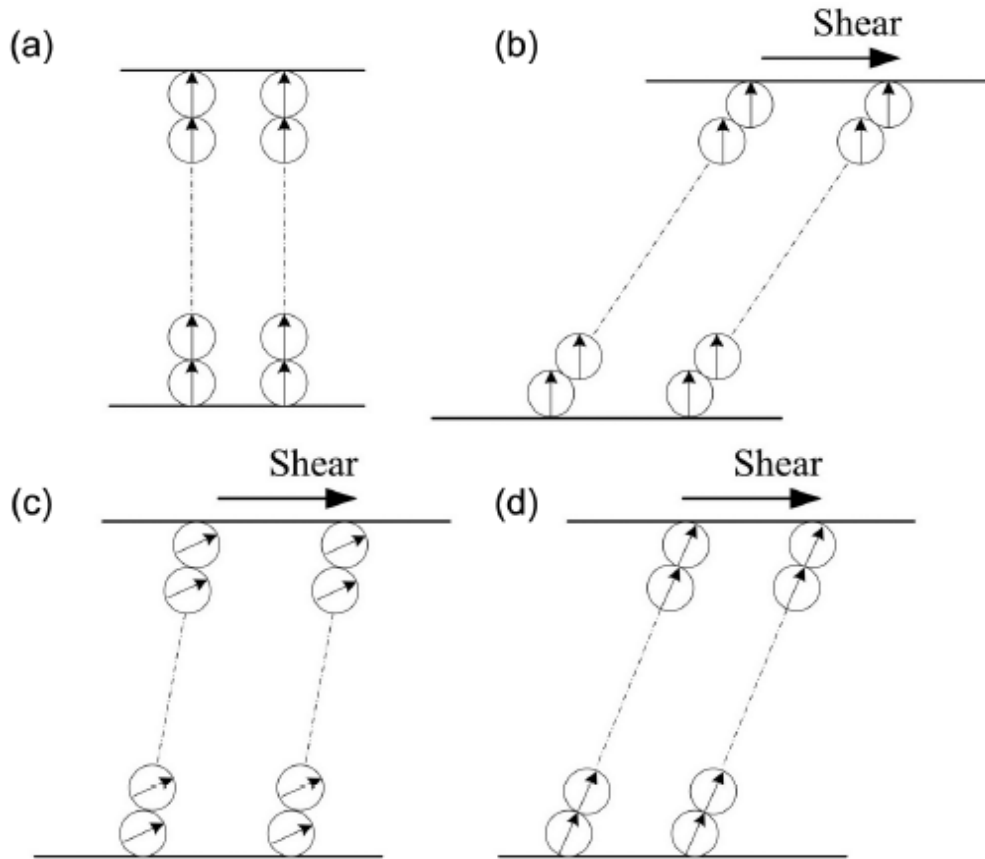


Fig. 5. Influence of the relaxation time of the ER fluids on their performance in the presence of an electric field: (a) the state when the electric field is on and no shearing is applied and the behaviour of ER fluids with (b) short, (c) large, and (d) moderate relaxation times in the shearing mode. Reprinted from Wang et al. [30].

## 1.4 Composition of electrorheological fluids

### 1.4.1 Liquid medium

A liquid medium, in which the dispersed phase of ER fluids is dispersed, should fulfil some criteria. The medium should be chemically, thermally and thermo-oxidatively stable. It should be able to operate in a broad temperature range and not to undergo a phase transition in the operating temperature region. It should also not interact with the particles in the negative way. In the case of ER fluids, the continuous phase should be also non-conducting and having a low relative permittivity [35, 36]. Therefore, the silicone or mineral oils are usually chosen as a continuous phase in ER fluids. The oils fulfil the above mentioned criteria and further various type with tuneable viscosity and composition are available, thus one can choose the liquid medium with the proper properties.

The choice of a liquid medium further strongly influences the ER efficiency (for closer description see *chapter 1.6 Requirements on electrorheological fluids*).

Even though the intrinsic viscosity of the chosen liquid medium does not significantly influence the ER effect, it directly determines the viscosity of ER fluid in the absence of an electric field. Therefore, with a liquid medium of lower viscosity the ER efficiency increases [31]. On the other hand, the use of liquid with low viscosity leads to faster sedimentation of the particles.

### 1.4.2 Dispersed phase

Electrorheological fluids are generally composed of non-conducting liquid medium (silicone and mineral oils) and electrically polarizable particles. These particles can be divided into two main groups – organic and inorganic. The latter is mainly represented by silica [37-40], titanates [14, 41-46], and clays [47-53]. Titanates are of high interest due to their low conductivity and substantial dielectric properties. These inorganic materials can be used for preparation of ER fluids with high yield stresses and low passing currents through the system due to low intrinsic conductivity of the particles. Major drawback is their high density in comparison with organic materials leading to their fast sedimentation.

Organic particles are dominantly represented by conducting polymers [22, 54-58] and various carbonaceous materials [59-66]. Conducting polymers are intensively studied materials in electrorheology due to their easy and inexpensive synthesis, and controllable conductivity, which should be approximately  $10^{-5}$ – $10^{-9}$  S cm<sup>-1</sup> for high ER effects, through the doping process [67, 68]. Polyaniline (Fig. 6), its derivatives, polypyrrole (PPy), and polythiophene are typical representatives of this group. The conductivity of conducting polymers is provided via their conjugated systems containing  $sp^2$  hybridized carbon atoms possessing delocalized electrons.

Recently, ER fluids based on novel organic conducting materials based on oligomers of conducting polymers have been introduced [69]. These materials miss the conjugated system (Fig. 7) and the conductivity mechanism is then provided through inter-molecular charge transport [70, 71], and therefore, doping mechanism and hydrogen bonds play a crucial role in the charge transport [72]. The former is responsible for the holes transport and the latter for electron transport. Doping mechanism is then crucial for high conductivities of these materials, and, thus, for high ER effects [69]. In the case of ER fluids based on aniline oligomers prepared in the various concentrations of methanesulfonic acid (MSA), the higher concentration of a dopant, the higher ER effects were observed (Fig. 8) [69]. The oligomers of conducting polymers represent a new class of conducting materials.

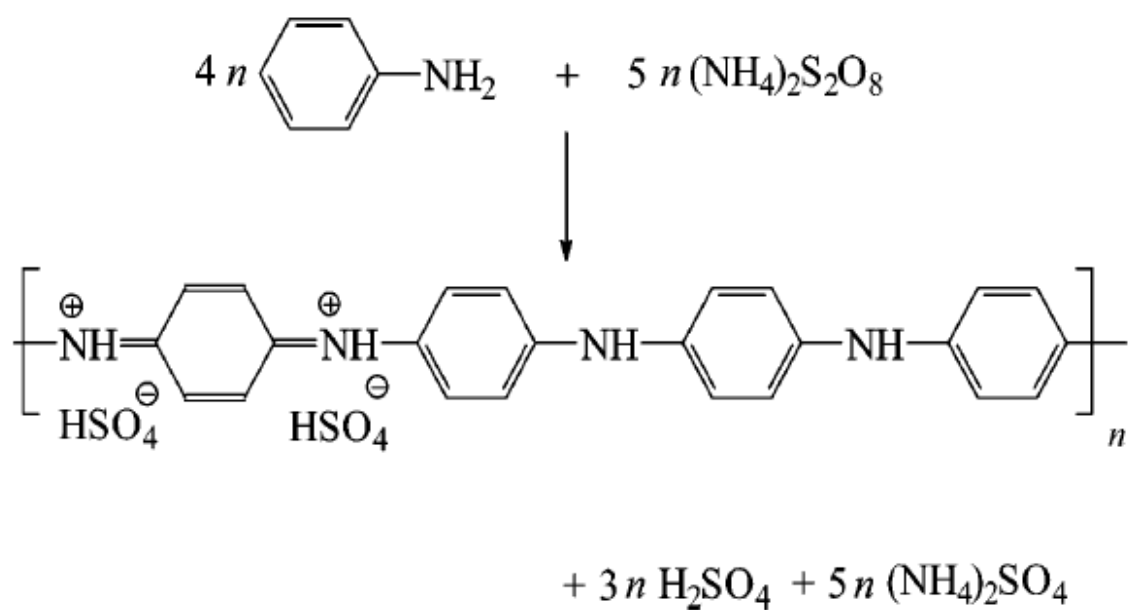


Fig. 6. The preparation and the chemical structure of PANI salt. Reprinted from Trchova et al. [73].

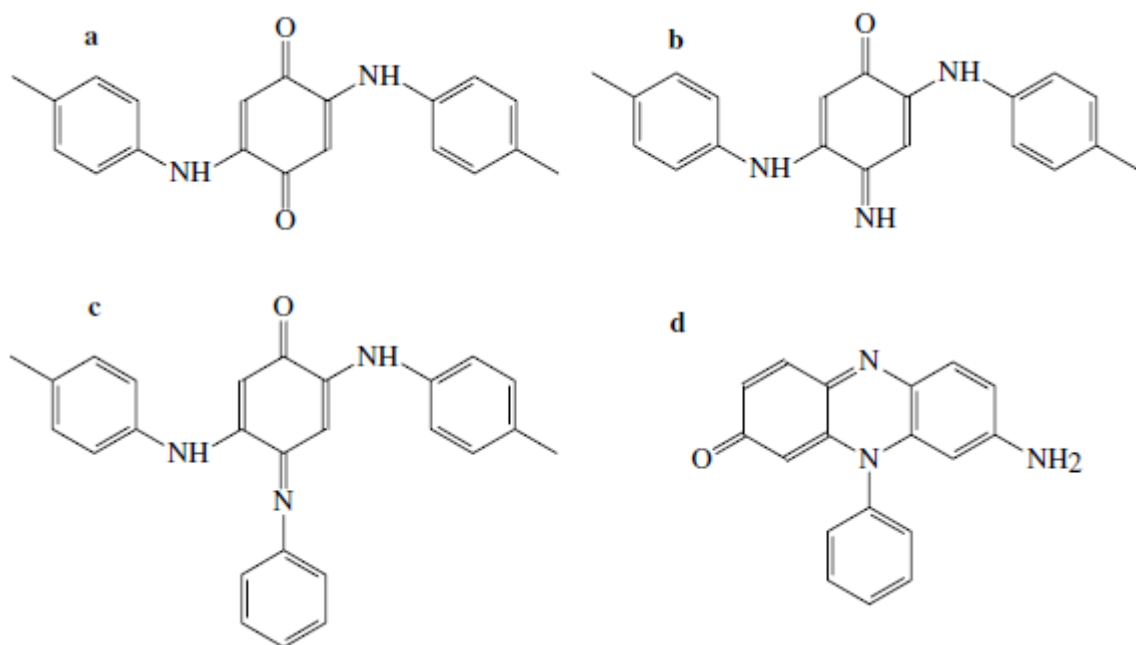


Fig. 7. Various possible aniline oligomers formation proposed by (a) Venancio et al. [74], (b) Surwade et al. [75], (c) Kriz et al. [76], and (d) Zujovic et al. [77]. Reprinted from Stejskal et al. [78].

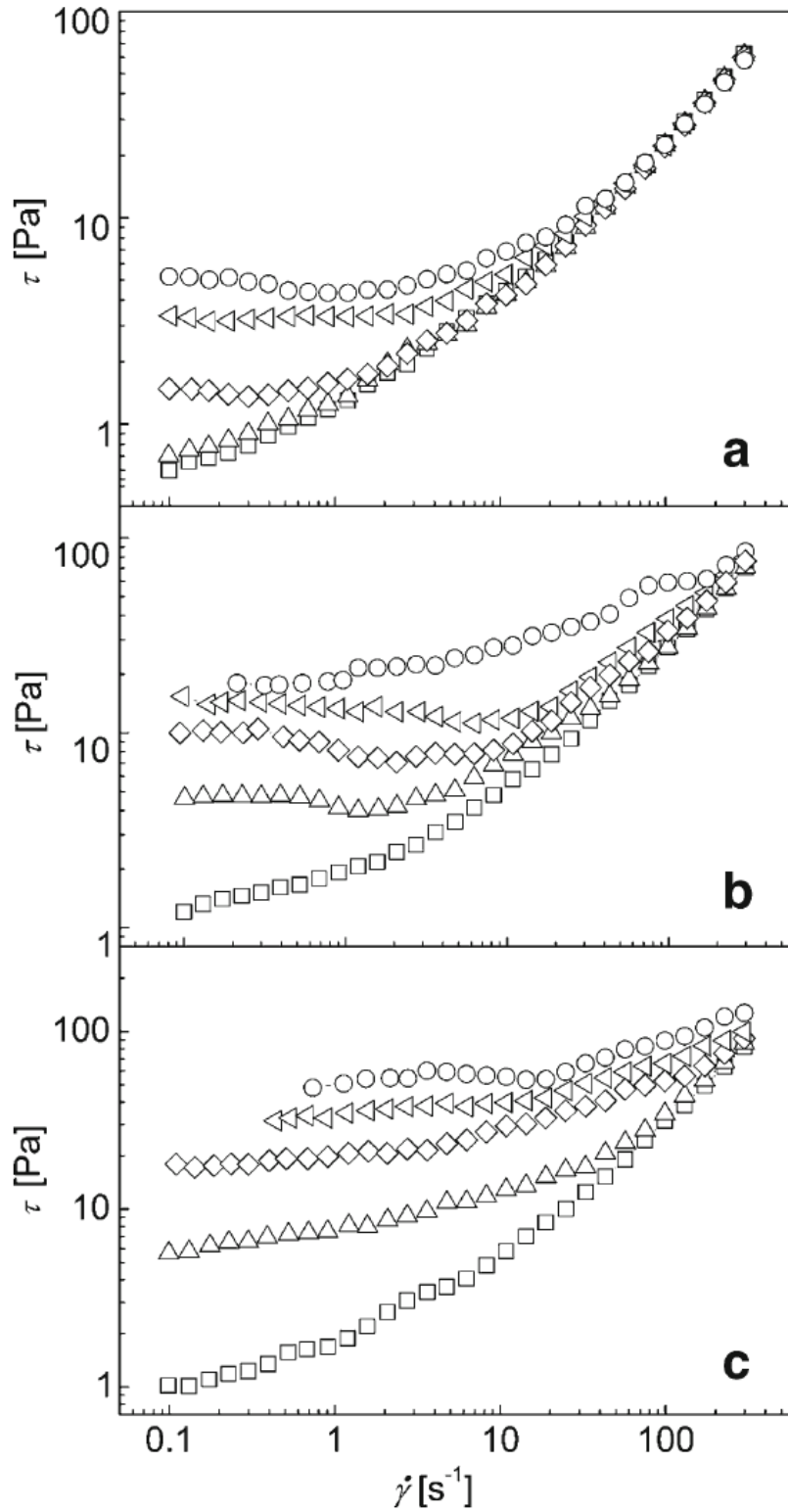


Fig. 8. Dependence of the shear stress,  $\tau$ , on the shear rate,  $\dot{\gamma}$ , of the ER fluids based on aniline oligomers particles prepared in the presence of (a) 0.1 M, (b) 0.2 M, and (c) 0.5 M MSA solutions at various external electric field strengths:  $0 \text{ kV mm}^{-1}$  (squares),  $0.5 \text{ kV mm}^{-1}$  (triangles),  $1 \text{ kV mm}^{-1}$  (diamonds),  $1.5 \text{ kV mm}^{-1}$  (left-pointing triangle), and  $2 \text{ kV mm}^{-1}$  (circle). Reprinted from Mrlik et al. [69].



In addition, few papers were recently published introducing a utilization of carbonization<sup>2</sup> process for a preparation of new electrically polarizable particles for ER fluids [80-84]. Carbonized particles possess high relative permittivity and large surface area. Both of these properties contribute to higher ER effect of their ER fluids in comparison with the ER fluids based on their non-carbonized analogues [80, 83]. Also the conductivity of the particles is strongly dependent on the carbonization temperature and can be thus controlled via carbonization process [83]. Qiao et al. [80] has used starch as an organic precursor containing carbon. The starch was carbonized at elevated temperatures in a nitrogen atmosphere and the particles were further mixed with silicone oil in order to prepare novel ER fluids. At elevated temperature, the starch underwent transition into carbonaceous structures possessing significantly higher surface area. This change positively contributed to an increase in interfacial polarization and their ER fluids then exhibited significantly higher ER effects than the ER fluids based on pure non-carbonized starch.

## 1.5 Factors influencing electrorheological effect

### 1.5.1 Electric field strength

Yield stresses exhibited by ER fluids considerably increase with increasing electric field strength. Higher electric field strengths evocate stronger dipole-dipole interactions between particles leading to significantly stiffer structures. The dependence of the  $\tau_y$  of ER fluids on the electric field strength obeys mostly the power law (eq. 8) [22]. Parameter  $q$  describes a rigidity of the system and  $\alpha$  is a slope of linear curve fitting the data.

$$\tau_y = q \times E^\alpha \quad (8)$$

In the case of ER fluids, it has further been demonstrated that for well-developed internal structures from the particles, the exponent  $\alpha$  should lie within 1.5-2 depending on the physical mechanism of holding the internal structures together [27, 85]. When the conductivity is the predominant factor determining the ER effect, the value 1.5 should be obtained [86], and a value 2 should be found in the case of polarization mechanism (Fig. 9).

---

<sup>2</sup> Carbonization is a process where organic materials are treated at elevated temperatures in an inert atmosphere. Recently, carbonized conducting polymers are a matter of an intensive research. When the nitrogen containing polymers are exposed to elevated temperatures in a nitrogen atmosphere, they undergo transition into nitrogen-enriched carbonaceous structures with unique properties [79].

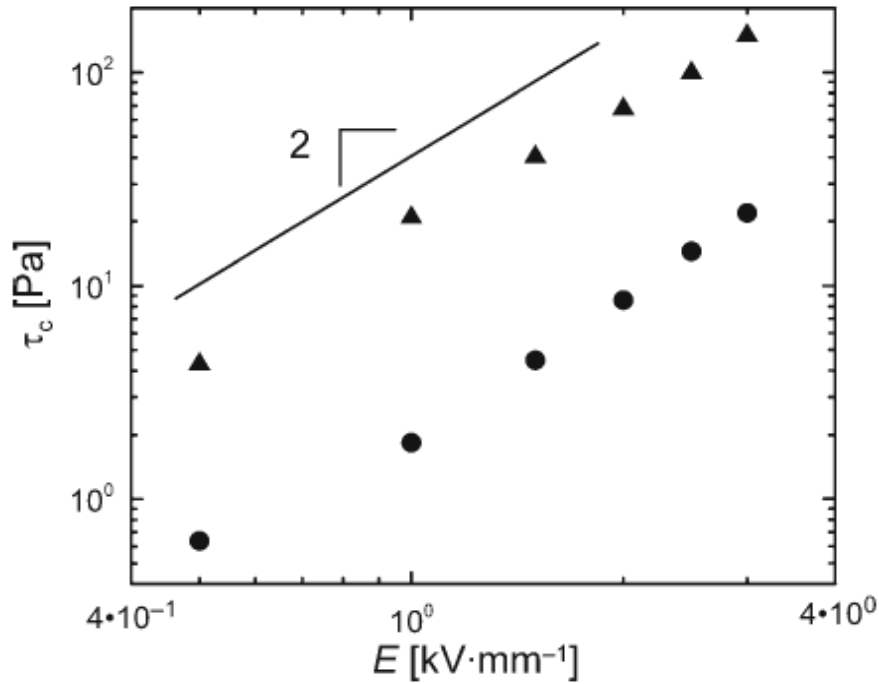


Fig. 9. Dependence of the shear stress values obtained at very low shear rates,  $\tau_c$ , on the electric field strength,  $E$ , for ER fluids based on  $\text{TiO}_2$  particles in (▲) rutile and (●) anatase form. The concentration of the dispersed phase was 15 wt%. Reprinted from Sedlacik et al. [34].

### 1.5.2 Particles size and morphology

The particles used as a dispersed phase in ER fluids can possess tremendous variations of morphologies [87]. The role of morphology is connected with the specific surface area and the inter-particle friction which occurs while orientating under the external electric field and deformation of the chain-like structures in the flow. It has been demonstrated that the ER fluids based on PANI or PPy rod-like (or fibrous) particles exhibit higher ER effects in comparison with the ER fluids based on PANI [58] or PPy [88] of the similar conductivities and the spherical morphology. Also in the case of ER effects of ER fluids based on various form of  $\text{TiO}_2$ , the ER fluids based on rutile form (rod-like particles) exhibit higher ER effect than the ER fluids based on anatase (spherical particles) (Fig. 9) [34]. In addition, the higher aspect ratio of the rods (fibrils) positively contributes to the ER effect [88].

In the case of using plate-like particles in ER fluids (Fig. 10), these ER fluids exhibit significantly higher ER effects than the ER fluids based on the spherical ones, [89, 90] mainly due to higher inter-particle friction [91].

The role of the particle size is more complex. Even though, it can be said that the bigger particles the bigger effects are observed. In the electrorheology, nevertheless, the highest ER effects have been observed for the ER fluid based

on dielectric nanoparticles [92, 93]. The smaller particles possess together higher specific surface area leading to increased amount of polar forces between them. The behaviour in the absence of an external physical field has to be also considered, since the nanoparticles-based suspensions typically exhibit higher viscosity due to higher particles-liquid medium interactions [18].

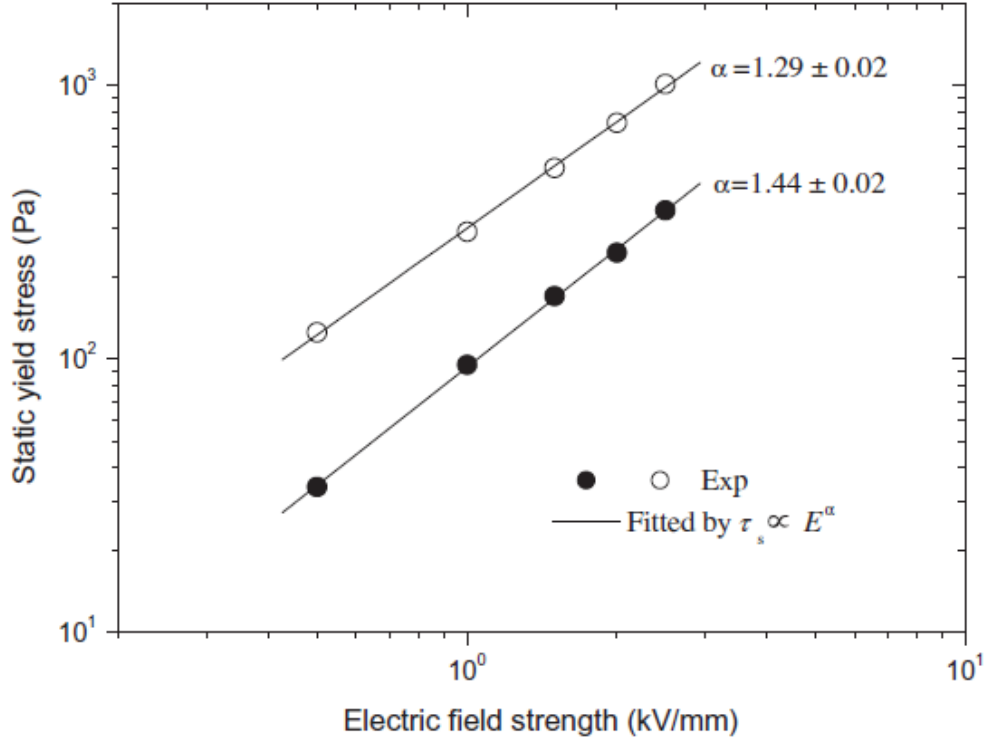


Fig. 10. The static yield stress vs. electric field strength for ER fluids based on graphene supported carbonaceous sheets (open symbols) and pure carbonaceous particles (solid symbols). Reprinted from de Yin et al. [90].

### 1.5.3 Temperature

Temperature is an important factor since the ER fluids should be able to operate in a wide temperature region and further temperature influences the physical properties of ER fluids. Generally, the ER effect of ER fluids increases with increasing temperature.

Many studies dealing with the temperature dependence of ER fluids [22, 41, 84, 94-99] have been introduced. The dispersed particles commonly used in ER fluids are semiconductors, whose conductivity and polarizability significantly increase with increasing temperature through thermally activated process [59, 70]. Increasing the temperature has generally several main positive impacts on the ER fluids: (i) an increase in the polarization magnitude, (ii) a shortening of  $t_{rel}$  of the ER fluids [84, 95], (iii) an increase in electrical conductivity of the dispersed particles [22, 98], and (iv) the viscosity of a liquid carrier decreases (Fig. 11) [22, 97]. All these effects of increased temperature lead to an enhancement of the ER effect (Fig. 11) and its stability at elevated temperature.

On the other hand, negative influence of the elevated temperature on the ER effect has also been observed [100].

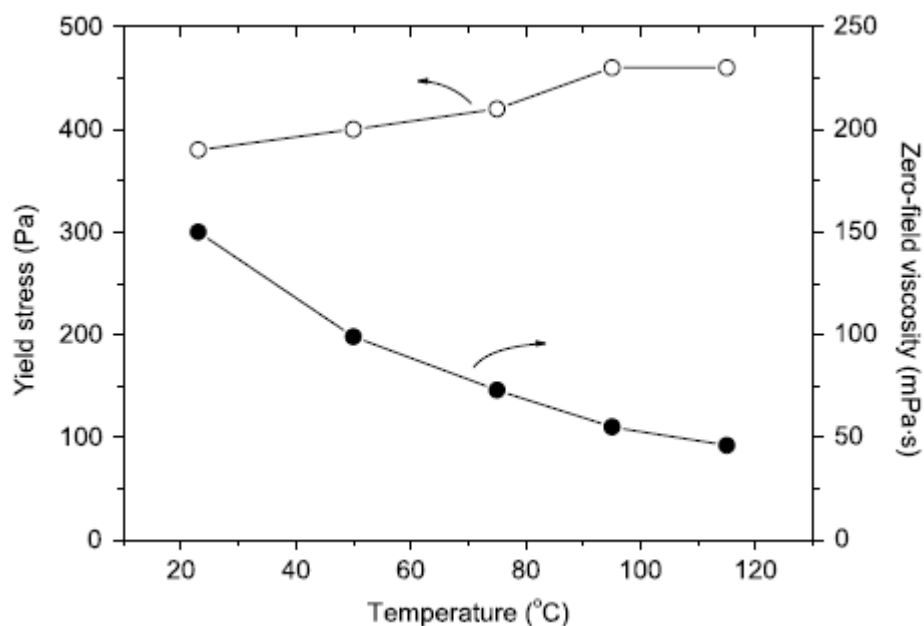


*Fig. 11. The values of yield stresses at  $3 \text{ kV mm}^{-1}$  and viscosity in the absence of an external electric field vs. temperature for ER fluids based on nitrogen-enriched carbonaceous nanotubes derivate from PANI of concentration 10 vol%. Reprinted from Yin et al. [84].*

#### **1.5.4 Particle concentration**

The ER effect of ER fluids is also highly influenced by the concentration of the dispersed phase. The higher amount of particles in ER fluids leads to a higher amount of particle-particle interactions increasing the sum of the electrostatic forces. Jiang and co-workers [101] or Kim and co-workers [102] investigated the influence of particle concentration on the ER effect of the ER fluids based on zeolite or dodecylbenzene-sulfonic acid doped PANI, respectively. In both studies the static yield stress significantly increased with increasing particle concentration (Fig. 12).

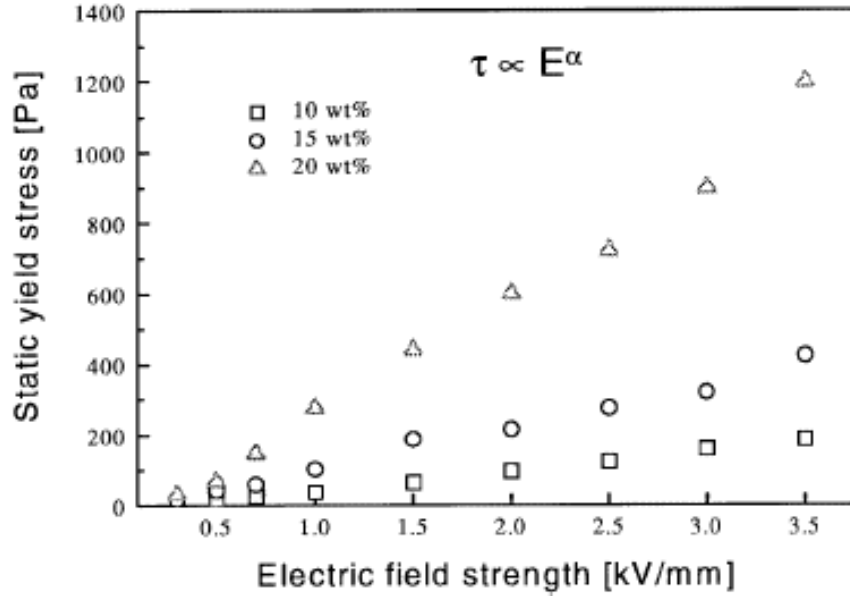


Fig. 12. The static yield stress vs. electric field strength for ER fluids based on dodecylbenzene-sulfonic acid doped PANI particles in silicone oil containing various particle concentration. Reprinted from Kim et al. [102].

Jiang et al. [101] further proposed a basic equation concerning the influence of particle concentration on the ER effect, which can be simplified according to Song et al. [103] to the form (eq. 9):

$$\tau_y = Ae^{C\varphi} \quad (9)$$

where A and C are constants dependent on the electrostatic properties of the particles dispersed in an ER fluid. On the other hand, the viscosity in the absence of an external electric field is also strongly dependent on  $\varphi$ . Lengalova et al. [104] focused on the ratio of the viscosity in presence of an electric field,  $\eta_E$ , and the viscosity in the absence of an external electric field,  $\eta_0$ , describing the effectivity of the system. Even though the yields stress increases with the higher volume fraction of the particles (Fig. 13a), the ER effectivity depending on  $\varphi$  had a certain maximum (Fig. 13b) due to increased  $\eta_0$ . Thus, the higher particle volume fraction of the particles in ER fluids leads to higher ER effects; however, it is something more challenging to propose the system with higher ER effectivity by changing the particle concentration.

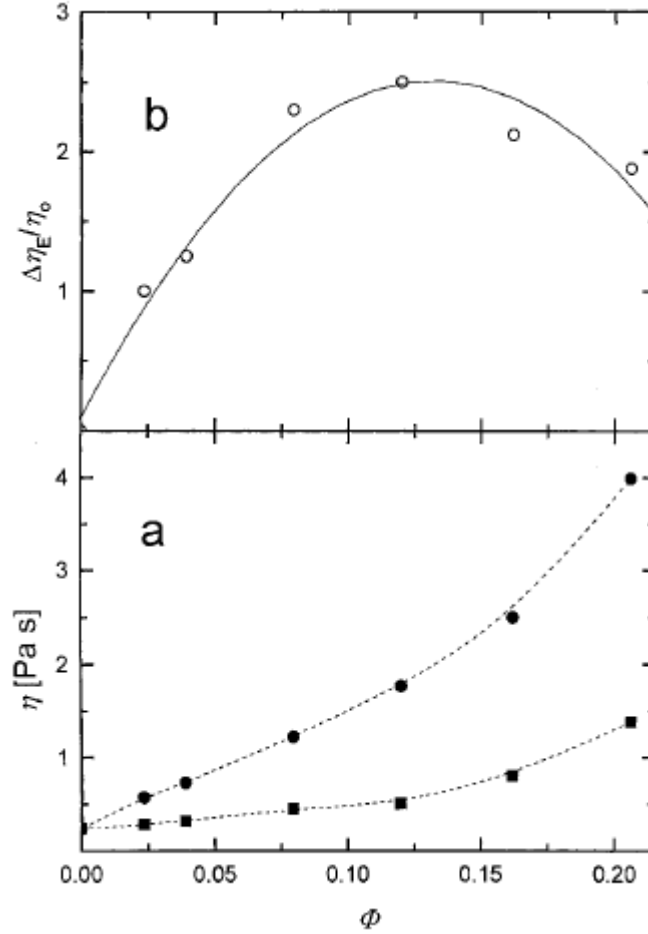


Fig. 13. (a) The dependence of the viscosity in the absence of an external electric field,  $\eta_0$ , (■) and viscosity in the presence of an external electric field,  $\eta_E$ , of strength  $2 \text{ kV mm}^{-1}$  (●); (b) the dependence of the ratio of  $\eta_E/\eta_0$  on the particles volume fraction for ER fluids based on PANI particles in silicone oil. Reprinted from Lengalova et al.[104].

## 1.6 Requirements on electrorheological fluids

Electrorheological fluids have to fulfil several requirements on their properties and behaviour in order to be implemented into the real applications. They have to exhibit high difference in the rheological properties in the presence and in the absence of an external electric field (high  $\tau_y$ ). This difference is well embodied in the eq. 10 [46, 57] for ER efficiency,  $e$ , where the  $\eta_0$  and  $\eta_E$  represent again the viscosity in the absence and in the presence of an external electric field, respectively.

$$e = \frac{\eta_E - \eta_0}{\eta_0} \quad (10)$$

The SFs have to be further physically (no sedimentation should occur) and thermo-oxidatively stable. They have to operate in a broad temperature region and they have to exhibit low electrical current passing density [26]. If sedimentation occurs, another important factor is the redispersibility of ER fluids. It represents how difficult is to redisperse the sediment within the ER fluids. The particles should also display no abrasion in order to keep their properties for a long-term use.

### **1.7 Shortcomings of electrorheological fluids**

The main drawback of ER fluids is the low ER effect. Their magnetic analogues (MR suspensions) exhibit significantly higher yield stresses in comparison with ER fluids; therefore, they have found a broader utilization in everyday life. In the case of ER fluids, their ER effects are still weak to be utilized in some of the industrial fields. The ER effect be increased with an addition of a huge amount of particles or substances with polar groups; however, this can lead to an undesirable increase in viscosity in the absence of an external electric field.

The other important issues are the sedimentation and thermo-oxidative stability. The particles used as a dispersed phase in ER fluids possess commonly higher density than the liquid medium in which they are dispersed. This leads to undesirable sedimentation problems and the ER fluid then do not fulfil the demand on the long-term stability. Many studies have been introduced on this topic and proposed some solutions to suppress sedimentation. In the case of conducting polymers the sedimentation is not that crucial as in the case of dense titanates due to their lower density. Sedlacik et al. [105] has prepared an ER fluid based on composite titanate/PPy particles. The presence of PPy led to a decrease in a bulk density of the material which enhanced the sedimentation stability of the ER fluid (Fig. 14). This approach, moreover, significantly promotes the ER effect of the ER fluid.

### **1.8 Application of smart fluids**

Many potential applications utilizing SFs as a functional medium have been proposed mainly in robotics and hydraulics. Some of them have already been utilized in an everyday life and some of them are of interest and are deeply researched recently. The possibility to control their rheological parameters can be involved for instance in damping systems, such as dampers [13], or in common devices such as washing machines. In automotive industry the SFs can be used in dampers [13], brakes, valves [7] and as a medium in electric clutches [4, 9]. Also their utilization in biomedicine as artificial joints [6] or artificial

muscles controllers [10] has been proposed. Last but not least, also inks and haptic displays using ER fluids have been suggested [8].

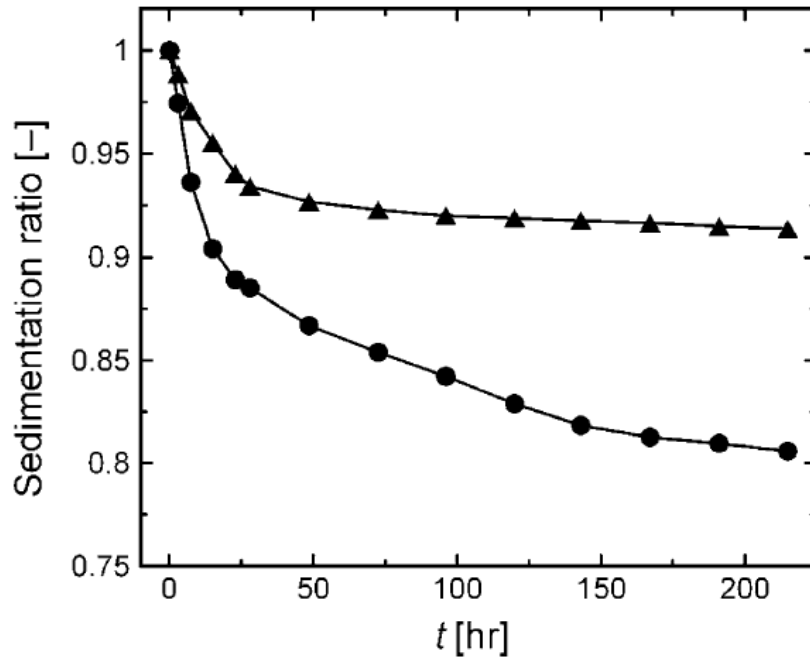


Fig. 14. The sedimentation stability of ER fluids of concentration 25 wt% based on  $TiO_2$  particles (●), and  $TiO_2/PPy$  composite particles (▲). Reprinted from Sedlacik et al. [105].



## **2. MOTIVATION AND AIMS OF THE DOCTORAL STUDY**

### **2.1 Motivation**

The ER fluids are materials exhibiting unique properties, which pronounced them for the use in many industrial applications. There are still physical issues that have to be solved in order to better understand and predict their behaviour. Another important topic is to find new compositions of ER fluids and materials to be utilized in them that would exhibit better rheological performance in the absence and in the presence of an external electric field.

### **2.2 Aims of the Doctoral Study**

- Preparation of new materials based on oligomers of conducting polymers which could be used as a dispersed phase in ER fluids in order to enhance their performance.
- Investigation of the possibility to use carbonization process as a new method for preparation of electrically polarizable particles for ER fluids with enhanced ER effect.
- Investigation of rheological parameters of the prepared ER fluids in the absence and in the presence of an external electric field.

### 3. EXPERIMENTAL PART

As mentioned above, the thesis investigates the possibility of preparation of novel particles for ER suspensions via carbonization process and the use of oligomers of conducting polymers.

Firstly, the possibility to prepare novel electrically polarizable particles by carbonization of poly(*p*-phenylenediamine) (ppPDA) was investigated. The results were introduced in *Paper I – An effect of carbonization on the electrorheology of poly(p-phenylenediamine)*. The ppPDA was prepared by an oxidative polymerization of *p*-phenylenediamine with ammonium peroxydisulfate. The prepared ppPDA particles were carbonized in a nitrogen atmosphere at various temperatures (200-800°C) in order to determine an impact of carbonization temperature on ER effect of their silicone-oil ER fluids. It is important to say, that the particles carbonized at 650°C and 800°C were too conductive and are therefore further omitted in the ER investigations. As it can be found in the literature [106], the carbonization temperature strongly influences the conductivity of the prepared particles.

The higher carbonization temperature during the carbonization of ppPDA, the higher specific surface area of the particles was achieved (Tab. 2) due to increased porosity of the particles and their reduced size while transformation into nitrogen-enriched carbonaceous structures.

*Table 2 – ppPDA particles specific surface area*

Carbonization temperature [°C]	Specific surface area [m <sup>2</sup> g <sup>-1</sup> ]
Original	30.4
200°C	33.7
400°C	69.3
600°C	259

The Raman spectroscopy confirmed the transformation of ppPDA particles into nitrogen-enriched carbonaceous structure by an exhibition of so-called G and D peaks which are typical for graphitic material. The G and D bands represent graphitic band (stretching of *sp*<sup>2</sup> carbons) and disorder band (stretching of carbon rings with some defect), respectively.

As mentioned above, the carbonization of the particles led to an increase in their specific surface area. This fact caused an increase in their silicone oil suspension viscosity in the absence of an external electric field, which was the highest for the particles carbonized at 600°C (Fig. 15a), due to higher interactions between particles and silicone oil. The carbonization process also significantly affects the ER effect of the prepared ER fluids. The highest ER effect was observed for the

ER fluid based on original particles (non-carbonized); even though the ER activity of the ER fluids based on particles carbonized at 200°C and 600°C was very similar (Fig. 15b). The ER fluid based on particles carbonized at 400°C exhibited clearly the lowest ER effect (Fig. 15b); probably because of a decomposition of conjugated system in ppPDA. With a further increase in a carbonization temperature, the loss of electric and dielectric properties which arose from the decomposition of conjugated systems is substituted with the transformation into carbonaceous structure possessing enhanced properties leading to increased ER effect of ER fluids based on such structures.

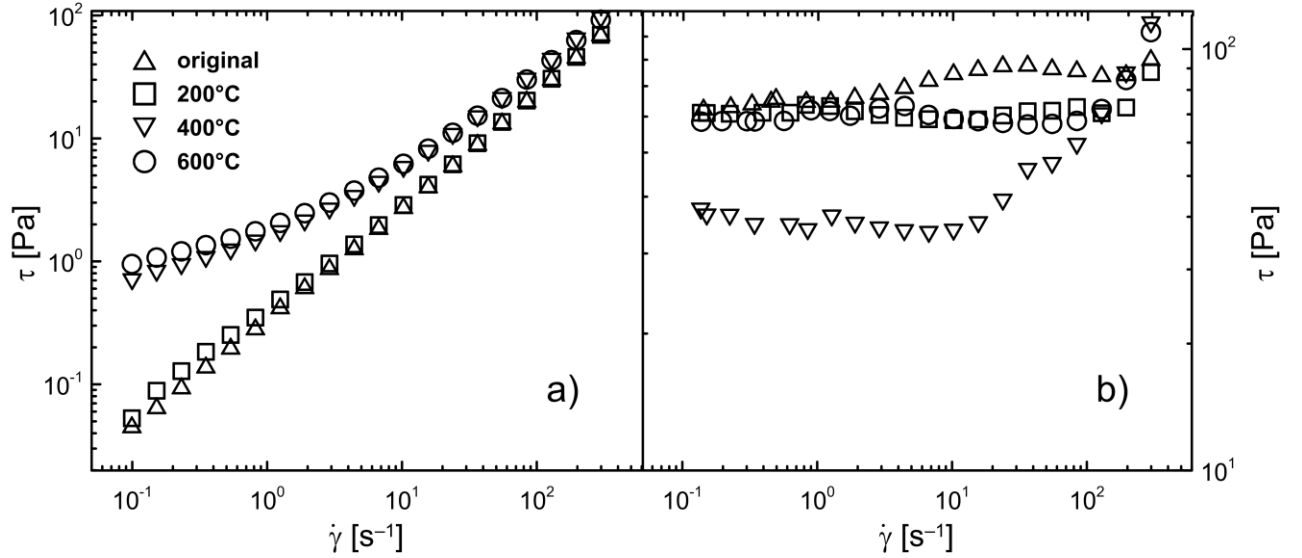


Fig. 15. The dependence of shear stress,  $\tau$ , on the shear rate,  $\dot{\gamma}$ , for ER fluids based on ppPDA and its carbonized analogues (a) in the absence of an external electric field, and (b) in the presence of an electric field of strength  $2 \text{ kV mm}^{-1}$ .

Even though the ER fluids based on original particles and particles carbonized at 200°C and 600°C show nearly the same ER effects, the ER efficiency (calculated according to eq. 10) is the highest for the first two ER fluids. The ER fluids based on particles carbonized at 600°C possessed significantly higher viscosity in the absence of an external electric field lowering the total ER efficiency of the fluid (Fig. 16).

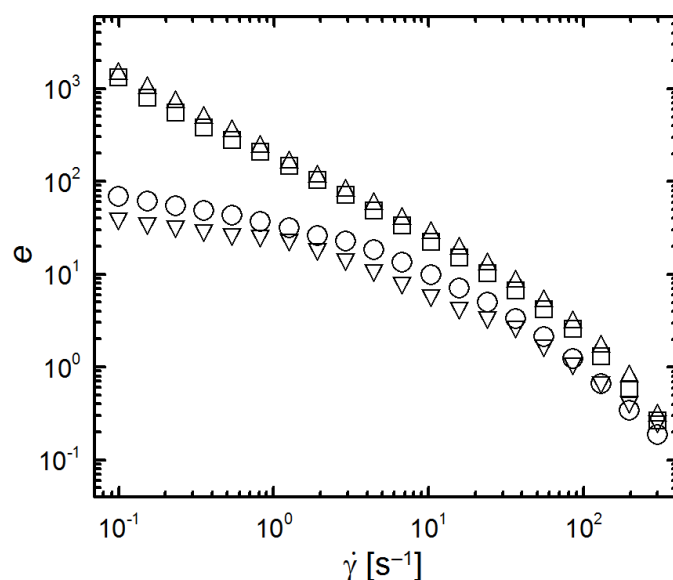
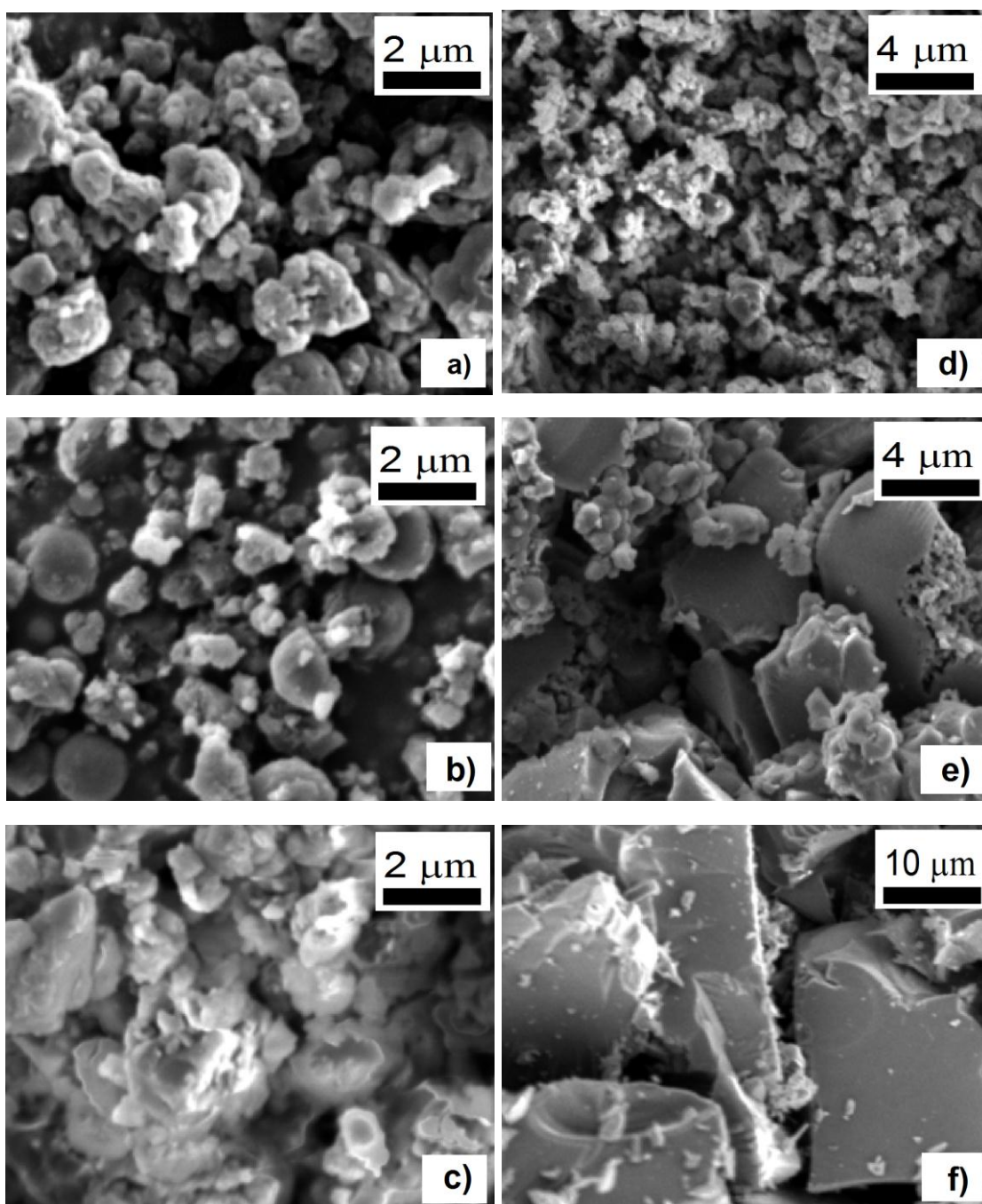


Fig. 16. The dependence of ER efficiency,  $e$ , calculated according to eq. 9 on the shear rate,  $\dot{\gamma}$ , for ER fluids based on ppPDA and its carbonized analogues. The meaning of the symbols is the same as in Fig. 15.

Carbonization was found as an interesting tool for preparation of new electric and dielectric particles, which are suitable for the use in ER fluids. The aniline oligomers were further prepared at various concentrations (0.1 M–2 M) of ammonium hydroxide ( $\text{NH}_4\text{OH}$ ) presented during their synthesis. Results are summarized in *Paper II – Carbonization of aniline oligomers to electrically polarizable particles and their use in electrorheology*. The prepared particles were further carbonized at  $650^\circ\text{C}$  in a nitrogen atmosphere; thus, aniline oligomers were prepared together with their carbonized analogues. In contrast to carbonization of ppPDA particles, the size of the aniline oligomers prepared at higher concentration ( $<0.2$  M) of  $\text{NH}_4\text{OH}$  increases, since the particles were sintered together at  $650^\circ\text{C}$  and during the cooling down, these were broken down into the sheets (Fig. 17). The particles prepared in the presence of 0.1 M  $\text{NH}_4\text{OH}$  possessed on their top a PANI layer, which protects the particles to be melted down, and therefore, their size was reduced after the treatment as it is usual for carbonized particles. Raman spectra of carbonized aniline oligomers particles again confirmed the transformation into carbonaceous structures exhibiting the typical G and D bands.



*Fig. 17. Scanning electron micrographs of aniline oligomers prepared in the presence of (a) 0.1 M, (b) 0.2 M, and (c) 2 M  $\text{NH}_4\text{OH}$  solution (d-f) and their carbonized analogues treated at  $650^\circ\text{C}$  in a nitrogen atmosphere.*

ER fluids of concentration of 10 wt% were prepared by mixing of prepared particles with silicone oil in a weight ratio 1:9. Generally, the ER fluids based on carbonized aniline oligomers exhibited higher ER effects than the ER fluid based on their non-carbonized analogues (Fig. 18). The ER fluids based on carbonized aniline oligomers in addition exhibited significantly higher ER effects than those ER fluids based on carbonized ppPDA keeping the same concentration of dispersed particles. The aniline oligomers formed larger particles after the carbonization process leading to a creation of stiffer structures.

The carbonization was thus confirmed as a suitable tool for preparation of electrically polarizable particles, whose ER fluids exhibit increased ER effects. Important findings, however, were observed by a comparison of the results obtained from steady-shear and oscillatory measurements. As it has been mentioned above, it is assumed that the interfacial polarization plays the major role on the rate of ER effect of ER fluids; thus, the higher dielectric relaxation strength, the higher ER effect should be observed. Prepared ER fluids based on carbonized aniline oligomers prepared in the presence of 0.1 M and 0.2 M  $\text{NH}_4\text{OH}$  have shown nearly the same ER effect in the steady-shear measurements, even though the dielectric relaxation strength of the former was 1.80 and of the latter one 1.18, which is significantly lower. In this case, the role of the relaxation time,  $t_{\text{rel}}$  has been as the crucial factor in prediction of the ER effect. The  $t_{\text{rel}}$  of ER fluid based on carbonized aniline oligomers prepared in the presence of 0.1 M and 0.2 M  $\text{NH}_4\text{OH}$  were  $1.9 \times 10^{-4}$  and  $5.6 \times 10^{-5}$  s, respectively. This stresses the importance of  $t_{\text{rel}}$  for generation of the ER effect. Moreover, in the case of oscillatory rheological measurements, the highest ER efficiency was observed for the case of the ER fluid based on carbonized aniline oligomers prepared in the presence of 0.2 M  $\text{NH}_4\text{OH}$  (Fig. 19); however, the ER efficiency for the ER fluids based on carbonized aniline oligomers prepared in the presence of 0.1 and 2 M  $\text{NH}_4\text{OH}$  were nearly the same, even though their ER fluids possess different dielectric properties. The latter have the dielectric relaxation strength and  $t_{\text{rel}}$  1.07 and  $1.2 \times 10^{-4}$  s, respectively. One of the factor could be also the larger size of the carbonized particles prepared in the presence of 2 M  $\text{NH}_4\text{OH}$ . Thus, the dielectric relaxation strength itself is not sufficient parameter for prediction the ER properties of ER fluids.

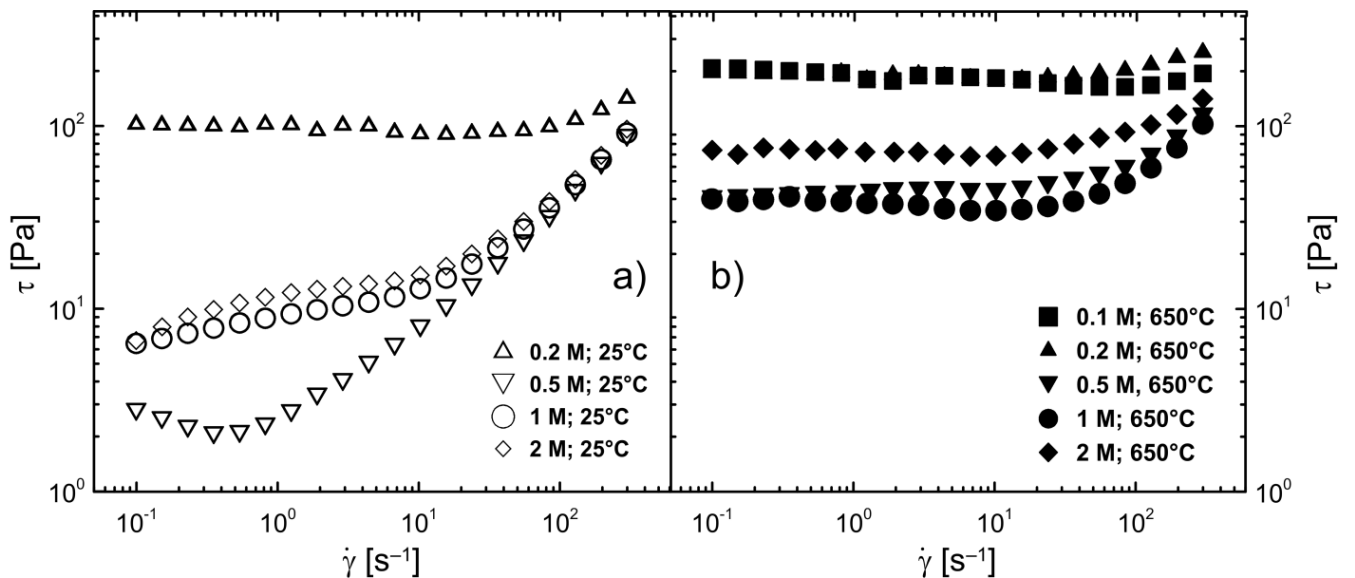


Fig. 18. The dependence of shear stress,  $\tau$ , on the shear rate,  $\dot{\gamma}$ , for suspensions based on (a) original and (b) carbonized aniline oligomers prepared in various concentrations of  $\text{NH}_4\text{OH}$  at electric field strength  $3 \text{ kV mm}^{-1}$ .

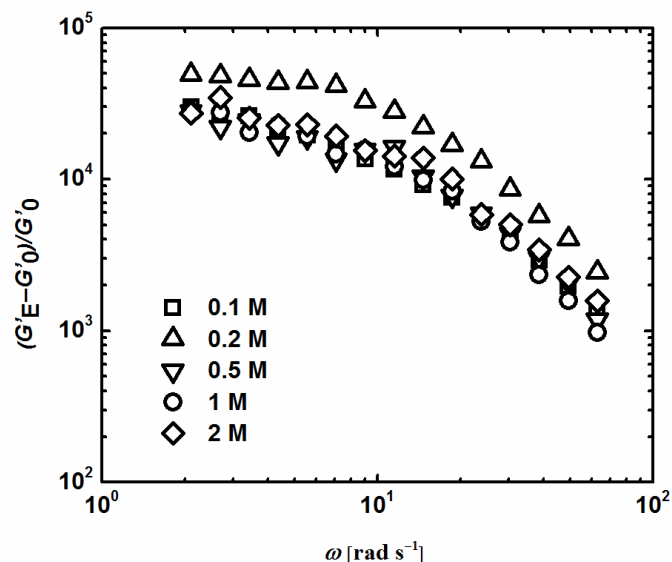


Fig. 19. The dependence of ER efficiency calculated from the values of elastic modulus in the presence of an electric field of strength  $3 \text{ kV mm}^{-1}$ ,  $G'_E$  and in its absence,  $G'_0$  on the angular frequency,  $\omega$ , for ER fluids based on carbonized aniline oligomers.

The dramatic change in ER performance of ER fluids based on aniline oligomers and their carbonized analogues has to be contributed to a dramatic change in dielectric properties. Only the ER fluids based on aniline oligomers prepared in the presence of 0.1 and 0.2 M  $\text{NH}_4\text{OH}$  among the ER fluids based on aniline oligomers exhibited relaxation process, even though, this was at high frequencies (Fig. 20). The rest of ER fluids based on aniline oligomers exhibited no relaxation at all in the measured region. The ER fluids based on carbonized samples, however, showed increased dielectric relaxation strength and all of them exhibited clear relaxation process which, moreover, was shifter to lower frequencies, where the interfacial polarization significantly influencing to high ER effects occurs (Fig. 21). The carbonization was thus confirmed as an excellent tool in a preparation of electrically polarizable particles for ER fluids.

These ER fluids based on carbonized aniline oligomers prepared in the presence of 0.1 M and 2 M  $\text{NH}_4\text{OH}$  were further used for investigation of the temperature influence on the ER effect (*Paper III – Temperature-dependent electrorheological effect and its description with respect to dielectric spectra*). The ER effect of these fluids was investigated in the range  $25\text{--}65^\circ\text{C}$  and was analyzed together with the results from dielectric spectroscopy of the ER fluids. As it implies from Fig. 18, as the dispersed phase particles with very various sizes were thus investigated.

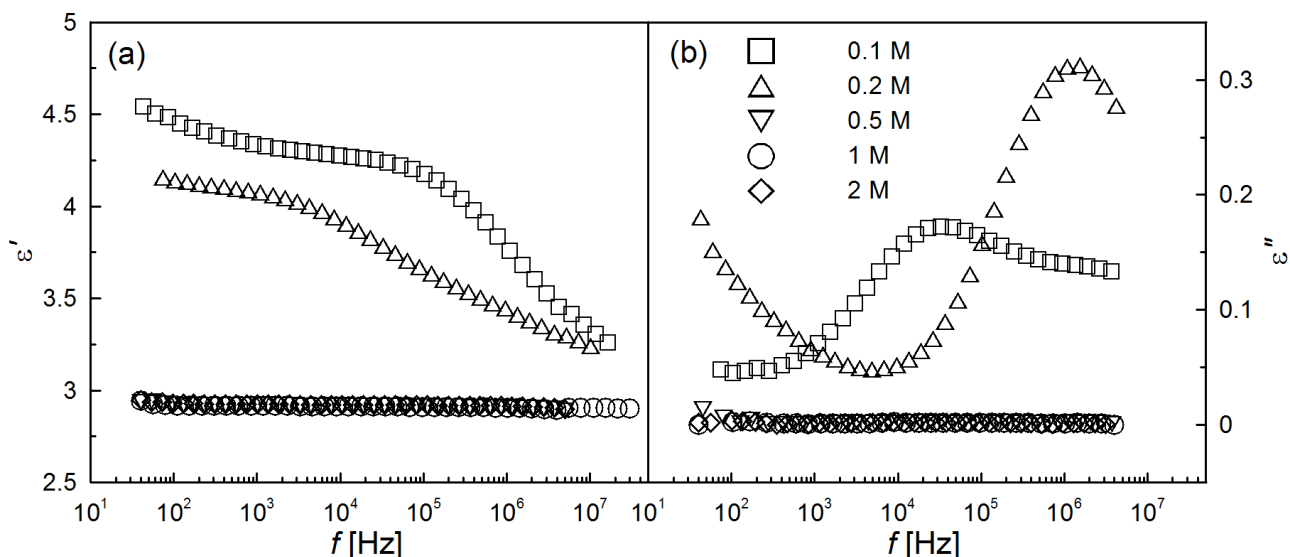


Fig. 20. (a) Real part,  $\epsilon'$ , and (b) imaginary part,  $\epsilon''$ , of complex permittivity dependence on frequency,  $f$ , for ER fluids based on aniline oligomers prepared in various concentrations of  $\text{NH}_4\text{OH}$ .

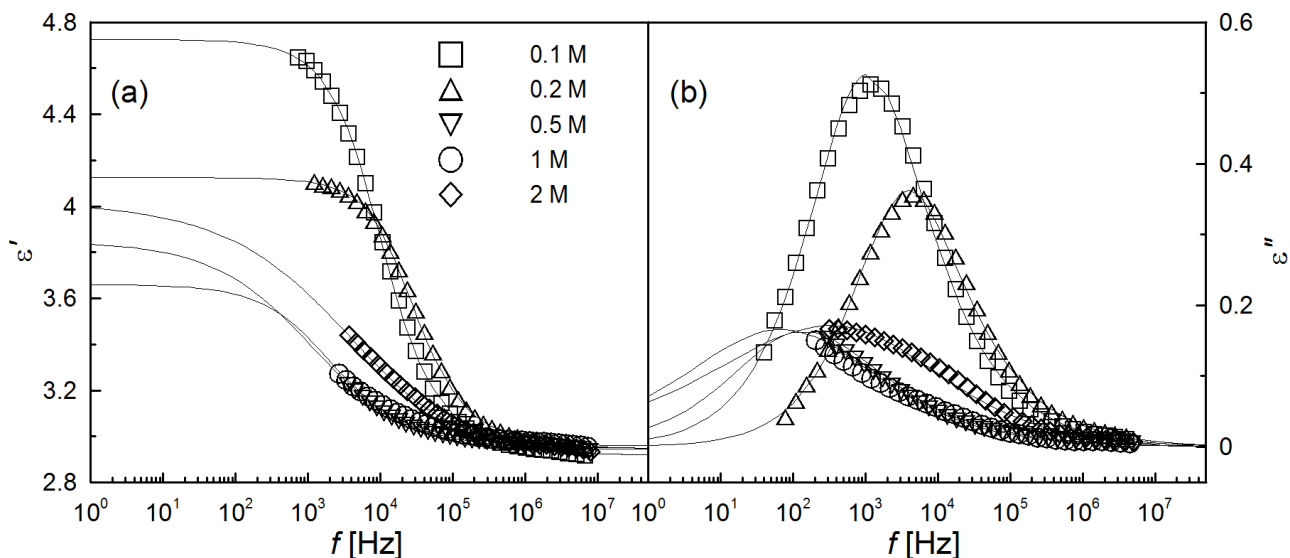


Fig 21. (a) Real part,  $\epsilon'$ , and (b) imaginary part,  $\epsilon''$ , of complex permittivity dependence on frequency,  $f$ , for ER fluids based on carbonized aniline oligomers prepared in various concentrations of  $\text{NH}_4\text{OH}$ .

For both ER fluids the ER effect increased with increasing temperature (Fig. 22) and, in addition, their viscosity in the absence of an external electric field decreases which fits well with the theory. The increment in the ER effect is commonly attributed to enhanced dielectric and electric properties. The dielectric spectra of these ER fluids were investigated in the temperature range 25–65°C since it is assumed that the dielectric parameters play an important role determining the ER effect. In the literature [70] it can be found that the dielectric



relaxation strength increases with the increasing temperature and it is accompanied also with shift of the  $t_{rel}$  to higher frequencies (the  $t_{rel}$  can be found shorter). Although both prepared ER fluids exhibited increased ER effects, their dielectric spectra showed different temperature dependence (Fig. 23,24). In the case of the ER fluids based on particles prepared in the presence of 2 M  $NH_4OH$  (bigger particles), the  $\Delta\epsilon'$  increases with an increase in temperature, however, in the case of the second ER fluid (based on significantly smaller particles),  $\Delta\epsilon'$  decreased. This is caused due to disturbances made by Brownian motion. Therefore, the increased of ER effect has to be connected with the shift of the  $t_{rel}$ , which is accompanied with the conductivity of the system, instead of purely with the  $\Delta\epsilon'$ , as it was often used in the literature [26].

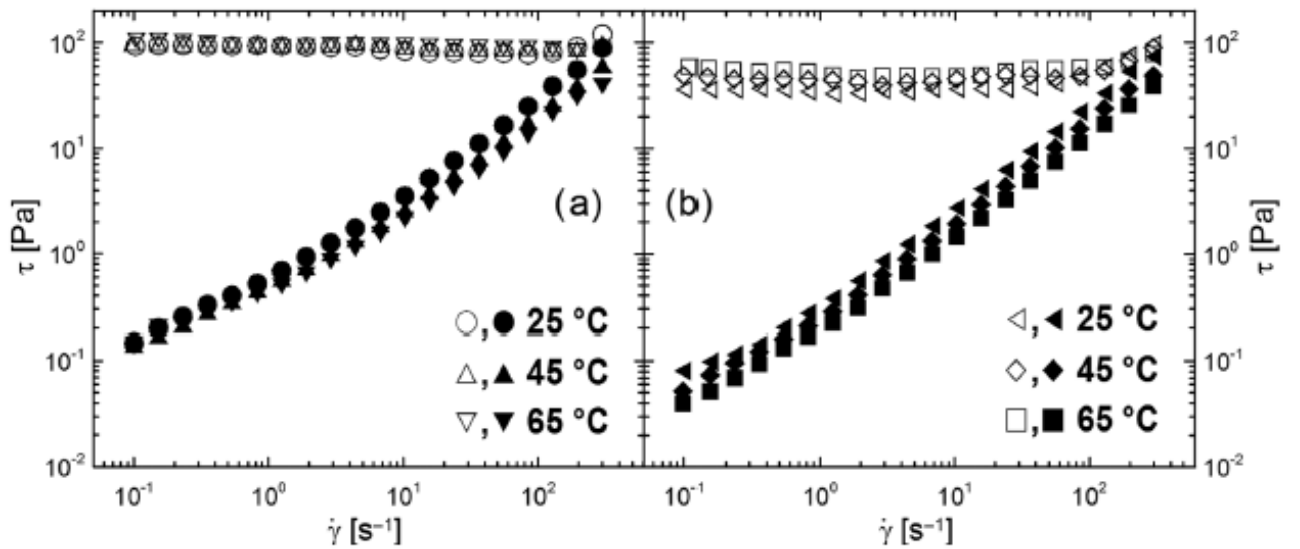


Fig. 22. The log-log dependence of the shear stress on the shear rate for ER fluids based on aniline oligomers prepared in the presence of (a) 0.1 M and (b) 0.2 M  $NH_4OH$  in the absence of an external electric field (full symbols) and in the presence of an external electric field of strength  $2 \text{ kV mm}^{-1}$ .

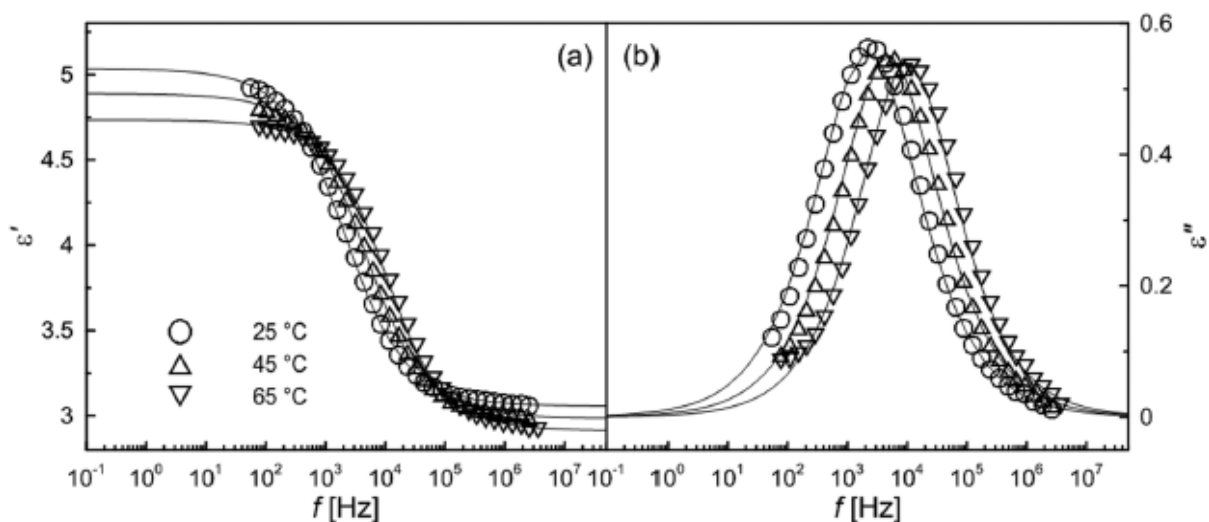


Fig. 23. (a) Real and (b) imaginary part of complex permittivity of the ER fluids based on aniline oligomers prepared in the presence of 0.1 M  $\text{NH}_4\text{OH}$  at various temperatures.

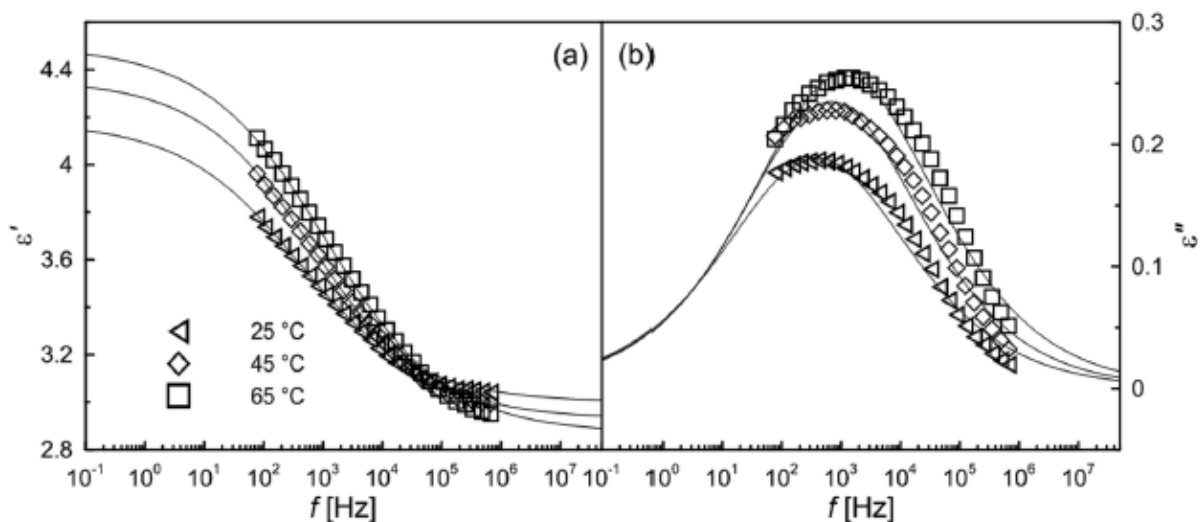


Fig. 24. (a) Real and (b) imaginary part of complex permittivity of the ER fluids based on aniline oligomers prepared in the presence of 2 M  $\text{NH}_4\text{OH}$  at various temperatures.

As another suitable material for electrorheology, the *p*-phenylenediamine oligomers were prepared, their conductivity was controlled via doping process, and, further, they were suspended in silicone oil in order to create novel ER fluids. These results are summarized in *Paper IV – The observation of a conductivity threshold on the electrorheological effect of p-phenylenediamine oxidized with p-benzoquinone*. The *p*-phenylenediamine was oxidized with *p*-benzoquinone in the presence of methanesulfonic acid solution of various concentrations. This approach led to a preparation of 2,5-(di-*p*-phenylenediamine)-1,4-benzoquinone trimmers with various conductivities depending on the concentration of MSA, which served as a dopant. In this manner chemically equivalent particles were obtained and the role of their

conductivities (determined through the amount of adsorbed ions) on the ER effect could be directly investigated. It has been found that with increasing amount of MSA acid presented during the synthesis the conductivity of the *p*-phenylenediamine oligomers increases, which led to an increase in ER effect (Fig. 25).

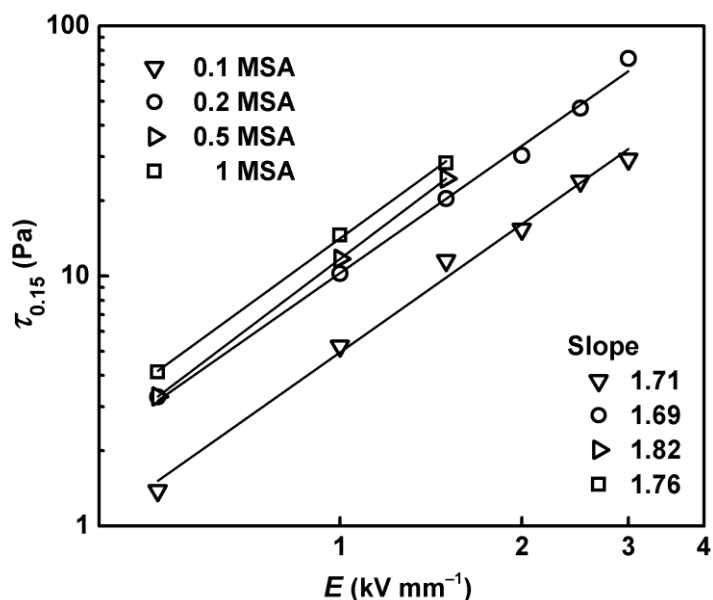


Fig. 25. The plot of shear stress values obtained at shear rate  $0.15 \text{ s}^{-1}$  vs electric field strength for ER fluids based on 2,5-(di-*p*-phenylenediamine)-1,4-benzoquinone trimmers prepared at various concentrations of MSA.

A nonlinear dependence between the yield stress and the conductivity of the particles, however, has been found (Fig. 26). Thus, the relationship between the conductivity of the particles and ER effects of their ER fluids is not proportional. It can be said that once the internal chain-like structures are organized, the further increment in the yield stress is not linearly proportional to the change of conductivity. Furthermore, even though the same values of  $\Delta\epsilon'$  were found for the ER fluids based on the particles prepared in the presence of 0.1 and 0.2 M MSA, their ER effects were significantly different. However, these two fluids exhibited different  $t_{\text{rel}}$  when the latter possessed the shorter one (Fig. 27). This conclusion supports an idea that relaxation time is much more significant parameter for predicting ER effect than the dielectric relaxation strength.

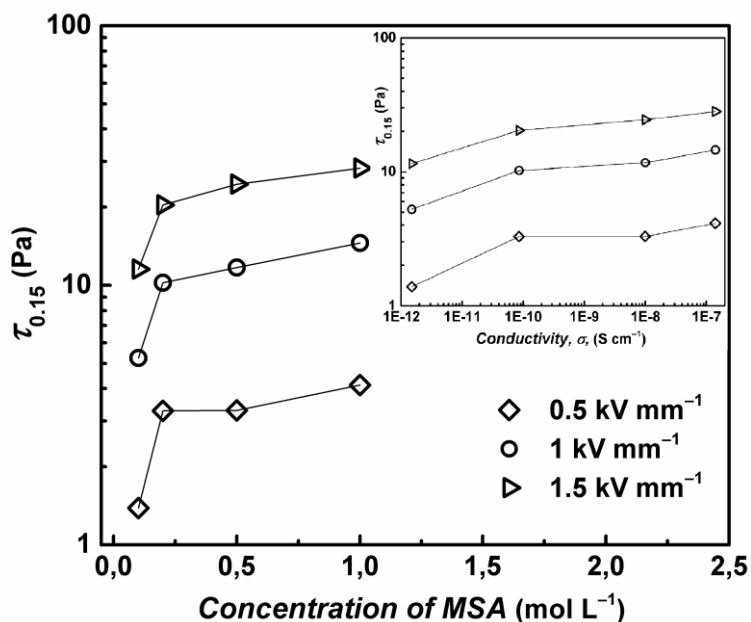


Fig. 26. The plot of shear stress values obtained at a shear rate of  $0.15 \text{ s}^{-1}$  vs. concentration of MSA presented during the synthesis of 2,5-(di-p-phenylenediamine)-1,4-benzoquinone trimmers for their 10 wt% ER fluids. The inset depicts shear stress values (Pa) obtained at a shear rate of  $0.15 \text{ s}^{-1}$ , vs. conductivity of the suspended particles.

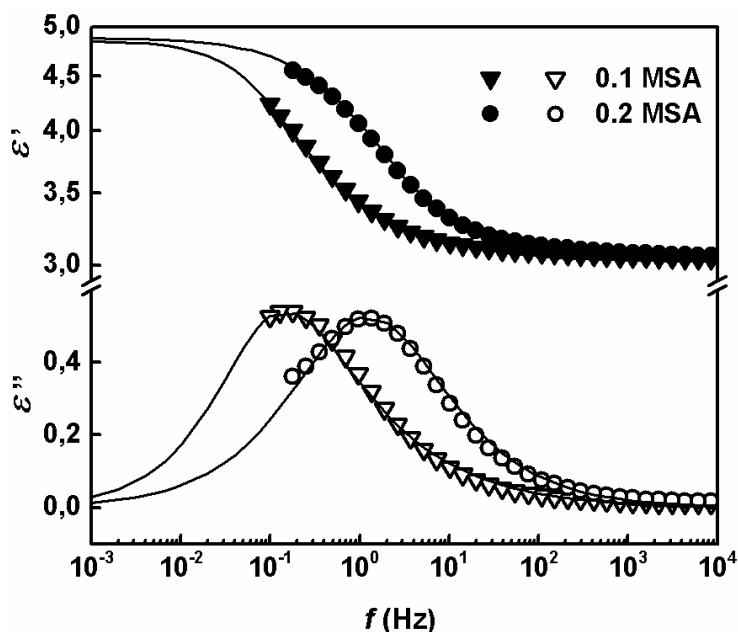


Fig. 27. Real and imaginary part of complex permittivity of the ER fluids based on 2,5-(di-p-phenylenediamine)-1,4-benzoquinone trimmers prepared at various concentrations of MSA.

## 4. THE THESIS CONTRIBUTION TO THE SCIENCE

Electrorheological fluids are well-known for several decades since they were firstly recognized by Winslow [1]. Their broader utilization, however, is limited due to their low effectiveness described by the difference between rheological parameters in the absence and in the presence of an electric field. New composition of ER fluids has to be found to increase their applicability in some of proposed industrial applications.

In the frame of this doctoral thesis, the aim was set to preparation of novel particle types which would be suitable for a use in ER suspensions. The chosen approach was to concentrate on carbonized particles of conducting polymers or their oligomers. The novel particles prepared by carbonization process exhibited increased ER effects together with enhanced ER efficiency. Thus the results showed the opportunity to prepare new materials which can be used as a dispersed phase in ER fluids, which are then closer to fulfill the demands on their properties.

In addition, it was found that the role of  $t_{rel}$  in determining the ER effect is usually underestimated when compared to  $\Delta\varepsilon'$ . In many scientific papers the major role of  $\Delta\varepsilon'$  is stressed, however, it was found that the values of  $t_{rel}$  should be rather considered to determine the ER effect. These findings should be investigated more deeply, and further it can significantly help to propose new ER materials, whose ER fluids would exhibit higher ER effects by not only considering the values of  $\Delta\varepsilon'$ , but also  $t_{rel}$ .

## LIST OF SYMBOLS AND ACRONYMS

ER	electrorheological	
MR	magnetorheological	
PANI	polyaniline	
PPy	polypyrrole	
MSA	methanesulfonic acid	
SF	smart fluid	
$\dot{\gamma}$	shear rate	(s <sup>-1</sup> )
$\tau_y$	yield stress	(Pa)
$\eta$	shear viscosity	(Pa s)
$\eta_s$	shear viscosity of a liquid medium	(Pa s)
$\eta_{pl}$	plastic viscosity	(Pa s)
$\varphi$	particles volume fraction	
$n$	Newtonian index	
$t_1, t_2$	time constants	(s)
$\eta_\infty$	viscosity at high shear rates	
$E$	electric field	(kV mm <sup>-1</sup> )
$E_L$	local electric field	(kV mm <sup>-1</sup> )
$\varepsilon_p$	relative permittivity of dispersed particles	
$\varepsilon_{lm}$	relative permittivity of a liquid medium	
$t_{rel}$	relaxation time	(s)
$\varepsilon^*$	complex permittivity	
$\omega$	angular frequency	(rad s <sup>-1</sup> )
$\varepsilon'_s$	real permittivity part at zero frequency	
$\varepsilon'_\infty$	real permittivity part at infinite frequency	
$\Delta\varepsilon'$	dielectric relaxation strength	
$\varepsilon''$	dielectric loss	
$e$	electrorheological efficiency	
$\eta_E$	viscosity in the presence of an electric field	
$\eta_0$	viscosity in the absence of an electric field	

## REFERENCES

- [1] Winslow WM. Induced fibrillation of suspensions. *J Appl Phys* 1949; 20(12):1137-40.
- [2] Rabinow J. The magnetic fluid clutch. *AIEE Transactions* 1948; 67:1308-15.
- [3] Bitaraf M, Ozbulut OE, Hurlebaus S, Barroso L. Application of semi-active control strategies for seismic protection of buildings with MR dampers. *Eng Struct* 2010; 32(10):3040-7.
- [4] Bucchi F, Forte P, Franceschini A, Frenzo F. Analysis of differently sized prototypes of an MR clutch by performance indices. *Smart Mater Struct* 2013; 22(10):10.
- [5] Chen ZQ, Wang XY, Ko JM, Ni YQ, Spencer BF, Yang G. MR damping system on Dongting Lake cable-stayed bridge. In: Liu SC, ed. *Smart Structures and Materials 2003: Smart Systems and Nondestructive Evaluation for Civil Infrastructures*. Bellingham: Spie-Int Soc Optical Engineering 2003, p. 229-35.
- [6] Johansson JL, Sherrill DM, Riley PO, Bonato P, Herr H. A clinical comparison of variable-damping and mechanically passive prosthetic knee devices. *Am J Phys Med Rehabil* 2005; 84(8):563-75.
- [7] Kamelreiter M, Kemmetmuller W, Kugi A. Digitally controlled electrorheological valves and their application in vehicle dampers. *Mechatronics* 2012; 22(5):629-38.
- [8] Liu YD, Lee BM, Park TS, Kim JE, Choi HJ, Booh SW. Optically transparent electrorheological fluid with urea-modified silica nanoparticles and its haptic display application. *J Colloid Interface Sci* 2013; 404:56-61.
- [9] Madeja J, Kesy Z, Kesy A. Application of electrorheological fluid in a hydrodynamic clutch. *Smart Mater Struct* 2011; 20(10):9.
- [10] Nagai S, Tomori H, Midorikawa Y, Nakamura T, Ieee. The position and vibration control of the artificial muscle manipulator by variable viscosity coefficient using MR brake. *Iecon 2011: 37th Annual Conference on Ieee Industrial Electronics Society*. New York: Ieee 2011.
- [11] Oh JS, Han YM, Lee SR, Choi SB. A 4-DOF haptic master using ER fluid for minimally invasive surgery system application. *Smart Mater Struct* 2013; 22(4):15.
- [12] Sarkar C, Hirani H. Theoretical and experimental studies on a magnetorheological brake operating under compression plus shear mode. *Smart Mater Struct* 2013; 22(11):12.
- [13] Zhu XC, Jing XJ, Cheng L. Magnetorheological fluid dampers: A review on structure design and analysis. *J Intell Mater Syst Struct* 2012; 23(8):839-73.
- [14] Plachy T, Mrlik M, Kozakova Z, Suly P, Sedlacik M, Pavlinek V, et al. The electrorheological behavior of suspensions based on molten-salt synthesized lithium titanate nanoparticles and their core-shell titanate/urea analogues. *ACS Appl Mater Interfaces* 2015; 7(6):3725-31.

- [15] Au PI, Foo B, Leong YK, Zhang WL, Choi HJ. Rheological analysis of graphene oxide coated anisotropic PMMA microsphere based electrorheological fluid from Couette flow geometry. *J Ind Eng Chem* 2015; 21:172-7.
- [16] Liu J, Wen XH, Liu ZP, Tan Y, Yang SY, Zhang P. Electrorheological performances of poly(o-toluidine) and p-toluenesulfonic acid doped poly(o-toluidine) suspensions. *Colloid Polym Sci* 2015; 293(5):1391-400.
- [17] Krieger IM. Rheology of monodisperse latices. *Adv Colloid Interface Sci* 1972; 3:111-36.
- [18] Macosko CW. Rheology. Principles, Measurements, and Applications. New York: Wiley-VCH; 1994.
- [19] Lopez-Lopez MT, de Vicente J, Bossis G, Gonzalez-Caballero F, Duran JDG. Preparation of stable magnetorheological fluids based on extremely bimodal iron-magnetite suspensions. *J Mater Res* 2005; 20(4):874-81.
- [20] Garakani AHK, Mostoufi N, Sadeghi F, Hosseinzadeh M, Fatourechi H, Sarrafzadeh MH, et al. Comparison between different models for rheological characterization of activated sludge. *Iran J Environ Health Sci Eng* 2011; 8(3):255-64.
- [21] Cho MS, Choi HJ, Jhon MS. Shear stress analysis of a semiconducting polymer based electrorheological fluid system. *Polymer* 2005; 46(25):11484-8.
- [22] Kim SG, Lim JY, Sung JH, Choi HJ, Seo Y. Emulsion polymerized polyaniline synthesized with dodecylbenzenesulfonic acid and its electrorheological characteristics: Temperature effect. *Polymer* 2007; 48(22):6622-31.
- [23] Shen R, Wang XZ, Lu Y, Wang D, Sun G, Cao ZX, et al. Polar-molecule-dominated electrorheological fluids featuring high yield stresses. *Adv Mater* 2009; 21(45):4631-5.
- [24] Hao T, Kawai A, Ikazaki F. Mechanism of the electrorheological effect: Evidence from the conductive, dielectric, and surface characteristics of water-free electrorheological fluids. *Langmuir* 1998; 14(5):1256-62.
- [25] Hao T. The interfacial polarization-induced electrorheological effect. *J Colloid Interface Sci* 1998; 206(1):240-6.
- [26] Hao T. Electrorheological suspensions. *Adv Colloid Interface Sci* 2002; 97(1-3):1-35.
- [27] Davis LC. Time-dependent and nonlinear effects in electrorheological fluids. *J Appl Phys* 1997; 81(4):1985-91.
- [28] Abdiryim T, Jamal R, Nurulla I. Doping effect of organic sulphonic acids on the solid-state synthesized polyaniline. *J Appl Polym Sci* 2007; 105(2):576-84.
- [29] Lee S, Yoon CM, Hong JY, Jang J. Enhanced electrorheological performance of a graphene oxide-wrapped silica rod with a high aspect ratio. *J Mater Chem C* 2014; 2(30):6010-6.



- [30] Wang ZY, Gong XL, Yang F, Jiang WQ, Xuan SL. Dielectric relaxation effect on flow behavior of electrorheological fluids. *J Intell Mater Syst Struct* 2015; 26(10):1141-9.
- [31] Mrlik M, Pavlinek V, Cheng QL, Saha P. Synthesis of titanate/polypyrrole composite rod-like particles and the role of conducting polymer on electrorheological efficiency. *Int J Mod Phys B* 2012; 26(2):1250007.
- [32] Havriliak S, Negami S. A complex plane representation of dielectric and mechanical relaxation processes in some polymers. *Polymer* 1967; 8(4):161-&.
- [33] Guo XS, Chen YL, Su M, Li D, Li GC, Li CD, et al. Enhanced electrorheological performance of Nb-doped TiO<sub>2</sub> microspheres based suspensions and their behavior characteristics in low-frequency dielectric spectroscopy. *ACS Appl Mater Interfaces* 2015; 7(48):26624-32.
- [34] Sedlacik M, Mrlik M, Kozakova Z, Pavlinek V, Kuritka I. Synthesis and electrorheology of rod-like titanium oxide particles prepared via microwave-assisted molten-salt method. *Colloid Polym Sci* 2013; 291(5):1105-11.
- [35] Gong XQ, Wu JB, Huang XX, Wen WJ, Sheng P. Influence of liquid phase on nanoparticle-based giant electrorheological fluid. *Nanotechnology* 2008; 19(16):7.
- [36] Rejon L, Castaneda-Aranda I, Manero O. Rheological behavior of electrorheological fluids: effect of the dielectric properties of liquid phase. *Colloid Surf A-Physicochem Eng Asp* 2001; 182(1-3):93-107.
- [37] Cheng QL, Pavlinek V, He Y, Lengalova A, Li CZ, Saha P. Structural and electrorheological properties of mesoporous silica modified with triethanolamine. *Colloid Surf A-Physicochem Eng Asp* 2008; 318(1-3):169-74.
- [38] Lengalova A, Pavlinek V, Saha P, Stejskal J, Kitano T, Quadrat O. The effect of dielectric properties on the electrorheology of suspensions of silica particles coated with polyaniline. *Phys A* 2003; 321(3-4):411-24.
- [39] Liu YD, Fang FF, Choi HJ. Silica nanoparticle decorated conducting polyaniline fibers and their electrorheology. *Mater Lett* 2010; 64(2):154-6.
- [40] Yoon C-M, Lee S, Hong SH, Jang J. Fabrication of density-controlled graphene oxide-coated mesoporous silica spheres and their electrorheological activity. *J Colloid Interface Sci* 2015; 438:14-21.
- [41] He Y, Cheng QL, Pavlinek V, Li CZ, Saha P. Synthesis and electrorheological characteristics of titanate nanotube suspensions under oscillatory shear. *J Ind Eng Chem* 2009; 15(4):550-4.
- [42] Hong JY, Lee E, Jang J. Electro-responsive and dielectric characteristics of graphene sheets decorated with TiO<sub>2</sub> nanorods. *J Mater Chem A* 2013; 1(1):117-21.
- [43] Jiang WQ, Jiang CX, Gong XL, Zhang Z. Structure and electrorheological properties of nanoporous BaTiO<sub>3</sub> crystalline powders prepared by sol-gel method. *J Sol-Gel Sci Technol* 2009; 52(1):8-14.

- [44] Miller DV, Randall CA, Bhalla AS, Newnham RE, Adair JH. Electrorheological properties of BaTiO<sub>3</sub> suspensions. *Ferroelectr, Lett Sect* 1993; 15(5-6):141-51.
- [45] Shang YL, Jia YL, Liao FH, Li JR, Li MX, Wang J, et al. Preparation, microstructure and electrorheological property of nano-sized TiO<sub>2</sub> particle materials doped with metal oxides. *J Mater Sci* 2007; 42(8):2586-90.
- [46] Yin JB, Zhao XP. Preparation and enhanced electrorheological activity of TiO<sub>2</sub> doped with chromium ion. *Chem Mat* 2004; 16(2):321-8.
- [47] Chae HS, Zhang WL, Piao SH, Choi HJ. Synthesized palygorskite/polyaniline nanocomposite particles by oxidative polymerization and their electrorheology. *Appl Clay Sci* 2015; 107:165-72.
- [48] Jang DS, Choi HJ. Conducting polyaniline-wrapped sepiolite composite and its stimuli-response under applied electric fields. *Colloid Surf A-Physicochem Eng Asp* 2015; 469:20-8.
- [49] Jang DS, Zhang WL, Choi HJ. Polypyrrole-wrapped halloysite nanocomposite and its rheological response under electric fields. *J Mater Sci* 2014; 49(20):7309-16.
- [50] Kim YJ, Liu YD, Choi HJ, Park SJ. Facile fabrication of pickering emulsion polymerized polystyrene/laponite composite nanoparticles and their electrorheology. *J Colloid Interface Sci* 2013; 394:108-14.
- [51] Meheust Y, Parmar KPS, Schjelderupsen B, Fossum JO. The electrorheology of suspensions of Na-fluorohectorite clay in silicone oil. *J Rheol* 2011; 55(4):809-33.
- [52] Parmar KPS, Meheust Y, Schjelderupsen B, Fossum JO. Electrorheological suspensions of laponite in oil: Rheometry studies. *Langmuir* 2008; 24(5):1814-22.
- [53] Rozynek Z, Zacher T, Janek M, Caplovicova M, Fossum JO. Electric-field-induced structuring and rheological properties of kaolinite and halloysite. *Appl Clay Sci* 2013; 77-78:1-9.
- [54] Choi HJ, Kim TW, Cho MS, Kim SG, Jhon MS. Electrorheological characterization of polyaniline dispersions. *Eur Polym J* 1997; 33(5):699-703.
- [55] Kim YD, Song IC. Electrorheological and dielectric properties of polypyrrole dispersions. *J Mater Sci* 2002; 37(23):5051-5.
- [56] Kwon SH, Liu YD, Choi HJ. Monodisperse poly(2-methylaniline) coated polystyrene core-shell microspheres fabricated by controlled releasing process and their electrorheological stimuli-response under electric fields. *J Colloid Interface Sci* 2015; 440:9-15.
- [57] Trlica J, Saha P, Quadrat O, Stejskal J. Electrorheological activity of polyphenylenediamine suspensions in silicone oil. *Physica A* 2000; 283(3-4):337-48.
- [58] Yin JB, Zhao XP, Xia X, Xiang LQ, Qiao YP. Electrorheological fluids based on nano-fibrous polyaniline. *Polymer* 2008; 49(20):4413-9.

- [59] Negita K, Misono Y, Yamaguchi T, Shinagawa J. Dielectric and electrical properties of electrorheological carbon suspensions. *J Colloid Interface Sci* 2008; 321(2):452-8.
- [60] Sim B, Zhang WL, Choi HJ. Graphene oxide/poly(2-methylaniline) composite particle suspension and its electro-response. *Mater Chem Phys* 2015; 153:443-9.
- [61] Yin JB, Shui YJ, Dong YZ, Zhao XP. Enhanced dielectric polarization and electro-responsive characteristic of graphene oxide-wrapped titania microspheres. *Nanotechnology* 2014; 25(4):045702.
- [62] Zhang K, Choi HJ. Smart polymer/carbon nanotube nanocomposites and their electrorheological response. *Materials* 2014; 7(5):3399-414.
- [63] Zhang WL, Choi HJ. Graphene oxide based smart fluids. *Soft Matter* 2014; 10(35):6601-8.
- [64] Zhang WL, Choi HJ. Graphene/graphene oxide: A new material for electrorheological and magnetorheological applications. *J Intell Mater Syst Struct* 2015; 26(14):1826-35.
- [65] Zhang WL, Choi HJ, Leong YK. Facile fabrication of graphene oxide-wrapped alumina particles and their electrorheological characteristics. *Mater Chem Phys* 2014; 145(1-2):151-5.
- [66] Zhang WL, Liu YD, Choi HJ. Graphene oxide nanocomposites and their electrorheology. *Mater Res Bull* 2013; 48(12):4997-5002.
- [67] Stenicka M, Pavlinek V, Saha P, Blinova NV, Stejskal J, Quadrat O. The electrorheological efficiency of polyaniline particles with various conductivities suspended in silicone oil. *Colloid Polym Sci* 2009; 287(4):403-12.
- [68] Stejskal J, Hlavata D, Holler P, Trchova M, Prokes J, Sapurina I. Polyaniline prepared in the presence of various acids: a conductivity study. *Polym Int* 2004; 53(3):294-300.
- [69] Mrlik M, Sedlacik M, Pavlinek V, Bober P, Trchova M, Stejskal J, et al. Electrorheology of aniline oligomers. *Colloid Polym Sci* 2013; 291(9):2079-86.
- [70] Mrlik M, Moucka R, Ilcikova M, Bober P, Kazantseva N, Spitalsky Z, et al. Charge transport and dielectric relaxation processes in aniline-based oligomers. *Synth Met* 2014; 192:37-42.
- [71] Stejskal J, Bober P, Trchová M, Horský J, Pilař J, Walterová Z. The oxidation of aniline with p-benzoquinone and its impact on the preparation of the conducting polymer, polyaniline. *Synth Met* 2014; 192:66-73.
- [72] Liu L, Yang GC, Tang XD, Geng Y, Wu Y, Su ZM. The effect of intermolecular interactions on the charge transport properties of thiazole/thiophene-based oligomers with trifluoromethylphenyl. *J Mol Graph* 2014; 51:79-85.
- [73] Trchova M, Moravkova Z, Dybal J, Stejskal J. Detection of aniline oligomers on polyaniline-gold interface using resonance raman scattering. *ACS Appl Mater Interfaces* 2014; 6(2):942-50.

- [74] Venancio EC, Wang PC, MacDiarmid AG. The azanes: A class of material incorporating nano/micro self-assembled hollow spheres obtained by aqueous oxidative polymerization of aniline. *Synth Met* 2006; 156(5-6):357-69.
- [75] Surwade SR, Dua V, Manohar N, Manohar SK, Beck E, Ferraris JP. Oligoaniline intermediates in the aniline-peroxydisulfate system. *Synth Met* 2009; 159(5-6):445-55.
- [76] Kriz J, Starovoytova L, Trchova M, Konyushenko EN, Stejskal J. NMR investigation of aniline oligomers produced in the early stages of oxidative polymerization of aniline. *J Phys Chem B* 2009; 113(19):6666-73.
- [77] Zujovic ZD, Laslau C, Bowmaker GA, Kilmartin PA, Webber AL, Brown SP, et al. Role of aniline oligomeric nanosheets in the formation of polyaniline nanotubes. *Macromolecules* 2010; 43(2):662-70.
- [78] Stejskal J, Trchova M. Aniline oligomers versus polyaniline. *Polym Int* 2012; 61(2):240-51.
- [79] Ciric-Marjanovic G, Pasti I, Gavrilov N, Janosevic A, Mentus S. Carbonised polyaniline and polypyrrole: towards advanced nitrogen-containing carbon materials. *Chem Pap* 2013; 67(8):781-813.
- [80] Qiao YP, Zhao X. Electrorheological effect of carbonaceous materials with hierarchical porous structures. *Colloid Surf A-Physicochem Eng Asp* 2009; 340(1-3):33-9.
- [81] Mrlik M, Ilcikova M, Plachy T, Pavlinek V, Spitalsky Z, Mosnacek J. Graphene oxide reduction during surface-initiated atom transfer radical polymerization of glycidyl methacrylate: Controlling electro-responsive properties. *Chem Eng J* 2016; 283:717-20.
- [82] Sedlacik M, Pavlinek V, Mrlik M, Moravkova Z, Hajna M, Trchova M, et al. Electrorheology of polyaniline, carbonized polyaniline, and their core-shell composites. *Mater Lett* 2013; 101:90-2.
- [83] Yin JB, Xia XA, Xiang LQ, Zhao XP. Conductivity and polarization of carbonaceous nanotubes derived from polyaniline nanotubes and their electrorheology when dispersed in silicone oil. *Carbon* 2010; 48(10):2958-67.
- [84] Yin JB, Xia XA, Xiang LQ, Zhao XP. Temperature effect of electrorheological fluids based on polyaniline derived carbonaceous nanotubes. *Smart Mater Struct* 2011; 20(1):015002.
- [85] Parthasarathy M, Klingenberg DJ. Electrorheology: Mechanisms and models. *Mater Sci Eng R-Rep* 1996; 17(2):57-103.
- [86] Davis LC. Polarization forces and conductivity effects in electrorheological fluids. *J Appl Phys* 1992; 72(4):1334-40.
- [87] Lengalova A, Pavlinek V, Saha P, Quadrat O, Stejskal J. The effect of dispersed particle size and shape on the electrorheological behaviour of suspensions. *Colloid Surf A-Physicochem Eng Asp* 2003; 227(1-3):1-8.
- [88] Xia XA, Yin JB, Qiang PF, Zhao XP. Electrorheological properties of thermo-oxidative polypyrrole nanofibers. *Polymer* 2011; 52(3):786-92.

- [89] Plachy T, Sedlacik M, Pavlinek V, Trchová M, Morávková Z, Stejskal J. Carbonization of aniline oligomers to electrically polarizable particles and their use in electrorheology. *Chem Eng J* 2014; 256:398-406.
- [90] Yin JB, Shui YJ, Chang RT, Zhao XP. Graphene-supported carbonaceous dielectric sheets and their electrorheology. *Carbon* 2012; 50(14):5247-55.
- [91] Yin JB, Wang XX, Chang RT, Zhao XP. Polyaniline decorated graphene sheet suspension with enhanced electrorheology. *Soft Matter* 2012; 8(2):294-7.
- [92] Cheng YC, Guo JJ, Liu XH, Sun AH, Xu GJ, Cui P. Preparation of uniform titania microspheres with good electrorheological performance and their size effect. *J Mater Chem* 2011; 21(13):5051-6.
- [93] Wen WJ, Huang XX, Yang SH, Lu KQ, Sheng P. The giant electrorheological effect in suspensions of nanoparticles. *Nat Mater* 2003; 2(11):727-30.
- [94] Belza T, Pavlinek V, Saha P, Quadrat O. Effect of field strength and temperature on viscoelastic properties of electrorheological suspensions of urea-modified silica particles. *Colloid Surf A-Physicochem Eng Asp* 2008; 316(1-3):89-94.
- [95] Jiang YP, Li XG, Wang SR, Xiao Y. Preparation of titanium dioxide nano-particles modified with poly (methyl methacrylate) and its electrorheological characteristics in Isopar L. *Colloid Polym Sci* 2015; 293(2):473-9.
- [96] Koyuncu K, Unal HI, Gumus OY, Erol O, Sari B, Ergin T. Electrokinetic and electrorheological properties of poly(vinyl chloride)/polyindole conducting composites. *Polym Adv Technol* 2012; 23(11):1464-72.
- [97] Liu Y, Liao FH, Li JR, Zhang SH, Chen SM, Wei CG, et al. The electrorheological properties of nano-sized SiO<sub>2</sub> particle materials doped with rare earths. *Scr Mater* 2006; 54(2):125-30.
- [98] Niu CG, Dong XF, Zhao H, Qi M. Properties of aniline-modified strontium titanate-based electrorheological suspension. *Smart Mater Struct* 2014; 23(7):8.
- [99] Yan RJ, Wu JH, Li C, Xu GJ, Zhou LW. Temperature effects of electrorheological fluids based on one-dimensional calcium and titanium precipitate. *Chin Phys Lett* 2013; 30(1):5.
- [100] Yilmaz H, Zengin H, Unal HI. Synthesis and electrorheological properties of polyaniline/silicon dioxide composites. *J Mater Sci* 2012; 47(13):5276-86.
- [101] Jiang JL, Tian Y, Meng YG. Structure parameter of electrorheological fluids in shear flow. *Langmuir* 2011; 27(10):5814-23.
- [102] Kim SG, Kim JW, Choi HJ, Suh MS, Shin MJ, Jhon MS. Synthesis and electrorheological characterization of emulsion-polymerized dodecylbenzenesulfonic acid doped polyaniline-based suspensions. *Colloid Polym Sci* 2000; 278(9):894-8.

- [103] Song ZY, Cheng YC, Wu JH, Guo JJ, Xu GJ. Influence of volume fraction on the yield behavior of giant electrorheological fluid. *Appl Phys Lett* 2012; 101(10):3.
- [104] Lengalova A, Pavlinek V, Saha P, Quadrat O, Kitano T, Stejskal J. Influence of particle concentration on the electrorheological efficiency of polyaniline suspensions. *Eur Polym J* 2003; 39(4):641-5.
- [105] Sedlacik M, Mrlik M, Pavlinek V, Saha P, Quadrat O. Electrorheological properties of suspensions of hollow globular titanium oxide/polypyrrole particles. *Colloid Polym Sci* 2012; 290(1):41-8.
- [106] Rozlivkova Z, Trchova M, Exnerova M, Stejskal J. The carbonization of granular polyaniline to produce nitrogen-containing carbon. *Synth Met* 2011; 161(11-12):1122-9.

## 5. LIST OF PAPERS

### Paper I

PLACHÝ, Tomáš; SEDLAČÍK, Michal; PAVLÍNEK, Vladimír; MORAVKOVA, Zuzana; HAJNA, Milena; STEJSKAL, Jaroslav. An effect of carbonization on the electrorheology of poly(p-phenylenediamine). *Carbon*, 2013, vol. 63, p. 187-195. ISSN 0008-6223. IF=6.196

### Paper II

PLACHÝ, Tomáš; SEDLAČÍK, Michal; PAVLÍNEK, Vladimír; TRCHOVÁ, Miroslava; MORÁVKOVÁ, Zuzana; STEJSKAL, Jaroslav. Carbonization of aniline oligomers to electrically polarizable particles and their use in electrorheology. *Chemical Engineering Journal*, 2014, vol. 256, p. 398-406. ISSN 1385-8947. IF=4.321

### Paper III

PLACHÝ, Tomáš; SEDLAČÍK, Michal; PAVLÍNEK, Vladimír; STEJSKAL, Jaroslav; GRAÇA, Manuel Pedro, COSTA, Luis Cadillon. Temperature-dependent electrorheological effect and its description with respect to dielectric spectra. *Journal of Intelligent Material Systems and Structures*. 2016, vol.27(7); p. 880-886. ISSN 1045-389X. IF=2.072

### Paper IV

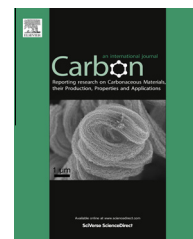
PLACHÝ, Tomáš; SEDLAČÍK, Michal; PAVLÍNEK, Vladimír; STEJSKAL, Jaroslav. The observation of a conductivity threshold on the electrorheological effect of p-phenylenediamine oxidized with p-benzoquinone. *Journal of Materials Chemistry C*. 2015, vol. 3(38); p. 9973-9980. ISSN 2050-7526. IF=4.696

# Paper I



Available at [www.sciencedirect.com](http://www.sciencedirect.com)

SciVerse ScienceDirect

journal homepage: [www.elsevier.com/locate/carbon](http://www.elsevier.com/locate/carbon)

# An effect of carbonization on the electrorheology of poly(*p*-phenylenediamine)

Tomas Plachy <sup>a,b</sup>, Michal Sedlacik <sup>a,c,\*</sup>, Vladimir Pavlinek <sup>a,b</sup>, Zuzana Morávková <sup>d</sup>, Milena Hajná <sup>d</sup>, Jaroslav Stejskal <sup>d</sup>

<sup>a</sup> Centre of Polymer Systems, University Institute, Tomas Bata University in Zlin, Nad Ovcirnou 3685, 760 01 Zlin, Czech Republic

<sup>b</sup> Polymer Centre, Faculty of Technology, Tomas Bata University in Zlin, T. G. Masaryk Sq. 275, 762 72 Zlin, Czech Republic

<sup>c</sup> Department of Production Engineering, Faculty of Technology, Tomas Bata University in Zlin, T. G. Masaryk Sq. 275, 762 72 Zlin, Czech Republic

<sup>d</sup> Institute of Macromolecular Chemistry, Academy of Sciences of the Czech Republic, Heyrovsky Sq. 2, 162 06 Prague 6, Czech Republic

## ARTICLE INFO

### Article history:

Received 29 March 2013

Accepted 19 June 2013

Available online 27 June 2013

## ABSTRACT

Particles of poly(*p*-phenylenediamine) were synthesized by the oxidation of *p*-phenylenediamine with ammonium peroxydisulfate at two oxidation levels. They were carbonized at 200–800 °C in inert atmosphere and subsequently tested in electrorheological (ER) suspensions. Scanning electron microscopy, Raman spectroscopy and thermogravimetric analysis were used to characterize an influence of the carbonization on the molecular structure and particles size and shape. Subsequently, ER suspensions were prepared by mixing polymer particles and silicone oil. In order to determine an effect of carbonization on the ER behaviour, a number of rheological measurements under various external electric fields were carried out. Dielectric spectroscopy was used for the evaluation of the influence of particles carbonization on the ER performance of suspensions as well. Although the particles carbonized at 600 °C exhibited nearly the same ER effect as the original particles due to significantly higher specific surface area, the efficiency of ER performance was the highest for original, i.e. non-carbonized particles. This is due to lower field-off viscosity in comparison to ER fluids based on carbonized particles.

© 2013 Elsevier Ltd. All rights reserved.

## 1. Introduction

Conducting polymers find their use in many applications. Not all of them, however, require high conductivity, and other electrical, optical, or redox properties typical for conducting polymers are exploited. Electrorheology belongs to the group of applications, where the electrical polarizability is a decisive property. An electrorheological (ER) effect is a phenomenon which causes abrupt changes of the viscosity of ER fluids upon the application of an electric field [1,2]. This reversible change from the liquid to a solid-like state appears in a very short time (within milliseconds) and is accompanied by a

distinct transition in rheological properties (viscosity, yield stress or viscoelastic moduli) [3–7]. This performance is highly desired by certain industrial fields, for example, in hydraulic and robotic applications [8]. ER fluids can be used in electrical clutches, torque transducers, dampers, etc. [9]. Nevertheless, there are still some shortcomings that hinder broader utilization of ER fluids in practice [10]. Many materials have been investigated for their ER performance as the dispersed phase with promising results. Unfortunately, they have not met all requirements on the ER fluids from the application point of view. Hao in his review [5] presents the most important properties that the proper ER fluid should have. Among these, a

\* Corresponding author: Fax: +42 57 603 1444.

E-mail address: [msedlacik@ft.utb.cz](mailto:msedlacik@ft.utb.cz) (M. Sedlacik).

0008-6223/\$ - see front matter © 2013 Elsevier Ltd. All rights reserved.

<http://dx.doi.org/10.1016/j.carbon.2013.06.070>

short response time of the system to the applied electric field, high yield stress, low conductivity, high ER efficiency, low field-off viscosity, and high stability belong [5,11].

Traditionally, an ER fluid is a two-phase system consisting of insulating carrier liquid and semi-conducting dispersed phase that can be either liquid or solid [5,12]. At the beginning of the research in the area, many ER systems containing water had been investigated. These suspensions were found unsuitable due to the content of water causing device corrosion. In addition, evaporation can negatively influence the liquid to solid-like state transition in time [13] and ER properties would be lost at elevated temperature. A substantial effort has recently been focused on investigation of polymeric materials for ER systems. Previous investigations have shown the possibility of utilization of conducting polymers as the dispersed phase. In particular, polyaniline (PANI), polypyrrole, poly(*p*-phenylene), poly(acene quinone) radicals, and their derivatives and composites are of concern [1,12,14–18]. These polymers display unique properties due to the conjugated system of  $\pi$ -bonds and presence of charge carriers that cause them to be electrically conducting. In other words, this structure enables charge transfer and, consequently, particle polarization in an electric field [5,13].

It is assumed that the interfacial polarization has a crucial effect on the ER phenomenon [5], thus dielectric and electric properties of particles are the dominant factors determining the intensity of ER effect [10]. The dispersed particles start to be polarized in electric field and their spatial distribution changes from random to highly organized. This transition leads to the creation of particle columns and chains oriented in the electric field direction. As a result, the system with oriented structure can withstand forces applied while the electric field is on [9,14].

Conducting polymers exposed to elevated temperature have recently been investigated as a new class of materials applicable in electrorheology [19–21]. They have been modified by heat treatment in air up to 300 °C [19,21,22]. This treatment reduces conductivity of these polymers, the property which often causes undesirable current drifts. The exposure to temperatures  $\approx$ 600 °C in inert atmosphere or in vacuum converts them to nitrogen-containing carbons [20,23,24]. The fact that the morphology is retained during carbonization belongs among interesting features of this process [23,25,26]. So far, attention has especially been paid to various PANI and polypyrrole morphologies [27]. For example, PANI [20,23,28–30] or polypyrrole [24] nanotubes/nanofibres were converted to analogous one-dimensional carbons. The ER response of carbonized conducting polymers, however, is still has to be investigated.

The above approach can be extended to other polymers, such as poly(*p*-phenylenediamine) (PpPDA). Trlica et al. [15] focused on the ER response of different isomers of polyphenylenediamine, i.e. a PANI derivate, particles in silicone oil. In this case, the best ER performance was achieved for the poly(*p*-phenylenediamine) isomer. Therefore, PpPDA particles were chosen as a reference material in the present study, which investigates the influence of various temperatures of PpPDA carbonization on its ER response. To evaluate the ER response rheological measurements comprising steady-state shear and oscillatory tests in the absence and in the presence

of electric field have been performed. Moreover, thermogravimetric analysis, Raman spectroscopy and scanning electron spectroscopy were used to follow changes in the structure of carbonized particles. Dielectric properties of the suspensions were also investigated as the interfacial polarization is assumed to be an important factor of the ER performance of ER suspensions.

## 2. Experimental

### 2.1. Synthesis of PpPDA

PpPDA was prepared by the oxidation of 0.2 M *p*-phenylenediamine (Fluka, Switzerland) with 0.25 M or 0.5 M ammonium peroxydisulfate (APS) (Lach:NER, Czech Republic) in 0.4 M hydrochloric acid at room temperature. Next day, the precipitated oxidation product was separated by filtration, rinsed with 0.4 M hydrochloric acid, then with acetone, and dried at room temperature. In the case of PANI, the conductivity of suspended particles is often too high for the use in ER suspensions due to drifting currents and they have to be at least partly deprotonated [31]. However, PpPDA prepared by Trlica et al. [15] had conductivity  $2.4 \times 10^{-10}$  S cm<sup>-1</sup> in the protonated state, which is sufficiently low for the use in ER suspensions. Therefore, the conductivity of prepared particles was not further controlled.

### 2.2. Carbonization

Thermogravimetric analysis was used at first as an analytical tool of PpPDA carbonization. This was performed in 50 cm<sup>3</sup> min<sup>-1</sup> nitrogen flow rate at a heating rate of 10 °C min<sup>-1</sup> with a TGA 7 Thermogravimetric Analyzer (Perkin Elmer, UK). A comparative experiment in air was also done for comparison.

At preparative scale, 5 g portions of the polymer were placed into an electric oven in nitrogen stream and the temperature was increased at 20 °C min<sup>-1</sup> to the target temperature. Then, the heating was switched off and the sample was left to cool down to room temperature still in nitrogen atmosphere.

### 2.3. Particles characterization

Measurement of specific surface area was carried out by nitrogen adsorption using a Gemini VII 2390 Analyzer (Micromeritics, Morcross, USA) and average particle size of samples was determined with dynamic light scattering in water (Zetasizer, Malvern Instruments, UK).

### 2.4. Raman spectroscopy

Raman spectra excited with a HeNe 633 nm laser were collected on an inVia Reflex Raman spectroscope (Renishaw, UK). A research-grade DM LM microscope (Leica, Germany) with an objective magnification $\times$ 50 was used to focus the laser beam on the sample placed on an X-Y motorized sample stage. The scattered light was analyzed by the spectrograph with holographic grating 1800 lines mm<sup>-1</sup> for HeNe laser. The dispersed light was registered by a Peltier-cooled CCD detector (576  $\times$  384 pixels).

## 2.5. Preparation of ER suspensions

The PpPDA particles were ground in a ball mill Lab Wizz 320 (Laarmann, The Netherlands), sieved on sieves with pores diameter of 45  $\mu\text{m}$ , and dried in a vacuum oven at 60  $^{\circ}\text{C}$  for 24 h. The suspensions of particles in silicone oil (Lukosiol M200, Chemical Works Kolín, Czech Republic, viscosity  $\eta_c = 200$  mPa s, conductivity  $\sigma_c \approx 10^{-11}$  S  $\text{cm}^{-1}$ ) were prepared in 6 vol% (10 wt%) concentration. Before each experiment, the suspension was stirred with a glass stick for ca 5 min and then sonicated for 1 min to insure homogeneous distribution of particles within a suspension.

## 2.6. Electrorheological measurements

The rheological measurements were carried out using a rotational rheometer Bohlin Gemini (Malvern Instruments, UK) with a plate-plate geometry (a diameter 40 mm with a gap of 0.5 mm between plates) at 2  $^{\circ}\text{C}$ . To determine the rheological parameters of ER fluids, steady-state shear tests were performed. Before each measurement step the suspensions were sheared for 60 s at a shear rate of 20  $\text{s}^{-1}$  to destroy residual internal structures.

In order to determine viscoelastic behaviour of suspensions, oscillatory tests were performed. Firstly, an amplitude (dynamic strain) sweep test was done to determine the linear viscoelastic region. Consequently, a frequency sweep test with fixed strain ( $\gamma = 0.0004$  obtained from amplitude sweep test) in this region within 0.1–1 Hz was carried out. External electric field strengths within 0.5–3 kV  $\text{mm}^{-1}$  were generated by a DC high-voltage source TREK 668B (TREK, USA). Prior to shearing the ER fluid in applied field, there was a 60 s delay to provide the particles time to build up the internal structures.

## 2.7. Dielectric measurements

An impedance analyzer Agilent 4524 (Agilent, Japan) was used for the investigation of dielectric properties. The data were collected in the frequency range 50–30  $\times 10^6$  Hz. The data were further fitted according to the Havriliak-Negami empirical model [32]:

$$\epsilon^* = \epsilon'_{\infty} + \frac{(\epsilon'_0 - \epsilon'_{\infty})}{(1 + (i\omega \cdot \tau_{rel})^a)^b} \quad (1)$$

where  $\epsilon^*$  stands for complex permittivity,  $\epsilon'_0$  and  $\epsilon'_{\infty}$  are static relative permittivity and theoretical relative permittivity at infinite frequency, respectively. Their difference expresses the dielectric relaxation strength,  $\Delta\epsilon'$ . Parameter  $\omega$  represents angular frequency,  $\tau_{rel}$  is the relaxation time, and  $a$  and  $b$  are shape parameters. Last two parameters enable to fit asymmetric relaxation peaks; the former one describing the width of the relaxation peak and the latter its asymmetry [32].

## 3. Results and discussion

### 3.1. Preparation of PpPDA

The oxidation of aniline in acidic aqueous media yields PANI. It may be proposed that a similar reaction performed with *p*-phenylenediamine would lead to a PANI-like structure

(Fig. 1a). The involvement of both amine groups could produce a “polyphenazine” ladder-like polymer, which can be regarded as being composed of two entwined PANI chains (Fig. 1b). The real situation is probably more complex and can involve the branching of chains at free amino groups, various oxidation states simulating the leucoemeraldine–emeraldine–pernigraniline transitions, possible involvement of oxygen-containing quinonoid groups, etc.

As the starting structure is not exactly known, it would be premature to speculate what happens after carbonization. For PANI, however, the production of cross-linked phenazine-containing structures has been proposed [23]. A similar structure of a nitrogen-containing carbon can probably be expected also in the present case.

### 3.2. Raman spectroscopy

To test the hypothesis concerning the molecular structure of PpPDA obtained with two oxidation levels, with 0.25 and 0.5 M APS, and to check if the carbonization was successful, the process was followed with Raman spectroscopy.

A Raman spectrum of PpPDA prepared with equimolar amount of oxidant (in Fig. 2 labeled as 1 $\times$ ) is similar to the spectrum of PpPDA observed by Sestrem et al. [33]. A shoulder at about 1647  $\text{cm}^{-1}$  belongs to the vibrations of phenazine- and oxazine-like structures [34,35]. The peak at 1597  $\text{cm}^{-1}$  is attributed to the ring-stretching vibrations, that at 1520  $\text{cm}^{-1}$  is connected with C=N stretching vibrations in quinoneimino or phenazine-like units [36–38]. The another one at 1455  $\text{cm}^{-1}$  with a shoulder at 1413  $\text{cm}^{-1}$  belongs to the skeletal vibrations and to the oxidized phenazine-like structure [37]. Two bands located at 1320 and 1178  $\text{cm}^{-1}$  were assigned to C–H bending on benzenoid or quinonoid ring vibrations, respectively [38]. These bands were observed for PpPDA but not for poly(*o*-phenylenediamine) [33]. The peak at 577  $\text{cm}^{-1}$  is attributed to the vibrations of phenazine-like linkages [39]. Finally, weak peaks at 498, 519, 457 and 411  $\text{cm}^{-1}$  are connected with skeletal deformations.

The spectrum of PpPDA prepared at doubled amount of oxidant (in Fig. 2 labelled as 2 $\times$ ) is not as clear as the previous spectrum and the bands are broader. The shoulder at 1647  $\text{cm}^{-1}$  is more pronounced, the shoulder at 1413  $\text{cm}^{-1}$  developed into a strong band. Small peaks below 500  $\text{cm}^{-1}$  are not observed. These changes may be connected with higher ratio of phenazine-like structures (Fig. 1b) and due to

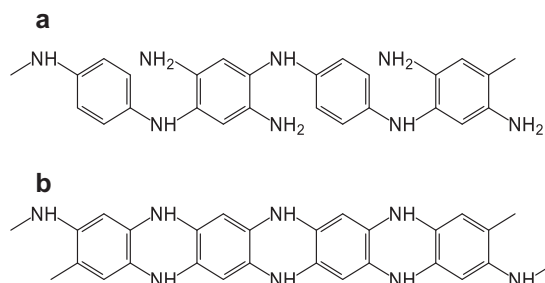


**Fig. 1** – Idealized structure of PpPDA produced by the oxidation of (a) one or (b) both amine groups in *p*-phenylenediamine.

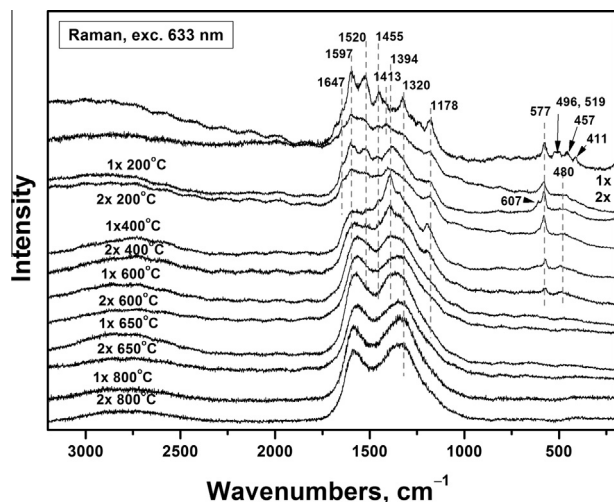


**Fig. 2** – Raman spectra of PpPDA prepared by oxidation of 0.2 M *p*-phenylenediamine with 0.25 (1x) or 0.5 M (2x) APS as prepared and after heating to various temperatures in nitrogen atmosphere.

the crosslinking. The bands connected with *para*-coupled chains are still present in the spectrum. The spectrum thus corresponds rather to a randomly linked and branched material than to a perfect ladder-like structure presented in Fig. 1b [40].

After heating to 200 °C (Fig. 2, 1x 200 °C and 2x 200 °C) a broad band at 1394  $\text{cm}^{-1}$  appears for both materials. This band is connected with short oligomers of aniline, the structures potentially containing phenazine-like and benzoquinone structures [41]. This band becomes even stronger after heating to 400 °C (Fig. 2, 1x 400 °C and 2x 400 °C). After heating to 600 °C or higher temperatures (Fig. 2, 1x or 2x, 600, 650, and 800 °C), two broad bands located around 1570 and 1330  $\text{cm}^{-1}$  are observed. These bands can be considered as G-band (“graphitic” band, stretching of any pair of  $\text{sp}^2$  carbons) and D-band (“disorder” band, breathing of hexagonal carbon rings activated by any defect included by a heteroatom), which are defined for graphitic material [42] and proved to be applicable for a nitrogen-containing analogue. The spectrum corresponds to the disordered nitrogen-containing graphitic material [19].

### 3.3. Particles analysis

PpPDA has an irregular morphology (Fig. 3a, b), the particle size being smaller when higher oxidant concentration had been used. Its features are preserved after carbonization at 600 °C (Fig. 3c, d).

Further, results showed that the specific surface area of the prepared particles increases with higher carbonization temperature (Table 1). Moreover, dynamic light scattering results showed that fraction of particles with size lower than 0.7 microns increases with higher carbonization temperature

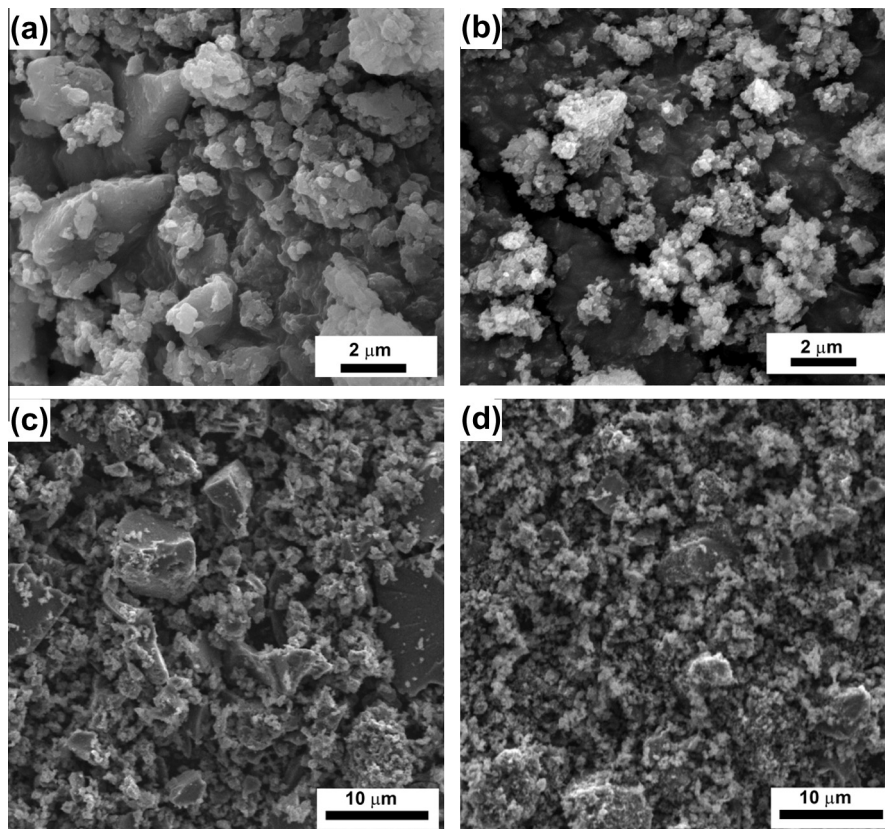


**Fig. 3** – Scanning electron micrographs of original samples prepared by oxidation of 0.2 M *p*-phenylenediamine with 0.25 (a) or 0.5 M (b) APS, and the same samples after carbonization at 600 °C in nitrogen atmosphere (c, d).

**Table 1 – PpPDA particles characterization.**

Carbonization temperature (°C)	Specific surface area (m <sup>2</sup> g <sup>-1</sup> )	Density (g cm <sup>-3</sup> )
Original	30.4	1.53
200	33.7	1.56
400	69.3	1.57
600	259	1.62

too. Therefore higher specific surface area of carbonized particles caused by structure decomposition under elevated temperatures together with reduced average particle size leads to higher field-off viscosity of their suspensions. The carbonization process also slightly increases density of prepared particles, which was determined by a pycnometer (Table 1).

### 3.4. Analytical carbonization: thermogravimetric analysis

The carbonization of PpPDA can be understood on the basis of thermogravimetric analysis, which is its analytical equivalent. As can be seen in Fig. 4, the PpPDA prepared at lower ox-

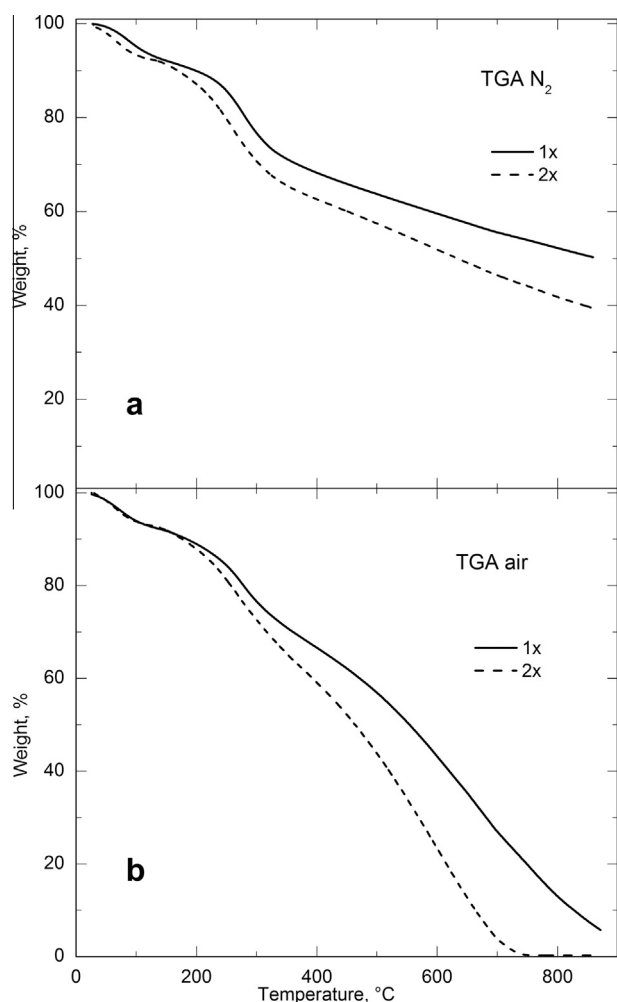


**Fig. 4 – Thermogravimetric analysis of PpPDA, prepared by oxidation of 0.2 M *p*-phenylenediamine with 0.25 (1×) or 0.5 M (2×) APS, in (a) nitrogen atmosphere and (b) in air.**

idant-to-monomer mole ratio is more stable both in nitrogen atmosphere (Fig. 4a) and in air (Fig. 4b). Carbonization in nitrogen leaves 40–50 wt% residue at exposure to 800 °C (Fig. 4a), while in air the samples are practically completely decomposed (Fig. 4b). However, it can be found that the modification at temperatures below 300 °C, used sometimes in the literature [19,21,22], leaves a sufficiently large residue similar for both environments.

### 3.5. Electrorheology

After carbonization of PpPDA at various temperatures, suspensions for ER measurements were prepared. However, particles carbonized at 650 and 800 °C were found not to be suitable for the use in ER suspensions because of their excessive conductivity that caused short circuits in the measuring device. Therefore, these materials are not discussed below. From synthesis of various types of PpPDA particles, those prepared with a double amount of APS showed more interesting ER responses in silicone oil suspensions and were analyzed in more detail.

For ER fluids a low field-off viscosity is one of key demands [11]. Therefore, this parameter was one of the important aspects in ER performance of the systems. Fig. 5 shows the dependence of the field-off viscosity,  $\eta_0$ , on the shear rate,  $\dot{\gamma}$ . The ER suspension of the original PpPDA particles, i.e. non-carbonized, exhibits the lowest field-off viscosity. With increasing carbonization temperature the field-off viscosity significantly rises. Especially at low shear rates the viscosity of investigated ER suspensions differs approximately by one order of magnitude. This can be explained as the consequence of higher specific surface area of the particles prepared at higher carbonization temperatures and their smaller size.

The generation of internal structures can be confirmed by the examination of flow properties of ER fluids in the presence of external electric field. Fig. 6a and Fig. 6b show

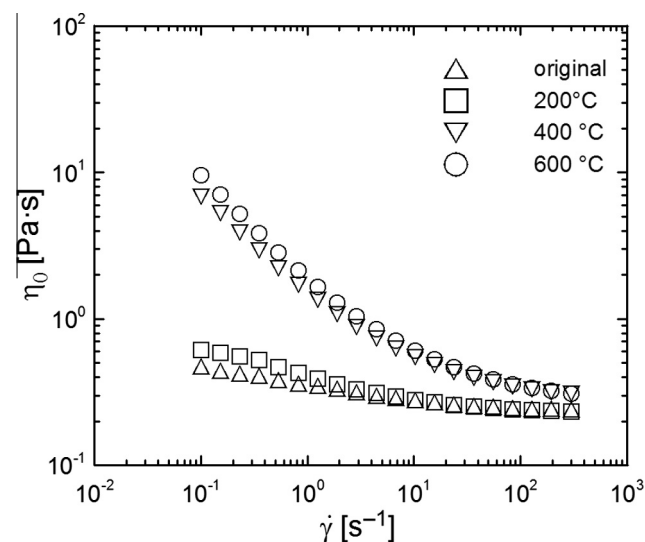


**Fig. 5 – Dependence of the field-off viscosity,  $\eta_0$ , on the shear rate,  $\dot{\gamma}$ , for 6 vol% ER fluids based on PpPDA particles carbonized under various temperatures in nitrogen atmosphere.**

rheological properties of ER fluids in the absence and in the presence of electric field of  $2 \text{ kV mm}^{-1}$ , respectively. A substantial increase in the shear stress reflecting the appearance of chain-like structures upon the application of electric field can be observed. This is caused by the formation of stiff internal structures within the system whose rupture occurs only above a yield stress,  $\tau_0$  [9].

The highest yield stress is observed for the ER suspension based on the original PpPDA particles. However, there is no substantial difference in the ER effect between these particles and those carbonized at 200 and 600 °C, while particles carbonized at 400 °C show the lowest response on the applied electric field. This can be partially explained as the consequence of conductivity of these particles. Rozlívková et al. [25] worked with carbonized granular PANI and their measurements revealed that electric conductivity increases for particles carbonized at 600 °C. These particles had the conductivity  $1.2 \times 10^{-8} \text{ S cm}^{-1}$ , while original PANI base conductivity was  $1.7 \times 10^{-10} \text{ S cm}^{-1}$ . Further, the particles exposed to 200 or 400 °C had a similar conductivity as the original PANI base or even lower by one order of magnitude, respectively. Thus, the low conductivity of particles carbonized at 400 °C could partially clarify the low ER effect. This can elucidate the ER performance of investigated particles in electric field, since PpPDA is a derivate of PANI, and thus similar behaviour can be expected. However, too high conductivity of particles can lead to shortcuts of the device in practical applications, as already mentioned.

The ER efficiency,  $e$ , is another important factor in ER systems as it evaluates the behaviour change of the system in the absence and in the presence of external electric field. It can be calculated according to Eq. (2) [8,43]:

$$e = \frac{(\eta_E - \eta_0)}{\eta_0} \quad (2)$$

where  $\eta_E$  is viscosity in the presence of the electric field and  $\eta_0$  is field-off viscosity. Fig. 7 shows the dependence of ER efficiency,  $e$ , on shear rate,  $\dot{\gamma}$ . As can be seen, the highest ER efficiency was achieved for suspensions based on original PpPDA particles. However, the suspension based on particles carbonized at 200 °C exhibited only slightly lower ER efficiency. A substantially lower ER response can be observed

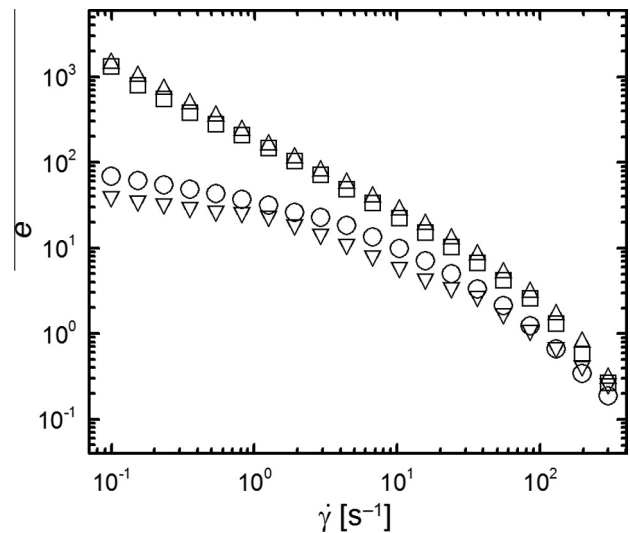


**Fig. 7 – Dependence of ER efficiency,  $e$ , (calculated from viscosity at 0 and  $2 \text{ kV mm}^{-1}$ ) for ER fluids based on PpPDA particles (carbonized under different temperatures in nitrogen atmosphere) on shear rate,  $\dot{\gamma}$ . The meaning of symbols is the same as in Fig. 5.**

for suspensions based on particles carbonized at 400 and 600 °C, which is caused by the low ER effect and the high field-off viscosity. At high shear rates, the differences in various ER fluids are reduced due to the dominance of hydrodynamic forces.

Even better description of these smart systems, in connection to applications, can be obtained from oscillatory tests represented by dynamic loadings. These tests give a picture of viscoelastic behaviour of the materials. Fig. 8 shows the dependence of storage and viscous moduli on angular frequency in the absence (a) and in the presence (b) of external electric field. It is evident that the loss (viscous) modulus,  $G''$ , dominates over the storage (elastic) modulus,  $G'$ , reflecting the viscous behaviour of the suspensions based on original particles and those carbonized at 200 °C. On the other hand, the behaviour of suspensions composed of particles carbonized at 400 and 600 °C is influenced by the specific sur-

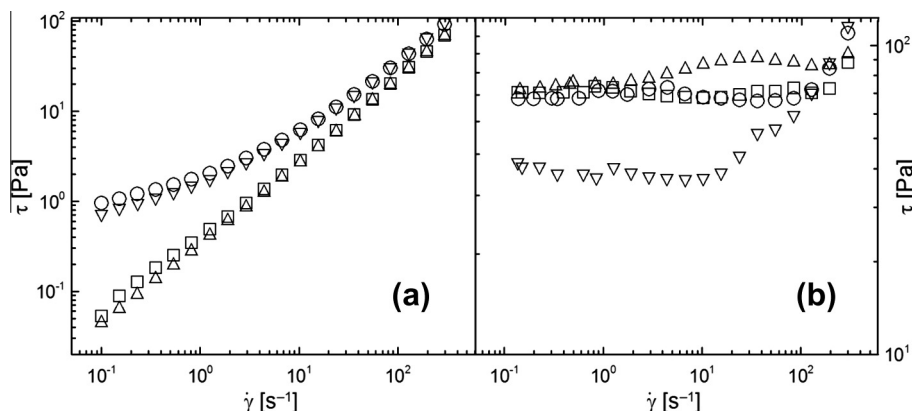


**Fig. 6 – The double-logarithmic plot of shear stress,  $\tau$ , in the absence (a) and in the presence of electric field strength of  $2 \text{ kV mm}^{-1}$  (b) on shear rate,  $\dot{\gamma}$ . The meaning of symbols is the same as in Fig. 5.**

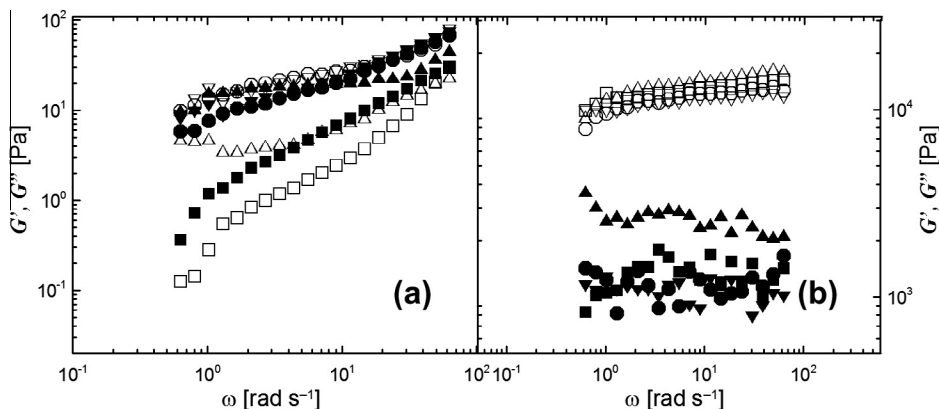


**Fig. 8** – Dependence of storage modulus (open symbols),  $G'$ , and viscous modulus (solid symbols),  $G''$ , on angular frequency,  $\omega$ , in the absence (a) and in the presence of electric field strength of  $2 \text{ kV mm}^{-1}$  (b). The meaning of symbols is the same as in Fig. 5.

**Table 2** – Dielectric parameters obtained from Havriliak-Negami model.

Parameter	Carbonization temperature [°C]			
	Original	200	400	600
$\varepsilon'_0$	4.06	4.07	4.35	4.63
$\varepsilon'_\infty$	3.10	3.05	3.00	2.03
$\Delta\varepsilon'$	0.96	1.02	1.35	1.60
$\tau_{\text{rel}}$ [s]	$2.68 \times 10^{-6}$	$8.54 \times 10^{-5}$	$4.02 \times 10^{-3}$	$5.50 \times 10^{-6}$
$a$	0.98	0.53	0.66	0.99
$b$	0.59	0.62	0.68	0.62

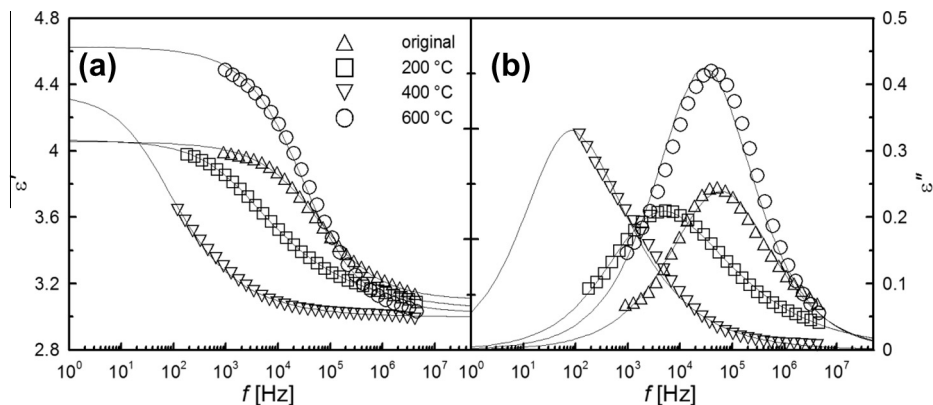


**Fig. 9** – Dielectric spectra of relative permittivity (a) and dielectric loss factor (b) for ER fluids based on original particles, and particles carbonized at 200, 400 and 600 °C.

face area and the small average particle size, i.e.  $G'$  is prevailing over  $G''$  already in the absence of electric field (Fig. 8a). However, after the application of the electric field (Fig. 8b)  $G'$  increases more significantly than  $G''$  and its dominance is apparent for all suspensions. This is connected with transition from the liquid to solid-like state caused by the formation of organized structure within the ER fluid. It can be seen that the highest storage modulus was achieved for original PpPDA particles.

### 3.6. Dielectric properties

It is assumed that interfacial polarization of particles plays a dominant role in the ER performance. It was proposed [5] that a good ER fluid should have its dielectric relaxation time between  $10^2$  and  $10^5$  Hz and the dielectric relaxation strength should be large. Thus, dielectric properties were analysed and Eq. (1) was applied for data evaluation. The obtained results are presented in Table 1.

Zhao et al. [44] demonstrated that highly mesoporous material with high specific surface area has positively influenced the dielectric relaxation strength of ER suspension based on this material, leading to the considerably high ER effect. In present study, the suspension based on particles carbonized at 600 °C (particles possess the highest specific surface area) exhibits the highest dielectric relaxation strength. Its ER effect, however, is comparable with the ER effect of suspensions based on original particles and particles carbonized at 200 °C. This indicates that the relaxation time, which is in this case similar for these three suspensions, has the significant importance on the ER performance of suspensions based on the PpPDA particles and its carbonized analogues (Table 2).

This can be seen also in Fig. 9, which shows the dependence of real,  $\epsilon'$ , and imaginary,  $\epsilon''$ , part of relative permittivity on the frequency,  $f$ . The relaxation time of the suspension based on the particles carbonized at 400 °C is  $4.02 \times 10^{-3}$  s, which means that it does not fulfil the above mentioned criterion for sufficient ER performance.

#### 4. Conclusion

Poly(*p*-phenylenediamine) particles were carbonized at different temperatures in inert nitrogen atmosphere. Carbonization was followed by thermogravimetric analysis, which showed the higher thermal stability of PpPDA particles prepared by a lower amount of oxidant. The conversion to the disordered nitrogen-containing carbon with increasing carbonization temperature was observed. Particles were subsequently used for the preparation of ER fluids which exhibit a distinct ER performance. With increasing electric field strength the ER response was higher. The highest ER efficiency was observed for original, i.e. non-carbonized sample. The ER efficiency decreased as the carbonization temperature increased, i.e. carbonization of PpPDA particles had a negative effect on ER behaviour in this case.

#### Acknowledgments

The authors wish to thank the Czech Grant Agency (202/09/1626) for the financial support. This research was also carried out with support of the Operational Programme Research and Development for Innovations co-funded by the European Regional Development Fund (ERDF) and national budget of the Czech Republic, within the framework of the Centre of Polymer Systems project (CZ.1.05/2.1.00/03.0111).

#### REFERENCES

- [1] Quadrat O, Stejskal J. Polyaniline in electrorheology. *J Ind Eng Chem* 2006;12:352–61.
- [2] Yin JB, Zhao XP. Electrorheology of nanofiber suspensions. *Nanoscale Res Lett* 2011;6:1–17.
- [3] Plocharski J, Drabik H, Wyciślik H, Ciach T. Electrorheological properties of polyphenylene suspensions. *Synth Met* 1997;88:139–45.
- [4] Sung JH, Cho MS, Choi HJ, Jhon MS. Electrorheology of semiconducting polymers. *J Ind Eng Chem* 2004;10:1217–29.
- [5] Hao T. Electrorheological suspensions. *Adv Colloid Interface Sci* 2002;97:1–35.
- [6] Davis LC. Time-dependent and nonlinear effects in electrorheological fluids. *J Appl Phys* 1997;81:1985–91.
- [7] Mrlik M, Sedlacik M, Pavlinek V, Bober P, Trchová M, Stejskal J et al. Electrorheology of aniline oligomers. *Colloid Polym Sci*. doi: <http://dx.doi.org/10.1007/s00396-013-2947-4>.
- [8] Trlica J, Saha P, Quadrat O, Stejskal J. Electrical and electrorheological behavior of poly(aniline-co-1,4-phenylenediamine) suspensions. *Eur Polym J* 2000;36:2313–9.
- [9] Pavlinek V, Saha P, Kitano T, Stejskal J, Quadrat O. The effect of polyaniline layer deposited on silica particles on electrorheological and dielectric properties of their silicone-oil suspensions. *Physica A* 2005;353:21–8.
- [10] Sedlacik M, Mrlik M, Pavlinek V, Saha P. Electrorheological properties of suspensions of hollow globular titanium oxide/pyrrole particles. *Colloid Polym Sci* 2012;290:41–8.
- [11] Yin J, Shui Y, Chang R, Zhao X. Graphene-supported carbonaceous dielectric sheets and their electrorheology. *Carbon* 2012;50:5247–55.
- [12] Kim DH, Kim YD. Electrorheological properties of polypyrrole and its composite ER fluids. *J Ind Eng Chem* 2007;13:879–94.
- [13] Choi HJ, Jhon MS. Electrorheology of polymers and nanocomposites. *Soft Matter* 2009;5:1562–7.
- [14] Sim IS, Kim JW, Choi HJ, Kim ChA, Jhon MS. Preparation and electrorheological characteristics of poly(*p*-phenylene)-based suspensions. *Chem Mater* 2001;13:1243–7.
- [15] Trlica J, Saha P, Quadrat O, Stejskal J. Electrorheological activity of polyphenylenediamine suspensions in silicone oil. *Physica A* 2000;283:337–48.
- [16] Choi HJ, Cho MS, To K. Electrorheological and dielectric characteristics of semiconductive polyaniline-silicone oil suspensions. *Physica A* 1998;254:272–9.
- [17] Choi HJ, Cho MS, Jhon MS. Electrorheological properties of poly(acene quinone) radical suspensions. *Polym Adv Tech* 1997;8:697–700.
- [18] Fang FF, Liu YD, Lee IS, Choi HJ. Well controlled core/shell type polymeric microspheres coated with conducting polyaniline: fabrication and electrorheology. *RSC Adv* 2011;1:1026–32.
- [19] Xia X, Yin JB, Qiang PF, Zhao XP. Electrorheological properties of thermo-oxidative polypyrrole nanofibers. *Polymer* 2011;52:786–92.
- [20] Yin JB, Xia X, Xiang LQ, Zhao XP. Temperature effect of electrorheological fluids based on polyaniline derived carbonaceous nanotubes. *Smart Mater Struct* 2011;20:015002 (1–8).
- [21] Yin JB, Xia X, Zhao XP. Conductivity, polarization and electrorheological activity of polyaniline nanotubes during thermo-oxidative treatment. *Polym Degrad Stab* 2012;97:2356–63.
- [22] Chen YZ, Wang BP, Dong SJ, Wang YP, Liu YN. Rectangular microscale carbon tubes with protuberant wall for high-rate electrochemical capacitors. *Electrochim Acta* 2012;80:34–40.
- [23] Trchová M, Konyushenko EN, Stejskal J, Kovářová J, Čirić-Marjanović G. The conversion of polyaniline nanotubes to nitrogen-containing carbon nanotubes and their comparison with multi-walled carbon nanotubes. *Polym Degrad Stab* 2009;94:929–38.
- [24] Bae JW, Jang JS. Fabrication of carbon nanotubes from conducting polymer precursor as field emitter. *J Ind Eng Chem* 2012;18:1921–4.
- [25] Rozlívková Z, Trchová M, Exnerová M, Stejskal J. The carbonization of granular polyaniline to produce nitrogen-containing carbon. *Synth Met* 2011;161:1122–9.



- [26] Yin J, Xia X, Xiang L, Zhao X. Conductivity and polarization of carbonaceous nanotubes derived from polyaniline nanotubes and their electrorheology when dispersed in silicone oil. *Carbon* 2010;48:2958–67.
- [27] Ćirić-Marjanović G, Pašti I, Gavrilov N, Janošević, Mentus S. Carbonised polyaniline and polypyrrole towards advanced nitrogen-containing carbon materials. *Chem Pap* 2013;67:781–813.
- [28] Gavrilov N, Pašti IA, Mitrić M, Travas-Sejdić J, Ćirić-Marjanović G, Mentus SV. Electrocatalysis of oxygen reduction reaction on polyaniline-derived nitrogen-doped carbon nanoparticle surfaces in alkaline media. *J Power Sources* 2012;220:306–16.
- [29] Yuan DS, Zhou TX, Zhou SL, Zou WJ, Mo SS, Xia NN. Nitrogen-enriched carbon nanowires from the direct carbonization of polyaniline nanowires and its electrochemical properties. *Electrochem Commun* 2011;13:242–6.
- [30] Yuan DS, Yuan XL, Zhou SL, Zou WJ, Zhou TX. N-Doped carbon nanorods as ultrasensitive electrochemical sensors for the determination of dopamine. *RSC Adv* 2012;2:8157–63.
- [31] Choi HJ, Kim TW, Cho MS, Kim SG, Jhon MS. Electrorheological characterization of polyaniline dispersions. *Eur Polym J* 1997;33:699–703.
- [32] Havriliak S, Negami S. A complex plane analysis of  $\alpha$ -dispersions in some polymer systems. *J Polym Sci* 1966;14:99–117.
- [33] Sestrem RH, Ferreira DC, Landers R, Temperini MLA, Do Nascimento GM. Structure of chemically prepared poly-(para)phenylenediamine investigated by spectroscopic techniques. *Polymer* 2009;50:6043–8.
- [34] Brolo AG, Sanderson AC. Surface-enhanced Raman scattering (SERS) from a silver electrode modified with oxazine 720. *Can J Chem* 2004;82:1474–80.
- [35] Do Nascimento GM, Silva CHB, Temperini MLA. Spectroscopic characterization of the structural changes of polyaniline nanofibers after heating. *Polym Degrad Stab* 2008;93:291–7.
- [36] Quillard S, Louarn G, Lefrant S, MacDiarmid AG. Vibrational analysis of polyaniline – a comparative study of leucoemeraldine, emeraldine, and pernigraniline bases. *Phys Rev B* 1994;50:12496–508.
- [37] Malinauskas A, Bron M, Holze R. Electrochemical and Raman spectroscopic studies of electrosynthesized copolymers and bilayer structures of polyaniline and poly(o-phenylenediamine). *Synth Met* 1998;92:127–37.
- [38] Boyer MI, Quillard S, Rebourt E, Louarn G, Buisson JP, Monkman A, et al. Vibrational analysis of polyaniline: a model compound approach. *J Phys Chem B* 1998;102:7382–92.
- [39] Do Nascimento GM, Silva CHB, Temperini MLA. Electronic structure and doping behaviour of PANI-NSA nanofibers investigated by resonance Raman spectroscopy. *Macromol Rapid Commun* 2006;27:255–9.
- [40] Baibarac M, Baltog I, Scocioreanu M, Ballesteros B, Mevellec JY, Lefrant S. One-dimensional composites based on single walled carbon nanotubes and poly(o-phenylenediamine). *Synth Met* 2011;161:2344–54.
- [41] Surwade SP, Dua V, Manohar N, Manohar SK, Beck E, Ferraris JP. Oligoaniline intermediates in the aniline–peroxydisulfate system. *Synth Met* 2009;159:445–55.
- [42] Dresselhaus MS, Jorio A, Hofman M, Dresselhaus G, Saito R. Perspectives on carbon nanotubes and graphene Raman spectroscopy. *Nano Lett* 2010;10:751–8.
- [43] Yin JB, Zhao XP. Preparation and enhanced electrorheological activity of TiO<sub>2</sub> doped with chromium ion. *Chem Mater* 2004;16:321–8.
- [44] Qiao Y, Zhao X. Electrorheological effect of carbonaceous materials with hierarchical porous structures. *Colloid Surface A* 2009;340:33–9.

## **Paper II**



# Carbonization of aniline oligomers to electrically polarizable particles and their use in electrorheology

T. Plachy<sup>a,b</sup>, M. Sedlacik<sup>a,\*</sup>, V. Pavlinek<sup>a</sup>, M. Trchová<sup>c</sup>, Z. Morávková<sup>c</sup>, J. Stejskal<sup>c</sup>

<sup>a</sup>Centre of Polymer Systems, University Institute, Tomas Bata University in Zlin, Nad Ovcírnou 3685, 760 01 Zlin, Czech Republic

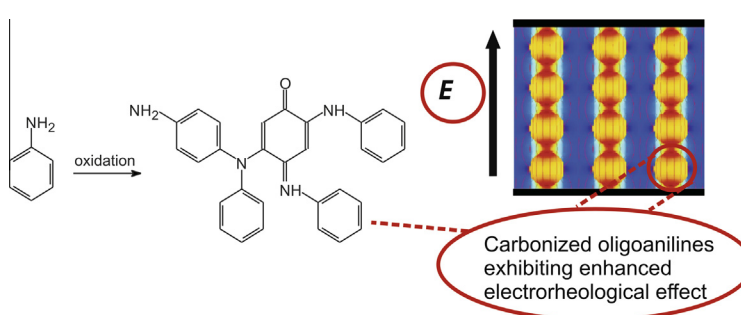
<sup>b</sup>Polymer Centre, Faculty of Technology, Tomas Bata University in Zlin, T. G. Masaryk Sq. 275, 762 72 Zlin, Czech Republic

<sup>c</sup>Institute of Macromolecular Chemistry, Academy of Sciences of the Czech Republic, Heyrovsky Sq. 2, 162 06 Prague 6, Czech Republic

## HIGHLIGHTS

- Aniline oligomers were prepared via the oxidation of aniline under alkaline conditions at various concentrations of ammonia.
- Carbonization process leads to the transition of particles' morphology from microspheres to two-dimensional plates.
- The electrorheological performance of suspensions increased with the carbonization of aniline oligomers particles.

## GRAPHICAL ABSTRACT



## ARTICLE INFO

### Article history:

Received 19 May 2014

Received in revised form 30 June 2014

Accepted 2 July 2014

Available online 14 July 2014

### Keywords:

Aniline  
Aniline oligomers  
Carbonization  
Electrorheology  
Dielectric spectroscopy  
Vibration spectroscopy

## ABSTRACT

Aniline oligomers prepared via the oxidation of aniline under alkaline conditions at various concentrations of ammonia were carbonized at 650 °C in inert atmosphere. Subsequently, the prepared particles were mixed with silicone oil and the suspensions were used as electrorheological fluids. After the carbonization, when the higher amount of ammonia was present during the synthesis, the transition of morphology of the particles from microspheres to two-dimensional plates was observed. This transition led to a significant increase of viscosity of silicone-oil suspensions in the presence of external electric field, while their field-off viscosity remained nearly unchanged. Thus, the carbonization had the desired effect on the treated particles leading to extremely high electrorheological efficiency of the suspensions based on such particles. The highest electrorheological efficiency was achieved for the suspension based on carbonized particles prepared in 0.2 M ammonia. The dielectric spectroscopy was used as an evaluative tool of electrorheological performance of suspensions, and data correspond well with the obtained results from electrorheological experiments.

© 2014 Elsevier B.V. All rights reserved.

## 1. Introduction

Electrorheological (ER) fluids are known as liquids altering their rheological parameters by application of an external electric field. Mostly, ER fluids are suspensions consisting of solid electrically polarizable particles dispersed in insulating liquid. In the absence

\* Corresponding author. Tel./fax: +42 57 603 1444.  
E-mail address: [msedlacik@ft.utb.cz](mailto:msedlacik@ft.utb.cz) (M. Sedlacik).

of an external electric field, particles are randomly distributed within the suspension. However, when an electric field is applied, particles start to create highly organized structures due to the interaction of induced dipoles. This formation of chains and column-like structures spanning the gap between electrodes is accompanied by an abrupt increase in viscoelastic moduli and viscosity, and suspensions start to act as Bingham fluids because electrostatic forces start to dominate over hydrodynamic ones. These changes are completely reversible and fast (within milliseconds).

In the presence of an external electric field, particles are oriented along the electric field direction thanks to dipole–dipole interaction. This phenomenon is called the ER effect. It is assumed that interfacial polarization and conductivity of the particles are dominant factors on the ER performance of ER suspensions [1]. Thanks to their unique properties, ER suspensions have been proposed for many applications, mainly in hydraulics and robotics, e.g., as dampers, clutches, torque transducers, in haptic masters for minimally invasive surgery systems [2] or haptic displays [3]. Both inorganic [4] and organic [5] materials have been used as a dispersed phase in ER suspensions. Also the composites consisting of combination of inorganic and organic materials were introduced [6,7]. The group of organic materials is particularly represented by conducting polymers. Among them polyaniline (PANI) [8,9] and polypyrrole [10] are of special interest. Polyaniline, as a material for electrorheology, has been reported in many scientific papers due to its easy and inexpensive synthesis [5,8,11–18]. Moreover, aniline-like oligomers with tuneable conductivities prepared by different reaction conditions or reaction substances have been introduced [19–21].

Conducting polymers, such as PANI, are unique among polymers in their ability to produce a variety of nanostructures [22,23]. Conducting PANI is produced by the oxidation of aniline with ammonium peroxydisulfate under acidic conditions. When oxidation of aniline is started under alkaline conditions, non-conducting aniline oligomers are produced as microspheres of several micrometres in diameter [24]. Their molecular structure is open to discussion but it is assumed that they are represented by condensed aniline molecules including oxygen atoms resulting from hydrolytic processes (Fig. 1). These are the objects of present study.

In recent studies, conducting polymers have been exposed to elevated temperature in inert atmosphere in order to obtain carbonaceous nitrogen-enriched structures [25–30]. In some cases, this treatment has positively influenced the ER performance of suspensions based on these materials.

Morávková et al. [31] have prepared carbonized aniline oligomers obtained by the oxidation of aniline under alkaline conditions. After the carbonization, the transition of morphology from microspheres into two-dimensional plates was observed. This phenomenon has been explained as a consequence of a transition, when the liquid content of the microspheres is rejected outside the microspheres above 200 °C and self-assembles into plates. In electrorheology, closely related aniline-like oligomers have been studied by Mrlik et al. [20]; however, there is no mention about their carbonized analogues.

Yin et al. [32] have introduced an ER suspension based on graphene-supported carbonaceous sheets, which has shown significantly higher increase in viscosity in the presence of the external electric field in comparison with carbonized PANI particles, which possess globular shape. However, there is a lack of studies which would describe ER behavior of two-dimensional carbonaceous enriched plates. Therefore, this study deals with aniline oligomers prepared under alkaline conditions and their subsequent

carbonization at 650 °C, which lead in some cases to creation of two-dimensional plates.

## 2. Experimental

### 2.1. Synthesis of aniline oligomers

Aniline (0.2 M; Sigma Aldrich) was oxidized with ammonium peroxydisulfate (0.2 M; Lach:NER, Czech Republic) in the aqueous solutions of 0.1, 0.2, 0.5, 1 and 2 M ammonium hydroxide (NH<sub>4</sub>OH; Lach:NER, Czech Republic) or in water at room temperature. Solutions of the monomer and the oxidant in water were mixed at room temperature to start the oxidation. So-prepared particles are labelled as 0.1, 0.2, 0.5, 1, or 2 M regarding the amount NH<sub>4</sub>OH presented during their synthesis. After the end of polymerization, the solids were collected on a filter after 2 h, rinsed with water, dried in air and then over the silica gel in a desiccator. A part of products deposited on silicon windows or in solid state was converted to bases by overnight immersion in 1 M NH<sub>4</sub>OH, followed by separation and drying.

### 2.2. Carbonization

The carbonization of PANI base exposed up to 800 °C in air and in nitrogen atmosphere has been studied [33,34]. According to the Raman spectra it was found that G and D bands characteristic for carbon-like structure (representing the graphitic and disordered modes of carbon) are well developed after PANI exposition at 650 °C in inert atmosphere. Therefore, the second set of the samples was prepared by an exposure of the particles to the temperature 650 °C in nitrogen. When the temperature was reached, the oven was switched off and the particles were left to cool to room temperature. These samples are further labelled as carbonized particles prepared in 0.1 M, 0.2 M, 0.5 M, 1 M or 2 M NH<sub>4</sub>OH solution.

### 2.3. Characterization

The course of oxidation was monitored by acidity changes recorded with a pH-meter. The morphology and dimensions of the particles were investigated using scanning electron microscopy (SEM; VEGA II LMU, Tescan, Czech Republic). UV–Vis spectra of the oxidation products dissolved in *N*-methylpyrrolidone (Sigma Aldrich) were collected with a Lambda 20 spectrometer (Perkin Elmer, UK). Infrared spectra in the range of 400–4000 cm<sup>-1</sup> were recorded at 64 scans per spectrum at 2 cm<sup>-1</sup> resolution using a Thermo Nicolet NEXUS 870 FTIR Spectrometer with a DTGS TEC detector. Samples were dispersed in potassium bromide and compressed into pellets. Raman spectra excited in the visible range with a HeNe 633 nm laser were collected on a Renishaw inVia Reflex Raman microspectrometer. The scattered light was analyzed by the spectrograph with a holographic grating (1800 lines mm<sup>-1</sup>). A Peltier-cooled CCD detector (578 × 385 pixels) registered the dispersed light. The conductivity of the original samples was measured by van der Pauw method using Electrometer Keithley 6517B (USA). The particles were pressed into the pellets of 13 mm diameter at pressure 15 MPa. Carbonized samples could not be pressed into pellets, thus their conductivity was not determined.

### 2.4. Preparation of suspensions

Experiments were performed with a fraction of samples grounded using a ball mill Lab Wizz 320 (Laarmann, The Netherlands), and sieved on a sieve with mesh diameter of 45 μm. Powders were mixed with silicone oil (Lukosiol M200, Chemical Works Kolin, Czech Republic, viscosity  $\eta_c = 194$  mPa s,

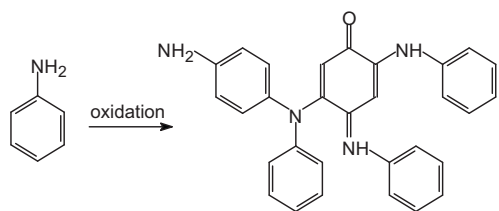


Fig. 1. A possible structure of aniline oligomers.

conductivity  $\sigma_c \approx 10^{-11} \text{ S cm}^{-1}$ ) in a ratio 1:9 (w/w). Before each experiment, the suspension was manually stirred for ca 5 min and then sonicated with a UZ Sonoplus HD 2070 kit (BANDELIN Electronic, Germany) for 1 min to assure homogeneous distribution of particles within the suspension.

### 2.5. Electrorheological experiments

Rheological behavior of prepared suspensions in the absence and in the presence of electric field was investigated using a rotational rheometer Bohlin Gemini (Malvern Instruments, UK) with parallel plate geometry (a diameter 40 mm with a gap of 0.5 mm between plates) at 25 °C. Electric fields of strength within 0.5–3 kV mm<sup>-1</sup> were generated by a DC high-voltage source TREK 668B (TREK, USA). The rheological measurements have been carried out in steady shear and oscillatory shear modes. Steady shear tests were performed at shear rate range 0.1–300 s<sup>-1</sup>. In the case of oscillatory tests, firstly, an amplitude (dynamic strain) sweep test was performed to determine the linear viscoelastic region (LVR). Subsequently, frequency sweep tests with fixed strain from LVR within 0.1–1 Hz were carried out. Before each measurement, the suspensions were sheared for 60 s at a shear rate of 20 s<sup>-1</sup> to destroy any residual internal structures. Prior to shearing the ER fluid in applied field, there was a 60 s delay to provide the time to build up the internal structures.

### 2.6. Dielectric measurements

An impedance analyzer Agilent 4524 (Agilent, Japan) together with a liquid test fixture Agilent 16452A were used for the investigation of dielectric properties. The data was collected in the frequency range 50–30 × 10<sup>6</sup> Hz and fitted with Havriliak–Negami empirical model [35]:

$$\varepsilon^* = \varepsilon'_\infty + \frac{(\varepsilon'_0 - \varepsilon'_\infty)}{(1 + (i\omega t_{\text{rel}})^a)^b} \quad (1)$$

where  $\varepsilon^*$  stands for complex permittivity. The difference of static relative permittivity,  $\varepsilon'_0$ , and theoretical relative permittivity at infinite frequency,  $\varepsilon'_\infty$ , is called dielectric relaxation strength,  $\Delta\varepsilon'$ . Parameter,  $\omega$ , represents angular frequency,  $t_{\text{rel}}$ , is the relaxation time, and,  $a$ , and,  $b$ , are shape-dependent parameters. The last two parameters enable to fit asymmetric relaxation peaks. The parameter,  $a$ , determines the width of the relaxation peak and the parameter,  $b$ , its asymmetry [35].

## 3. Results and discussion

### 3.1. Formation of oligoaniline microspheres in alkaline media

When the oxidation of aniline starts in an alkaline medium, the reaction is fast and exothermic and, consequently, the temperature increases during the reaction. Two hydrogen atoms are abstracted from each aniline molecule during their oxidative coupling, and they are released as protons; thus, the pH of the reaction mixture decreases (Fig. 2) [24].

The oxidation of 0.2 M aniline with 0.2 M ammonium peroxydisulfate gradually generates 0.2 M sulfuric acid. The acid is partly neutralized by aniline or reaction intermediates containing primary amino groups, and especially with NH<sub>4</sub>OH which is the strongest base in the system. At its 0.1 M concentration, NH<sub>4</sub>OH becomes completely neutralized, and the pH drops to acidic values (Fig. 2). The formation of polyaniline thus becomes possible in the advanced stages of oxidation. The 0.5 and 1 M NH<sub>4</sub>OH was sufficient to maintain the reaction alkaline throughout the oxidation.

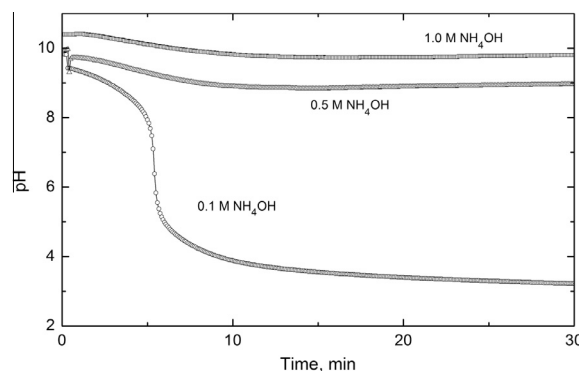


Fig. 2. pH profiles during the oxidation of 0.2 M aniline with 0.2 M ammonium peroxydisulfate in 0.1, 0.5, and 1.0 M NH<sub>4</sub>OH.

### 3.2. UV–visible spectra

UV–Vis spectra of aniline oligomers prepared in 0.5 and 1 M NH<sub>4</sub>OH display a local maximum at 348 nm and a characteristic long tail extending to longer wavelengths (Fig. 3). The absorption band of PANI (emeraldine) base having the maximum above 600 nm is absent in aniline oligomers. This result confirms that the products prepared at low NH<sub>4</sub>OH concentration, i.e. 0.1 and 0.2 M, contain a fraction of PANI in addition to aniline oligomers. The absorption maximum appears in the case of oxidation in 0.2 M NH<sub>4</sub>OH and in water, when the pH drops to acidic values and the formation of polyaniline (emeraldine) becomes possible (Fig. 3).

### 3.3. FTIR spectra

In the infrared spectra of samples prepared in 0.2, 0.5, and 1.0 M NH<sub>4</sub>OH (Fig. 4), the bands due to quinonoid and benzenoid ring-stretching vibrations are situated at 1581 and 1503 cm<sup>-1</sup>. A shoulder observed at about 1630 cm<sup>-1</sup> corresponds most probably to N–H scissoring vibrations of aromatic amines or to the presence of phenazine units. The contribution of benzoquinones is possible. The sharp band at 1445 cm<sup>-1</sup> is attributed to the skeletal C–C stretching vibration of the substituted aromatic ring [36]. The broad band in the 1300–1230 cm<sup>-1</sup> region indicates the presence of the C–N stretching vibration of a primary aromatic amine, which confirms the oligomeric nature of the oxidation products. The band at about 1035 cm<sup>-1</sup> is assigned to the symmetric stretching vibrations in sulfonic groups linked by covalent bonds to the benzene

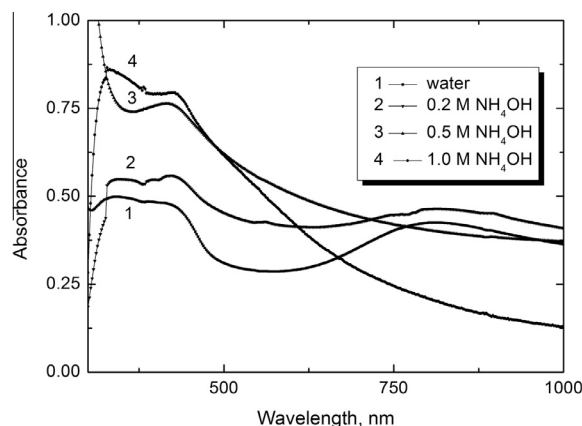
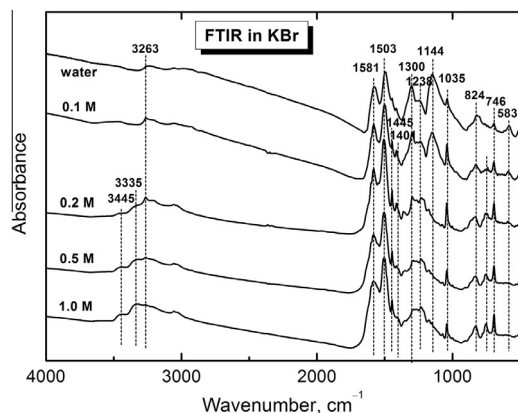


Fig. 3. UV–Vis spectra of the powders obtained by the oxidation of aniline in water and in 0.2, 0.5, and 1.0 M NH<sub>4</sub>OH, and dissolved in *N*-methylpyrrolidone.



**Fig. 4.** Infrared spectra of the powders obtained by the oxidation of 0.2 M aniline with 0.2 M ammonium peroxydisulfate in 0.1, 0.2, 0.5, and 1 M  $\text{NH}_4\text{OH}$  and in water.

ring. A prominent band at  $824\text{ cm}^{-1}$  in the substitution region  $900\text{--}650\text{ cm}^{-1}$  in the spectrum of the PANI base is due to the C–H out-of-plane bending vibrations of dominating *para*-coupled constitutional units. The bands at  $746$  and  $691\text{ cm}^{-1}$  correspond to the C–H out-of-plane bending and out-of-plane ring deformations of a mono-substituted phenylene ring, respectively [24,36]. The spectrum of the oligomers displays bands at  $3440$  and  $3324\text{ cm}^{-1}$  of asymmetric and symmetric free N–H stretching vibrations, supporting the contribution of the N–H scissoring vibration. The peaks at  $3266$  and  $3195\text{ cm}^{-1}$  corresponding to the hydrogen-bonded N–H vibrations are detected in the spectrum of aniline oligomers. They are connected with hydrogen bonding of N–H groups with sulfonic or carbonyl groups [24]. The infrared spectra of samples prepared in  $0.1\text{ M NH}_4\text{OH}$  and in water display a broad absorption band at wavenumbers higher than  $2000\text{ cm}^{-1}$ , an increased absorption of the bands at  $1300$  and  $1238\text{ cm}^{-1}$ , and a broad band centred at  $1144\text{ cm}^{-1}$ , which are characteristic of the conducting protonated form of polyaniline [36].

### 3.4. Morphology

Fig. 5 shows images of prepared particles obtained by the scanning electron microscopy. It can be seen that, regardless of the concentration of  $\text{NH}_4\text{OH}$  during the synthesis of aniline oligomers, the original particles are all spherical or rather irregular. Their dimensions slightly increase with the increasing concentration of  $\text{NH}_4\text{OH}$  present during the synthesis. After the carbonization at  $650^\circ\text{C}$ , the particles produced in the presence of the lowest amount of  $\text{NH}_4\text{OH}$  ( $0.1\text{ M}$ ) became slightly smaller and possessing much rougher surface than their original analogues (Fig. 5a and d). It may be connected with the presence of a thin PANI layer on its surface. However, increasing concentration of  $\text{NH}_4\text{OH}$  led to a considerable increase of dimensions of carbonized particles and creation of two-dimensional plates (Fig. 5d–f). It has been described by the group of Stejskal and coworkers [31] that probably those particles arose from larger plates which were sintered together and that broke down during the cooling from the melt to ambient temperature. Also on their surface higher aniline oligomers are produced during synthesis instead of PANI layer.

### 3.5. Spectroscopic evidence of carbonization

Raman spectroscopy is a useful tool in the structural characterization of graphitic materials [37]. The Raman spectra of the samples prepared in  $0.2\text{ M}$  and  $1.0\text{ M NH}_4\text{OH}$  obtained with  $633\text{ nm}$  excitation line exhibit a strong fluorescence on which

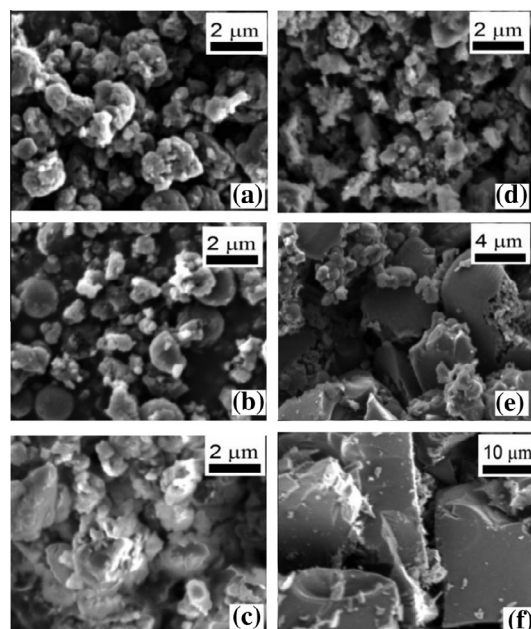


**Fig. 5.** SEM images of original samples prepared in (a)  $0.1\text{ M}$ , (b)  $0.2\text{ M}$ , and (c)  $2.0\text{ M NH}_4\text{OH}$  and (d–f) their carbonized analogues after treatment at  $650^\circ\text{C}$ .

one can distinguish the dominant peak of C=C stretching vibration in quinonoid units situated at about  $1600\text{ cm}^{-1}$  with a shoulder at about  $1626\text{ cm}^{-1}$ , and the peaks at  $1543$ ,  $1368$ ,  $1340$ ,  $1150$  and  $616\text{ cm}^{-1}$  in the spectrum of sample prepared in  $0.2\text{ M NH}_4\text{OH}$  (Fig. 6a). They are slightly shifted to  $1529$ ,  $1350$ ,  $1155$ , and  $614\text{ cm}^{-1}$  in the spectrum of the sample prepared in  $1.0\text{ M NH}_4\text{OH}$  (Fig. 6b) with respect to former sample, which contains a thin overlayer of PANI on particle surface. The spectra have recently been interpreted in [31,38].

After heating to  $650^\circ\text{C}$  in inert atmosphere Raman spectra confirm the conversion of the aniline-like oligomers to graphite-like carbon displaying two typical peaks located at about  $1600$  and  $1340\text{ cm}^{-1}$  that are assigned to graphitic (G) and disordered (D) modes, respectively [25,37].

### 3.6. Electrorheological behavior

As it has been shown in previous studies [26,27], suspensions based on carbonized materials usually possess a higher viscosity in the absence of electric field than the suspensions based on the original samples. This was a result of smaller particles size or higher porosity of carbonized particles leading to much higher specific surface area. Therefore, in this study, a field-off viscosity was also investigated, since low field-off viscosity is one of the crucial parameters for ER suspensions from the application point of view.

Fig. 7 shows the dependence of field-off viscosity on the shear rate for silicone oil suspensions based on (a) original and (b) carbonized particles. As it was mentioned above, with increase of  $\text{NH}_4\text{OH}$  presented during the synthesis the dimensions of particles undergoing the transformation into two-dimensional plates increased after carbonization; and thus as a consequence, except the carbonized sample prepared in  $0.1\text{ M NH}_4\text{OH}$  solution, the field-off viscosity of suspensions based on carbonized particles was not significantly increased in comparison with field-off viscosity of suspensions based on original samples. The thin PANI layer on their surface transformed into cross-linked two-dimensional molecular structures [33,39]. Only in the case of the suspension based on carbonized sample prepared in  $0.1\text{ M NH}_4\text{OH}$  solution, the particles became smaller after the carbonization. As a result,

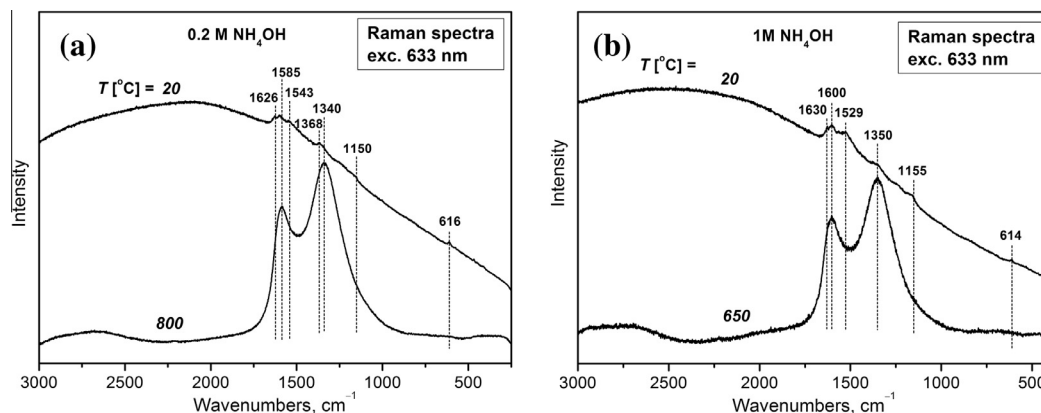


Fig. 6. Raman spectra of the powders obtained by the oxidation of 0.2 M aniline with 0.2 M ammonium peroxydisulfate in (a) 0.2 M and (b) 1 M  $\text{NH}_4\text{OH}$  and their carbonized analogues.

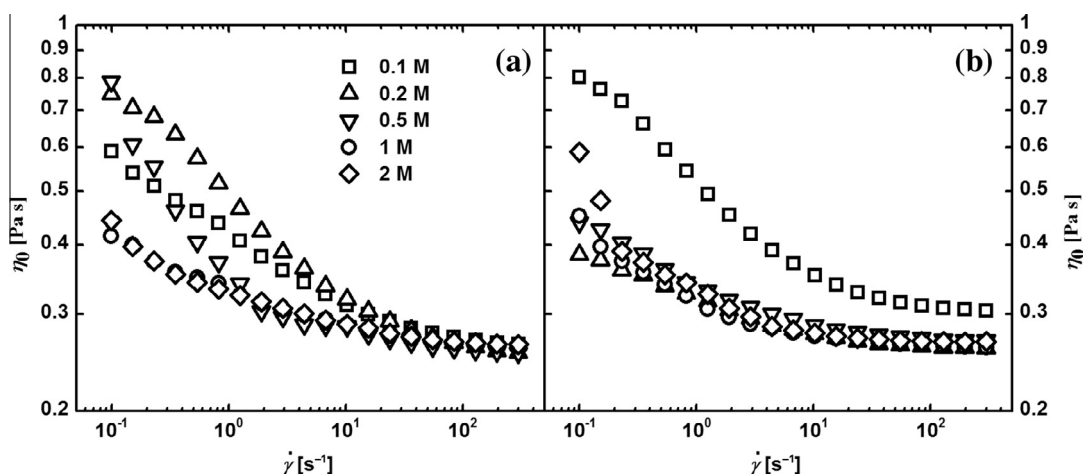


Fig. 7. The dependence of shear viscosity,  $\eta_0$ , on the shear rate,  $\dot{\gamma}$  in the absence of the electric field for suspensions based on (a) original and (b) carbonized aniline oligomers prepared at various concentrations of  $\text{NH}_4\text{OH}$ .

the suspension based on these particles possesses higher field-off viscosity than its original analogue.

The carbonization process significantly increased ER effect of suspensions based on such particles as illustrated on the rheological behavior of the suspensions in steady shear flow upon the

application of electric field (Fig. 8). In the case of the suspension based on original particles prepared in 0.1 M  $\text{NH}_4\text{OH}$  solution the results are not included in the plot, owing to high conductivity (Table 1) of this suspension which caused short-circuit of the measuring apparatus. This is connected with the presence of

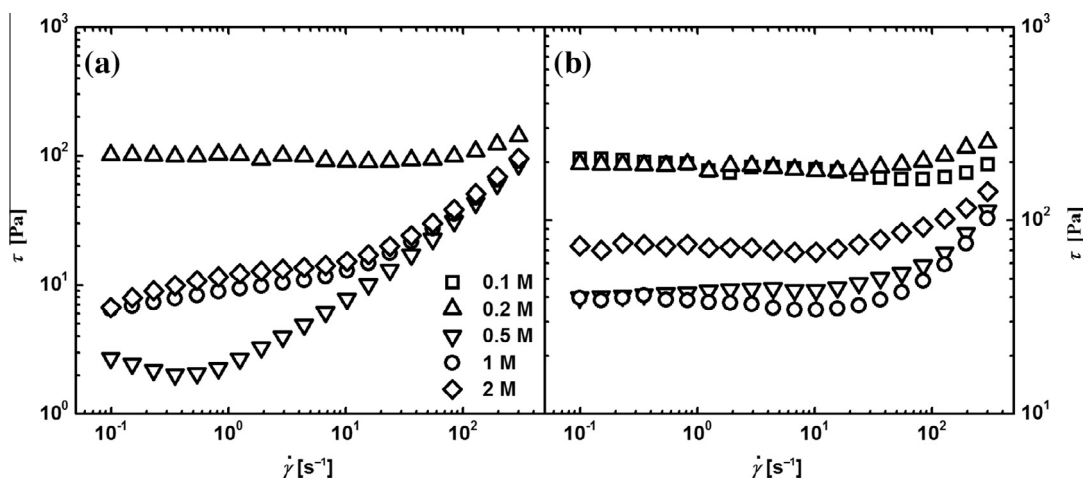


Fig. 8. The dependence of shear stress,  $\tau$ , on the shear rate,  $\dot{\gamma}$ , for suspensions based on (a) original and (b) carbonized aniline oligomers prepared in various concentrations of  $\text{NH}_4\text{OH}$  at electric field strength  $3 \text{ kV mm}^{-1}$ .

**Table 1**  
The conductivity of original particles.

Sample	Conductivity, $\sigma$ , [S cm <sup>-1</sup> ]
0.1 M	$1.58 \times 10^{-5}$
0.2 M	$9.90 \times 10^{-8}$
0.5 M	$6.07 \times 10^{-9}$
1 M	$7.06 \times 10^{-9}$
2 M	$5.82 \times 10^{-9}$

conducting PANI layer on the particle surfaces. As can be seen, the carbonization process and the transformation of particles into two-dimensional plates considerably increased ER performance of the suspensions. Suspensions based on carbonized particles prepared in 0.1 M and 0.2 M NH<sub>4</sub>OH solution exhibit the highest ER effect. The yield stresses of these suspensions are around 200 Pa, which is comparable with some of the magnetorheological suspensions [40].

The aniline oligomers were completely de-doped in the presence of 0.5 M and higher concentration of NH<sub>4</sub>OH solution, which can elucidate the very close conductivity of particles prepared in 0.5 M, 1 M and 2 M NH<sub>4</sub>OH solution (Table 1). The increased ER effect of suspension based on particles prepared in 2 M NH<sub>4</sub>OH solution in comparison with suspensions based on particles prepared in 1 M and 0.5 M NH<sub>4</sub>OH solution can be explained as the result of higher amount of nitrogen in the structure of the particles as a result of higher amount of nitrogen presented during the particles synthesis. Introduction of polar groups leads to a creation of stiffer structures due to the creation of stronger local electric field as it has been demonstrated [41]. The suspension based on particles prepared in 0.2 M NH<sub>4</sub>OH solution, which possess the conductivity higher by more than one order of magnitude than the above mentioned samples due to the presence of PANI on the surface, exhibits the highest increase in shear stress in the presence of electric field from the original samples. The suspension based on the original sample prepared in 0.5 M NH<sub>4</sub>OH solution exhibits the lowest ER effect. It also shows the typical decrease in shear stress at low shear rates for an ER fluid with a small ER effect, which has been previously commented in the literature [42,43]. Such behavior is caused by breaking of internal structures together with their difficult reformation under the shear flow.

Large difference between viscosity in the presence and in the absence of the electric field is of high importance from the application point of view. This difference can be expressed by the formula:

$$e = (\eta_E - \eta_0) / \eta_0 \quad (2)$$

where the parameter  $e$  stands for electrorheological efficiency, and  $\eta_E$  and  $\eta_0$  are the viscosities in the presence and in the absence of an electric field, respectively. In this study, the carbonization is very promising process in the preparation of new electrically polarizable particles for the ER suspensions with high ER efficiency, since above the amount of 0.1 M NH<sub>4</sub>OH present during the synthesis, the carbonization did not negatively affect the viscosity in the absence of electric field and, at the same time, it led to the increase of viscosity upon the application of electric field. Fig. 9 shows the dependence of ER efficiency on the shear rate for the suspensions based on carbonized particles. The suspension based on carbonized particles prepared in 0.2 M NH<sub>4</sub>OH solution exhibits the highest ER efficiency in the whole shear-rate range thanks to the lowest field-off viscosity and highest ER effect. Although the suspension based on the carbonized particles prepared in 0.1 M NH<sub>4</sub>OH solution exhibits the highest field-off viscosity, its ER efficiency is still higher than that of the rest of the prepared suspensions, because those exhibit lower ER effect leading to lower ER efficiency. It can be also seen, that ER efficiency is significantly higher at low shear rates compared to high shear rates, since at low shear rates, the hydrodynamic forces are

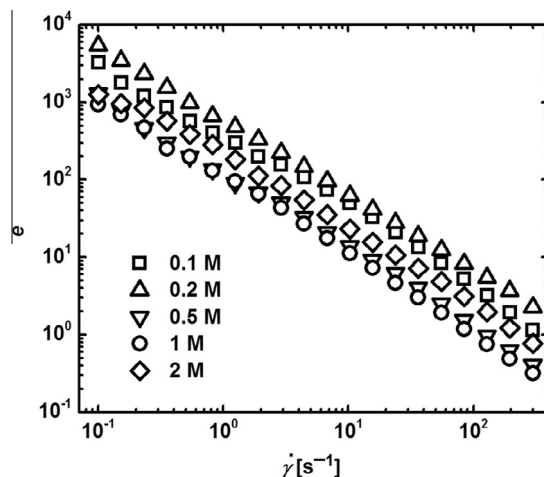


**Fig. 9.** The dependence of ER efficiency,  $e$ , on the shear rate,  $\dot{\gamma}$ , for suspensions based on carbonized aniline oligomers prepared at various concentrations of NH<sub>4</sub>OH.

low and a domination of electrostatic forces leads to high ER efficiency. However, with increasing shear rates the hydrodynamic forces increase, while electrostatic forces stay the same; thus, the hydrodynamic forces start to dominate at high shear rates (the viscosity of the ER suspension starts to be the same regardless whether an electric field is applied or not).

From the application point of view, the rheological behavior of ER suspensions under dynamic oscillatory loading is of high interest. Therefore, oscillatory tests at single strain from LVR ( $\gamma = 10^{-4}$ ) were carried out. The results are shown only for the suspensions based on carbonized samples, since their ER effect is of higher interest in comparison with their original analogues. In the absence of the electric field (Fig. 10a), the elastic modulus of the suspensions is low, which demonstrates only small portion of elastic behavior. However, when the electric field of strength 3 kV mm<sup>-1</sup> is applied, the particles start to join together thanks to electrostatic forces and span the electrodes. This leads to steep increase by several orders of magnitude in the elastic modulus (Fig. 10b) approving the transition to significantly more solid state. Unlike the steady shear tests, the highest storage modulus is achieved for the suspension based on carbonized particles prepared in 0.2 M NH<sub>4</sub>OH solution. The storage modulus is significantly higher than that achieved for suspension based on carbonized particles prepared in 0.1 M NH<sub>4</sub>OH solution, i.e. those particles with the highest ER activity in steady shear experiments. This can be explained as a consequence of shorter relaxation time of the suspension based on carbonized particles prepared in 0.2 M NH<sub>4</sub>OH solution and smaller particles of suspension based on carbonized particles prepared in 0.1 M NH<sub>4</sub>OH solution. It seems that, under dynamic oscillation loading, the structures created by smaller particles (sample 0.1 M) do not exhibit as high toughness as the structures created by two-dimensional plates. From comparison of elastic modulus of suspensions based on carbonized particles prepared in 0.1 M and 2 M NH<sub>4</sub>OH solution, whose relaxation times are the same (Table 2), it seems that in oscillatory measurements the contribution of larger particles to stronger ER effect is more considerable than in steady-shear mode. This is again a consequence of the carbonized PANI on their surface. Thus, it can be assumed that in the dynamic loading the increase in storage modulus upon an application of electric field is rather dependent on the relaxation time and the dimensions of the particles than on the dielectric relaxation strength. Similar behavior was observed in the previous study [26].



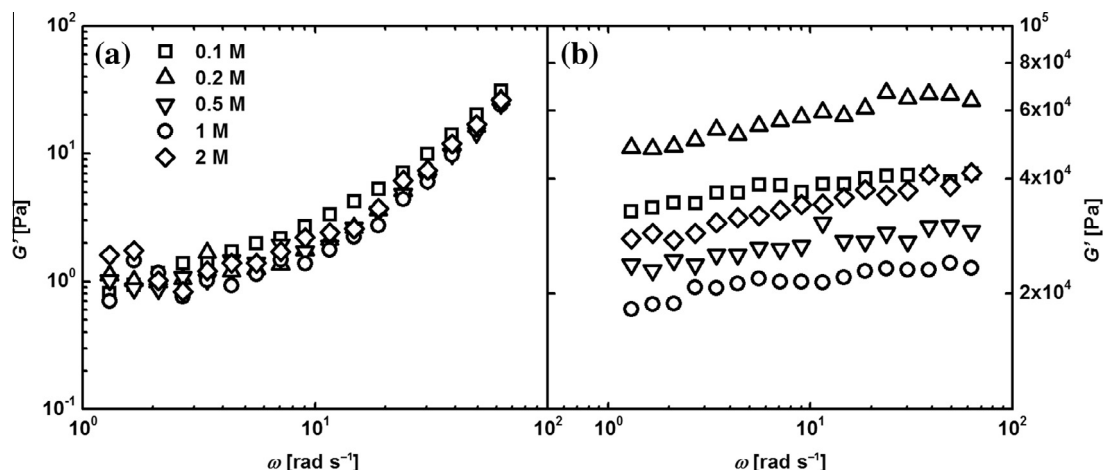


**Fig. 10.** The dependence of the elastic modulus,  $G'$ , on the angular frequency,  $\omega$ , (a) in the absence of electric field, and (b) in the presence of electric field of strength  $3 \text{ kV mm}^{-1}$  for the prepared ER suspensions based on carbonized oligomers.

**Table 2**

Dielectric parameters of ER suspensions based on carbonized aniline oligomers obtained from Havriliak–Negami model.

Parameter	Sample suspension				
	0.1 M	0.2 M	0.5 M	1 M	2 M
$\epsilon'_0$	4.72	4.12	3.66	3.85	4.01
$\epsilon'_\infty$	2.92	2.94	2.94	2.96	2.94
$\Delta\epsilon'$	1.80	1.18	0.72	0.89	1.07
$t_{\text{rel}} [\text{s}]$	$1.9 \times 10^{-4}$	$5.6 \times 10^{-5}$	$1.8 \times 10^{-3}$	$1.8 \times 10^{-3}$	$1.2 \times 10^{-4}$
$a$	0.71	0.77	0.60	0.44	0.35
$b$	0.82	0.76	0.73	1.13	1.67

carbonized particles prepared in 0.2 M  $\text{NH}_4\text{OH}$  solution was the second highest in steady shear experiments; under dynamic oscillatory loading it is similar as for the suspensions based on two-dimensional carbonized particles prepared in 0.5 M, 1 M and 2 M  $\text{NH}_4\text{OH}$  solution, which possess significantly higher dimensions than carbonized particles prepared in 0.1 M  $\text{NH}_4\text{OH}$  solution. (The role of PANI layers on the first particles may be of more importance than their dimensions, or the smaller dimension is a consequence of the PANI on the surface). In other words, the increase in the storage modulus upon the application of external electric field is not so high in the case of smaller particles as in the system composed of significantly bigger particles, in this case of two-dimensional plates.

### 3.7. Dielectric properties

The ER effect is closely linked to dielectric properties of ER suspensions, since it is assumed that the interfacial polarization of the ER suspension plays one of the dominant roles in their ER performance. The interfacial polarization occurs in the frequency region  $10^2$ – $10^5$  Hz. Therefore, the relaxation time should lie within this frequency range and the dielectric relaxation strength should be large in this region for high ER effect. Preferably, the relaxation time should be closer to the upper limit of this region. The complex study of dielectric behavior of aniline-based oligomers prepared in the presence of methanesulfonic acid has been introduced by Mrlik et al. [44].

Figs. 12 and 13 show the dependence of real and imaginary part of the complex permittivity on the frequency for suspensions based on original and carbonized particles, respectively.

In rheological measurements, the suspension based on particles prepared in 0.1 M  $\text{NH}_4\text{OH}$  could be measured only in electric field up to  $0.5 \text{ kV mm}^{-1}$ . The dielectric data obtained for this suspension declare too high electric conductivity of the particles, since the result shows clear electrode polarization, which occurs in highly conducting suspensions. The peak in range of higher frequencies (Fig. 13b) corresponds then to its relaxation process. Fig. 12a also shows that suspensions based on original particles do not exhibit clear relaxation in the desired frequency region which corresponds well with ER measurements and low intensity of ER effect. The suspension based on particles prepared in 0.2 M  $\text{NH}_4\text{OH}$  solution exhibited the highest ER effect among the original samples. However, it also does not show clear relaxation within the desired frequency. These problems are connected with the conducting PANI present on the surface of these particles. The wide peak of the suspension based on particles prepared in 0.2 M  $\text{NH}_4\text{OH}$  reflects the

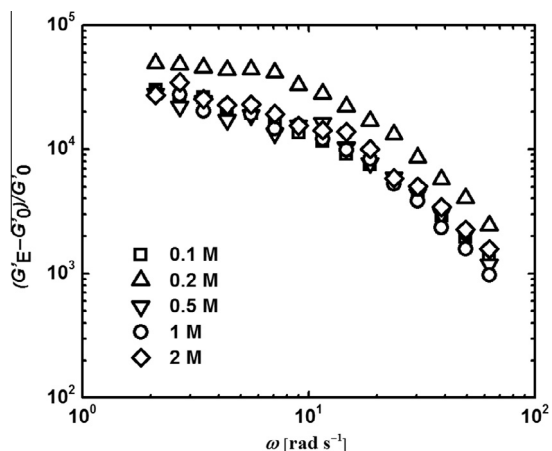


**Fig. 11.** The dependence of ER efficiency calculated from elastic modulus in the presence of electric field of strength  $3 \text{ kV mm}^{-1}$ ,  $G'_E$ , and elastic modulus in the absence of electric field,  $G'_0$ , on the angular frequency,  $\omega$ , for suspensions based on carbonized aniline oligomers.

This can be also seen in Fig. 11, which depicts the ER efficiency for suspensions based on carbonized particles in an oscillation mode,  $e_0$ :

$$e_0 = (G'_E - G'_0)/G'_0 \quad (3)$$

where  $G'_E$  stands for elastic modulus in the presence of electric field of strength  $3 \text{ kV mm}^{-1}$ , and  $G'_0$  stands for elastic modulus in the absence of electric field. The efficiency is again the highest for the suspension based on carbonized particles prepared in 0.2 M  $\text{NH}_4\text{OH}$  solution. Although the ER efficiency of the suspension based on

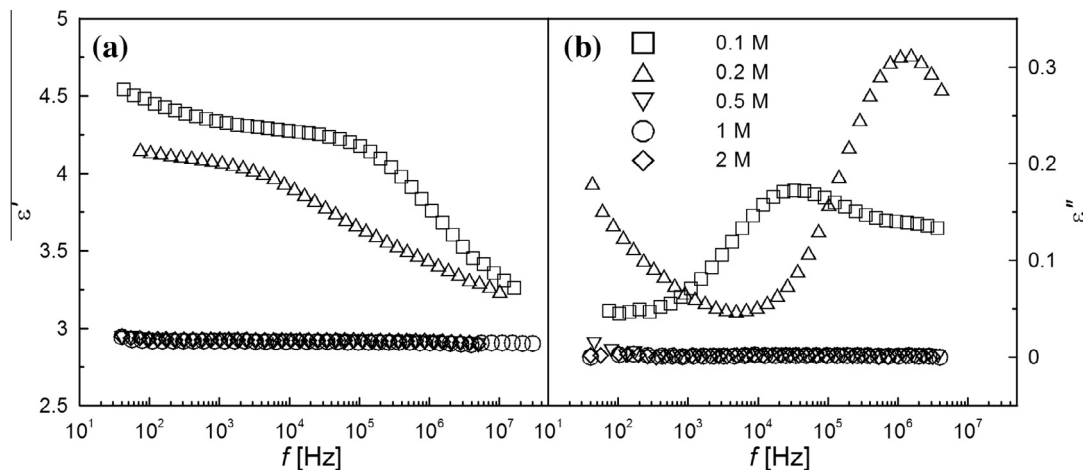


**Fig. 12.** Dielectric spectra of (a) relative permittivity and (b) dielectric loss factor for the ER suspensions based on aniline oligomers prepared at various concentrations of  $\text{NH}_4\text{OH}$ .

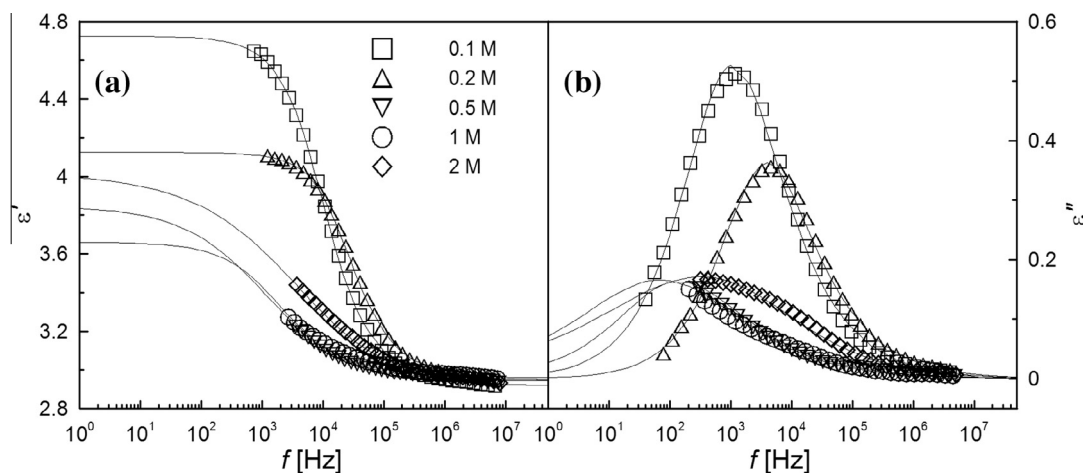


**Fig. 13.** Dielectric spectra of (a) relative permittivity and (b) dielectric loss factor for ER suspensions based on carbonized aniline oligomers prepared at various concentrations of  $\text{NH}_4\text{OH}$ .

broad spectrum of the particles with different relaxation times; and in the low frequencies the measured data are influenced by electrode polarization. This suspension exhibits the ER effect; however in comparison with carbonized samples, its effect is nearly two times lower. The suspensions based on particles prepared in 0.5 M, 1 M and 2 M  $\text{NH}_4\text{OH}$  solution show absolutely no relaxation in the measured region. These particles were synthesized in the presence of higher concentration of  $\text{NH}_4\text{OH}$ , which did not allow the formation of the conducting PANI form. In other words, these particles have the lowest conductivity, and, thus the response of the suspensions based on these materials to the electric field is not of interest. On the other hand, the suspensions based on carbonized samples prepared in 0.1 and 0.2 M  $\text{NH}_4\text{OH}$  show clear interfacial polarization, which results in symmetric narrow peaks. The spectra for the suspensions based on carbonized samples prepared in higher amount of  $\text{NH}_4\text{OH}$  exhibit relaxation shifted to the lower frequencies out of the region where the interfacial polarization occurs.

The suspensions based on carbonized particles exhibit significantly higher ER effects in comparison with their non-carbonized analogues. Their dielectric spectra also better fulfil demands for high performance of ER suspensions. As can be seen from Fig. 13b, the suspension based on carbonized particles prepared

in 0.2 M  $\text{NH}_4\text{OH}$  solution particles exhibits faster relaxation process, i.e. the relaxation time is lower, than that of the suspension based on carbonized particles prepared in 0.1 M  $\text{NH}_4\text{OH}$  solution. This is connected with the transformation of the conducting PANI to a non-conducting PANI base [33,34]. Thus, although the suspension based on carbonized particles prepared in 0.1 M  $\text{NH}_4\text{OH}$  solution shows significantly higher dielectric relaxation strength, it seems that in this case the relaxation time plays more important role in determination of high ER effect than dielectric relaxation strength. The dielectric relaxation strengths for the suspensions based on carbonized particles prepared in 0.5 M, 1 M and 2 M  $\text{NH}_4\text{OH}$  solution do not significantly differ (Fig. 13a). However, the significantly higher ER effect of the suspension based on carbonized particles prepared in 2 M  $\text{NH}_4\text{OH}$  solution is again the consequence of its shorter relaxation time in comparison with the suspensions based on carbonized particles prepared in 0.5 and 1 M  $\text{NH}_4\text{OH}$  solution (Table 2, Fig. 13b).

#### 4. Conclusions

The carbonization of aniline oligomers prepared by oxidation of aniline under alkaline conditions at various concentrations of

ammonia leads to new materials suitable for ER suspensions with enhanced ER efficiency. After the carbonization, the morphology transformation of aniline oligomers from microspheres to two-dimensional plates can be observed. The carbonization significantly contributes to the extremely high ER efficiency of their ER suspensions. The suspensions based on the prepared carbonized aniline oligomers exhibit higher viscosity under the external electric field than the suspensions based on their original analogues. The dielectric spectroscopy provides precise correlation between dielectric properties of suspensions and their rheological performance in the presence of external electric field. Although the prepared suspensions exhibit similar dielectric relaxation strength, the shorter relaxation time of the electrorheological suspensions contributes considerably to the high electrorheological effect. The highest ER efficiency and effect are observed for the suspension based on carbonized particles prepared in 0.2 M NH<sub>4</sub>OH, and their 10 wt% silicone oil suspension exhibited a yield stress around 200 Pa. In the case of dynamic oscillatory loading, the presence of two-dimensional plates significantly contributes to enhanced ER efficiency of the suspensions in comparison with the suspension consisted of small particles. Thus, in dynamic oscillatory loading the ER efficiency seems to be more dependent on the size of particles and relaxation time than on the dielectric relaxation strength.

### Acknowledgements

The authors thank the Internal Grant Agency of Tomas Bata University (IGA/FT/2014/017) and the Czech Science Foundation (P205/12/0911, 13-08944S) for the financial support. This research was also carried out with support of the Operational Program Research and Development for Innovations co-funded by the European Regional Development Fund (ERDF) and national budget of the Czech Republic, within the framework of the Centre of Polymer Systems project (CZ.1.05/2.1.00/03.0111).

### References

- [1] J.H. Sung, M.S. Cho, H.J. Choi, M.S. Jhon, *Electrorheology of semiconducting polymers*, *J. Ind. Eng. Chem.* 10 (2004) 1217–1229.
- [2] J.S. Oh, Y.M. Han, S.R. Lee, S.B. Choi, A 4-DOF haptic master using ER fluid for minimally invasive surgery system application, *Smart Mater. Struct.* 22 (2013) 15.
- [3] Y.D. Liu, B.M. Lee, T.S. Park, J.E. Kim, H.J. Choi, S.W. Booh, *Optically transparent electrorheological fluid with urea-modified silica nanoparticles and its haptic display application*, *J. Colloid Interface Sci.* 404 (2013) 56–61.
- [4] M. Sedlacik, M. Mrlik, Z. Kozakova, V. Pavlinek, I. Kuritka, *Synthesis and electrorheology of rod-like titanium oxide particles prepared via microwave-assisted molten-salt method*, *Colloid Polym. Sci.* 291 (2013) 1105–1111.
- [5] H.J. Choi, T.W. Kim, M.S. Cho, S.G. Kim, M.S. Jhon, *Electrorheological characterization of polyaniline dispersions*, *Eur. Polym. J.* 33 (1997) 699–703.
- [6] H.J. Choi, M.S. Jhon, *Electrorheology of polymers and nanocomposites*, *Soft Matter* 5 (2009) 1562–1567.
- [7] M. Mrlik, V. Pavlinek, P. Saha, O. Quadrat, *Electrorheological properties of suspensions of polypyrrole-coated titanate nanorods*, *Appl. Rheol.* 21 (2011) 7.
- [8] Y.D. Liu, H.J. Choi, *Electrorheological response of polyaniline and its hybrids*, *Chem. Pap.* 67 (2013) 849–859.
- [9] O. Quadrat, J. Stejskal, *Polyaniline in electrorheology*, *J. Ind. Eng. Chem.* 12 (2006) 352–361.
- [10] D.H. Kim, Y.D. Kim, *Electrorheological properties of polypyrrole and its composite ER fluids*, *J. Ind. Eng. Chem.* 13 (2007) 879–894.
- [11] H.J. Choi, M.S. Cho, K. To, *Electrorheological and dielectric characteristics of semiconductive polyaniline-silicone oil suspensions*, *Physica A* 254 (1998) 272–279.
- [12] A. Lengalova, V. Pavlinek, P. Saha, J. Stejskal, T. Kitano, O. Quadrat, *The effect of dielectric properties on the electrorheology of suspensions of silica particles coated with polyaniline*, *Physica A Stat. Mech. Appl.* 321 (2003) 411–424.
- [13] M. Stenicka, V. Pavlinek, P. Saha, N.V. Blinova, J. Stejskal, O. Quadrat, *The role of particle conductivity in electrorheology of suspensions of variously protonated polyaniline*, *J. Phys: Conf. Ser.* 149 (2009) 012027.
- [14] M. Stenicka, V. Pavlinek, P. Saha, N.V. Blinova, J. Stejskal, O. Quadrat, *Electrorheology of suspensions of variously protonated polyaniline particles under steady and oscillatory shear*, *Appl. Rheol.* 20 (2010).
- [15] B.M. Lee, J.E. Kim, F.F. Fang, H.J. Choi, J.F. Feller, *Rectangular-shaped polyaniline tubes covered with nanorods and their electrorheology*, *Macromol. Chem. Phys.* 212 (2011) 2300–2307.
- [16] M. Stenicka, V. Pavlinek, P. Saha, N.V. Blinova, J. Stejskal, O. Quadrat, *Effect of hydrophilicity of polyaniline particles on their electrorheology: steady flow and dynamic behaviour*, *J. Colloid Interface Sci.* 346 (2010) 236–240.
- [17] M. Stenicka, V. Pavlinek, P. Saha, N.V. Blinova, J. Stejskal, O. Quadrat, *Structure changes of electrorheological fluids based on polyaniline particles with various hydrophilicities and time dependence of shear stress and conductivity during flow*, *Colloid Polym. Sci.* 289 (2011) 409–414.
- [18] J.B. Yin, X. Xia, X.P. Zhao, *Conductivity, polarization and electrorheological activity of polyaniline nanotubes during thermo-oxidative treatment*, *Polym. Degrad. Stab.* 97 (2012) 2356–2363.
- [19] B. Gercek, M. Yavuz, H. Yilmaz, B. Sari, H.I. Unal, *Comparison of electrorheological properties of some polyaniline derivatives*, *Colloid Surf. A* 299 (2007) 124–132.
- [20] M. Mrlik, M. Sedlacik, V. Pavlinek, P. Bober, M. Trchová, J. Stejskal, P. Saha, *Electrorheology of aniline oligomers*, *Colloid Polym. Sci.* 291 (2013) 2079–2086.
- [21] J. Stejskal, P. Bober, M. Trchová, J. Horský, J. Pilař, Z. Walterová, *The oxidation of aniline with p-benzoquinone and its impact on the preparation of the conducting polymer, polyaniline*, *J. Phys: Conf. Ser.* 192 (2014) 66–73.
- [22] J. Stejskal, I. Sapurina, M. Trchová, *Polyaniline nanostructures and the role of aniline oligomers in their formation*, *Prog. Polym. Sci.* 35 (2010) 1420–1481.
- [23] J. Stejskal, I. Sapurina, M. Trchová, E.N. Konyushenko, *Oxidation of aniline: polyaniline granules, nanotubes, and oligoaniline microspheres*, *Macromolecules* 41 (2008) 3530–3536.
- [24] J. Stejskal, M. Trchová, *Aniline oligomers versus polyaniline*, *Polym. Int.* 61 (2012) 240–251.
- [25] G. Ciric-Marjanovic, I. Pasti, N. Gavrilov, A. Janosevic, S. Mentus, *Carbonised polyaniline and polypyrrole: towards advanced nitrogen-containing carbon materials*, *Chem. Pap.* 67 (2013) 781–813.
- [26] T. Plachy, M. Sedlacik, V. Pavlinek, Z. Morávková, M. Hajná, J. Stejskal, *An effect of carbonization on the electrorheology of poly(p-phenylenediamine)*, *Carbon* 63 (2013) 187–195.
- [27] Y.P. Qiao, X. Zhao, *Electrorheological effect of carbonaceous materials with hierarchical porous structures*, *Colloid Surf. A* 340 (2009) 33–39.
- [28] M. Sedlacik, V. Pavlinek, M. Mrlik, Z. Morávková, M. Hajná, M. Trchová, J. Stejskal, *Electrorheology of polyaniline, carbonized polyaniline, and their core-shell composites*, *Mater. Lett.* 101 (2013) 90–92.
- [29] J.B. Yin, X.A. Xia, L.Q. Xiang, X. Zhao, *Temperature effect of electrorheological fluids based on polyaniline derived carbonaceous nanotubes*, *Smart Mater. Struct.* 20 (2011) 015002.
- [30] J.B. Yin, X.A. Xia, L.Q. Xiang, X.P. Zhao, *Conductivity and polarization of carbonaceous nanotubes derived from polyaniline nanotubes and their electrorheology when dispersed in silicone oil*, *Carbon* 48 (2010) 2958–2967.
- [31] Z. Morávková, M. Trchová, E. Tomšik, A. Zhigunov, J. Stejskal, *Transformation of oligoaniline microspheres to platelike nitrogen-containing carbon*, *J. Phys. Chem. C* 117 (2013) 2289–2299.
- [32] J.B. Yin, Y.J. Shui, R.T. Chang, X.P. Zhao, *Graphene-supported carbonaceous dielectric sheets and their electrorheology*, *Carbon* 50 (2012) 5247–5255.
- [33] Z. Rozlívková, M. Trchová, M. Exnerová, J. Stejskal, *The carbonization of granular polyaniline to produce nitrogen-containing carbon*, *Synth. Met.* 161 (2011) 1122–1129.
- [34] M. Trchová, P. Matějka, J. Brodinová, A. Kalendová, J. Prokeš, J. Stejskal, *Structural and conductivity changes during the pyrolysis of polyaniline base*, *Polym. Degrad. Stab.* 91 (2006) 114–121.
- [35] S. Havriliak, S. Negami, *A complex plane analysis of alpha-dispersions in some polymer systems*, *J. Polym. Sci. Part C Polym. Symp.* (1966). 99–8.
- [36] M. Trchová, J. Stejskal, *Polyaniline: the infrared spectroscopy of conducting polymer nanotubes (IUPAC Technical Report)*, *Pure Appl. Chem.* 83 (2011) 1803–1817.
- [37] A. Jorio, R. Saito, G. Dresselhaus, M.S. Dresselhaus, *Raman Spectroscopy in Graphene Related Systems*, Wiley-VCH Verlag GmbH & Co. KGaA, 2011.
- [38] M. Trchová, Z. Morávková, M. Bláha, J. Stejskal, *Raman spectroscopy of polyaniline and oligoaniline thin films*, *Electrochim. Acta* 122 (2014) 28–38.
- [39] M. Trchová, E.N. Konyushenko, J. Stejskal, J. Kovářová, G. Ciric-Marjanovic, *The conversion of polyaniline nanotubes to nitrogen-containing carbon nanotubes and their comparison with multi-walled carbon nanotubes*, *Polym. Degrad. Stab.* 94 (2009) 929–938.
- [40] M. Sedlacik, R. Moucka, Z. Kozakova, N.E. Kazantseva, V. Pavlinek, I. Kuritka, O. Kaman, P. Peer, *Correlation of structural and magnetic properties of Fe3O4 nanoparticles with their calorimetric and magnetorheological performance*, *J. Magn. Magn. Mater.* 326 (2013) 7–13.
- [41] R. Shen, X.Z. Wang, Y. Lu, D. Wang, G. Sun, Z.X. Cao, K.Q. Lu, *Polar-molecule-dominated electrorheological fluids featuring high yield stresses*, *Adv. Mater.* 21 (2009) 4631–4635.
- [42] F.F. Fang, Y.D. Liu, I.S. Lee, H.J. Choi, *Well controlled core/shell type polymeric microspheres coated with conducting polyaniline: fabrication and electrorheology*, *RSC Adv.* 1 (2011) 1026–1032.
- [43] Y.D. Liu, H.J. Choi, *Electrorheological fluids: smart soft matter and characteristics*, *Soft Matter* 8 (2012) 11961–11978.
- [44] M. Mrlik, R. Moučka, M. Ilčíková, P. Bober, N. Kazantseva, Z. Špitálský, M. Trchová, J. Stejskal, *Charge transport and dielectric relaxation processes in aniline-based oligomers*, *Synth. Met.* 192 (2014) 37–42.

## **Paper III**

# Temperature-dependent electrorheological effect and its description with respect to dielectric spectra

Tomas Plachy<sup>1,2</sup>, Michal Sedlacik<sup>1</sup>, Vladimir Pavlinek<sup>1</sup>, Jaroslav Stejskal<sup>3</sup>, Manuel Pedro Graça<sup>4</sup> and Luís Cadillon Costa<sup>4</sup>

## Abstract

Electrorheological fluids consisting of large number and type of electrically polarizable particles have been presented in the literature. Nevertheless, there is a lack of temperature-dependent electrorheological effect analysis, which is their major feature from the application point of view. In this work, aniline oligomers were synthesized and carbonized in order to obtain suitable materials to be used in electrorheological fluids. The silicone oil suspensions were prepared and their temperature-dependent electrorheological performance was investigated in the temperature range between 25°C and 65°C. The electrorheological fluid based on particles with larger size exhibits higher sensitivity to the increase in temperature than the electrorheological fluid based on smaller particles. As an evaluative tool, dielectric spectra of the prepared electrorheological fluids were investigated. It has been shown that the activation energy of the relaxation process is higher for the electrorheological fluid based on larger size particles. The enhanced electrorheological effect at high temperature was ascribed to the shift of dielectric relaxation of the electrorheological fluids to higher frequencies.

## Keywords

Electrorheology, aniline oligomers, carbonization, impedance spectroscopy

## Introduction

Electrorheological (ER) fluids are suspensions altering their rheological parameters via an external electric field due to a formation of organized chain-like structures from electrically polarizable particles spanning the electrodes (Chae et al., 2015; Jang and Choi, 2015; Mrlik et al., 2013a; Plachy et al., 2015; Sim et al., 2015). These materials with controlled rheological parameters are highly demanded in high technological applications, like in robotics (Oh et al., 2013) and hydraulics devices (Kamelreiter et al., 2012). Although one of the key requirements of the ER fluids from the application point of view is their broad operational temperature region, there is still a lack of studies dealing with the temperature dependence of their rheological characteristics in the absence and in the presence of an external electric field.

The so far presented studies dealing with the dependence of ER effect on the temperature (Belza et al., 2008; He et al., 2009; Jiang et al., 2015; Kim et al., 2007; Koyuncu et al., 2012; Liu et al., 2006; Niu et al., 2014; Yan et al., 2013; Yin et al., 2011) have

shown that for dry-based ER fluids, the ER effect increases with the increasing temperature. In the case of water-based ER fluids, the water tends to evaporate at high temperature which leads to a decrease in the ER effect. Increasing the temperature has generally two main positive impacts affecting the dispersed particles: (1) increase in the polarization magnitude and (2) increase in the polarization rate of the particles leading to an enhancement of the ER effect and its stability at elevated temperature (Jiang et al., 2015; Yin et al., 2011). The elevated temperature also increases the

<sup>1</sup>Centre of Polymer Systems, University Institute, Tomas Bata University in Zlín, Zlín, Czech Republic

<sup>2</sup>Polymer Centre, Faculty of Technology, Tomas Bata University in Zlín, Zlín, Czech Republic

<sup>3</sup>Institute of Macromolecular Chemistry, Academy of Sciences of the Czech Republic, Prague, Czech Republic

<sup>4</sup>IN and Physics Department, University of Aveiro, Aveiro, Portugal

## Corresponding author:

Tomas Plachy, Polymer Centre, Faculty of Technology, Tomas Bata University in Zlín, T. G. Masaryk Sq. 275, 762 72 Zlín, Czech Republic.  
Email: plachy@ft.utb.cz

electrical conductivity of the dispersed particles, influencing positively the ER effect (Kim et al., 2007). The increase in the conductivity is noted by a steep increase in the leakage current density (Niu et al., 2014). Moreover, the viscosity of a liquid medium tends to decrease with increasing temperature, making easier the formation of stiffer chain-like structures due to lowering of the frictional forces between particles and the viscous medium (Kim et al., 2007; Liu et al., 2006). On the other hand, negative influence of the elevated temperature on the ER effect has also been observed (Yilmaz et al., 2012).

The aim of this work concerns the study of the temperature-dependent ER performance of ER fluids based on aniline oligomers investigating the influence of the particles size on their temperature-dependent ER performance.

## Experimental

### Preparation of the particles

The particles were prepared as it has been described by Plachy et al. (2014). Briefly, aniline (0.2 M; Sigma-Aldrich, USA) was oxidized with ammonium peroxydisulphate (0.2 M; Lach:NER, Czech Republic) in the aqueous solutions of 0.1 M (product is further labelled as S1) and 2 M (product is further labelled as S2) ammonium hydroxide (NH<sub>4</sub>OH; Lach:NER, Czech Republic). After drying, the particles were thermal treated at 650°C in nitrogen atmosphere in order to obtain carbonaceous nitrogen-enriched structures. When the target temperature was reached, the oven was switched off and the products were left to cool down slowly to the room temperature. The density of prepared particles was determined by a pycnometer.

### Preparation of ER fluids

ER fluids of concentration 10 wt% (due to very similar densities of both samples, this corresponds approximately to 7 vol% for both prepared fluids) were prepared by mixing the dry particles and dry silicone oil (Lukosiol M200; Chemical Works Kolín, Czech Republic; viscosity  $\eta_c = 194$  mPa s; conductivity  $\sigma_c \approx 10^{-11}$  S cm<sup>-1</sup>). Before each measurement, the ER fluid was manually stirred with a glass stick for  $\approx 5$  min and then sonicated (ultrasound frequency 24 kHz, 50% amplitude) for 60 s in order to homogenize the ER fluids.

### Rheological measurements

Rheological parameters of the prepared ER fluids in the absence and in the presence of an external electric field were measured using a rotational rheometer

Bohlin Gemini (Malvern Instruments, UK) with a coaxial-cylinder geometry (length of 27.4 mm, inner cylinder separated by a gap of 0.7 mm) at 25°C, 45°C and 65°C. The external electric field of strength within 0.5–2 kV mm<sup>-1</sup> was produced by a DC high-voltage supplier TREK 668B (TREK, USA). The electric field was applied 1 min before starting shearing in order to provide enough time for particles to create internal structures. The experiments were performed in a steady shear mode in the shear rate range of 0.1–300 s<sup>-1</sup>. After each measurement, the fluid was sheared at a shear rate of 40 s<sup>-1</sup>, for 1 min, in order to destroy the residual structures.

### Scanning electron microscopy

Morphology and dimensions of the particles were investigated using scanning electron microscopy (SEM; VEGA II LMU, Tescan, Czech Republic).

### Dielectric measurements

Dielectric properties of the ER fluids were investigated by a high-precision impedance analyser Agilent 4294A (Agilent, Japan) in the frequency range from 40 to 10<sup>7</sup> Hz at temperatures of 25°C, 45°C and 65°C.

### Optical microscopy

Formation of structures created within the ER fluids upon an application of the electric field of strength 1 kV mm<sup>-1</sup> was observed using an optical microscope (N 400M, China) linked to a digital camera. In this experience, the fluid, consisting of 0.5 wt% (ca. 0.3 vol%) of particles, was placed between two copper electrodes, with a gap of 1 mm, which were connected to a high-voltage DC source (Keithley 2400; Keithley, USA).

## Results and discussion

### Characterization of the particles

SEM proved that the particles prepared in 0.1 M NH<sub>4</sub>OH solution (S1; Figure 1(a)) are significantly smaller than those prepared in 2 M NH<sub>4</sub>OH solution (S2; Figure 1(b)). While the former possess a thin polyaniline layer on their surface preventing them from sintering upon the high temperature, the oligomers prepared in 2 M NH<sub>4</sub>OH solution were probably fused during the carbonization and they broke down to the smaller pieces during the cooling process (Morávková et al., 2013; Plachy et al., 2014). The measured density of the S1 and S2 particles was 1.35 and 1.41 g cm<sup>-3</sup>, respectively.

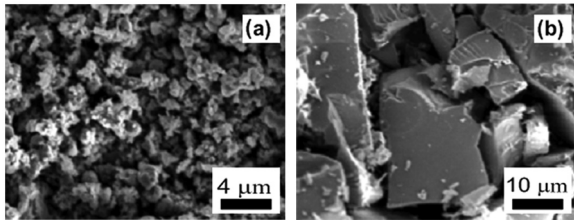


**Figure 1.** SEM images of (a) S1 and (b) S2 particles.

### Rheological properties

Figure 2 shows that the ER fluid based on S1 particles behaves as a pseudoplastic liquid (Figure 2(a)) at low shear rates in the absence of an external electric field due to the small size of the particles since these possess high specific surface area leading to higher interactions between particles and silicone oil. The ER fluid based on the S2 particles acts nearly as a Newtonian fluid over the whole shear rate region (Figure 2(b)). After the application of the electric field of strength  $2 \text{ kV mm}^{-1}$ , however, both ER fluids start to act as Bingham fluids. In this condition, the S1-based fluid exhibits higher yield stresses than the S2 fluid. With increasing temperature, the yield stresses for both fluids increase (Figure 3). This fact can be a consequence of an enhancement of the conductivity and/or polarizability of the particles together with a reduction in the viscosity of silicone oil (Jiang et al., 2015; Kim et al., 2007; Niu et al., 2014; Yin et al., 2011). The dispersed particles commonly used in ER fluids are semiconductors, whose conductivity and polarizability significantly increase with increasing temperature through thermally activated process (Mrlik et al., 2014; Negita et al., 2008). This behaviour stands in opposition to magnetorheological (MR) fluids, which are magnetic analogues of ER fluids. It was found that shear stress of MR suspensions based on carbonyl iron particles slightly decreases with increasing temperature in the presence

of magnetic field (Chooi and Oyadiji, 2005; Ocalan and McKinley, 2013; Trendler and Bose, 2007). This effect was explained by a loss of saturation magnetization at elevated temperatures (Wang et al., 2014). On the other hand, Mrlik et al. (2013b) and Machovsky et al. (2014) have described MR suspensions based on coated carbonyl iron particles exhibiting increased MR effect at elevated temperature.

The ER behaviour of the fluid based on larger particles is more sensitive to the temperature than the fluid prepared from smaller particles. These findings are represented by steeper increase in shear stress values with increasing temperature obtained by linear regression (slope 0.60) in comparison with the values for ER fluid based on S1 (slope 0.28) (Figure 3). The decrease in the shear stress in the absence of external electric field with increasing temperature is also more significant for the fluid based on the S2.

Another key demand on the ER fluids is a high difference in viscosity observed in the presence of an electric field,  $\eta_E$ , and the viscosity in the absence of an electric field,  $\eta_0$ . This difference is well embodied in the formula of ER efficiency,  $e = (\eta_E - \eta_0)/\eta_0$  (Yin and Zhao, 2004). For both prepared ER fluids, the ER efficiency increases with increasing temperature (Figure 4). At  $25^\circ\text{C}$ , the ER efficiency is higher for the fluid based on S1. In a low shear rate region at a temperature of  $65^\circ\text{C}$ , however, the ER efficiency is higher for the fluid based on S2 as a result of its significantly enhanced ER effect and lowered field-off viscosity. Lower ER efficiency of the ER fluid based on S1 at low shear rates is a consequence of its high pseudoplastic behaviour in the absence of electric field.

### Dielectric properties

Figure 5 shows the dielectric response of S1 sample at room temperature, using the Cole–Cole plot. The

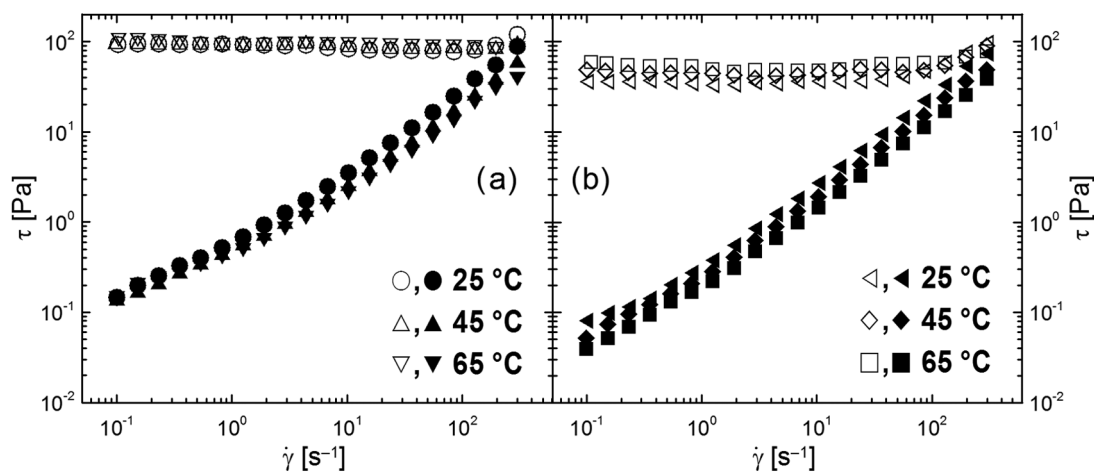


**Figure 2.** The log–log dependence of shear stress,  $\tau$ , on the shear rate,  $\dot{\gamma}$ , for ER fluids based on (a) S1 particles and (b) S2 particles in the absence (solid symbols) and in the presence of electric field of strength  $2 \text{ kV mm}^{-1}$  (open symbols) at various temperatures.

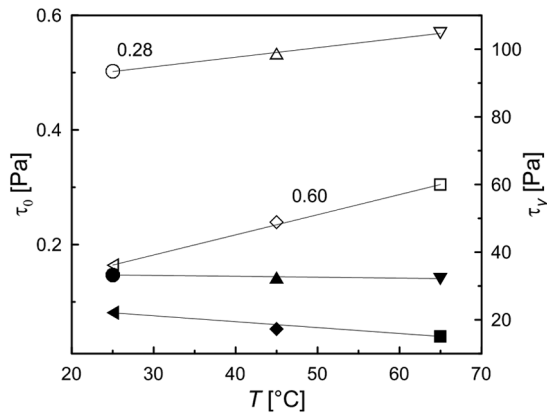


**Figure 3.** Values of the shear stress for prepared ER fluids in the absence (solid symbols;  $\tau_0$ ) and in the presence of electric field of strength  $2 \text{ kV mm}^{-1}$  (open symbols;  $\tau_\gamma$ ) at shear rate of  $0.1 \text{ s}^{-1}$  at various temperatures. The meaning of the symbols is the same as in Figure 2.

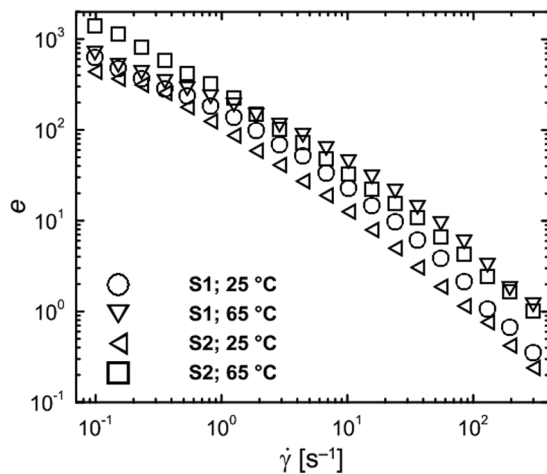


**Figure 4.** The dependence of the ER efficiency,  $e$ , on the shear rate,  $\dot{\gamma}$ , for ER fluids based on S1 and S2 particles in the presence of the electric field of strength  $2 \text{ kV mm}^{-1}$  at  $25^\circ\text{C}$  and  $65^\circ\text{C}$ .

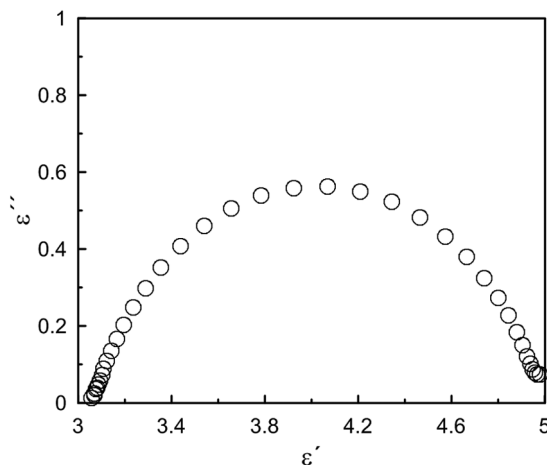


**Figure 5.** Cole–Cole plot of the ER fluid based on S1 particles at  $25^\circ\text{C}$ .

observed dielectric relaxation process cannot be explained by the Debye model, as the centre of the semicircle is not in the abscissa axis, indicating the existence of a relaxation time distribution. Due to the spectrum symmetry, the Cole–Cole formalism was employed for data analysis (Cole and Cole, 1941)

$$\epsilon^* = \epsilon_\infty + \frac{(\epsilon_S - \epsilon_\infty)}{1 + (i\omega \cdot \tau_{rel})^{1-\alpha}} \quad (1)$$

where  $\epsilon^*$  stands for the complex permittivity,  $\epsilon_S$  and  $\epsilon_\infty$  are the ‘static’ and ‘infinite frequency’ relative permittivities, respectively,  $\omega$  represents the angular frequency and  $\tau_{rel}$  represents the relaxation time.  $\Delta\epsilon$ , known as dielectric strength, is the algebraic difference between  $\epsilon_S$  and  $\epsilon_\infty$ . The  $\alpha$  parameter, which is called the Cole–Cole exponent, describes the broadness of the relaxation time distribution (Cole and Cole, 1941).

It was observed that with the increase in the temperature,  $\Delta\epsilon$  decreases for the ER fluid based on S1 (Figure 6), while it increases for the fluid based on S2 (Table 1; Figure 7). The decrease in  $\Delta\epsilon$  can be caused by the disturbances of the smaller particles through the Brownian motion. The significant increase in the dielectric relaxation strength of ER fluid based on S2 is also confirmed by its higher relaxation peaks at  $45^\circ\text{C}$  and  $65^\circ\text{C}$  when compared with the one at  $25^\circ\text{C}$  (Figure 7(b)). By increasing the temperature, the relaxation times, obtained from the peak maximum of dielectric loss factor as  $\tau_{rel} = 1/2\pi f_{max}$  (Liu and Choi, 2012), significantly shift to higher frequencies for both ER fluids (Figures 6(b) and 7(b)). It has been found that, for the high ER effect, the relaxation time of the fluids should fall within frequencies of  $10^2$ – $10^5$  Hz and preferably closer to the higher frequency limit ( $10^5$  Hz) (Hao, 1998, 2002). It must be noted that in this frequency range the interfacial polarization, which is responsible for the ER effect, also occurs. Despite almost similar  $\Delta\epsilon$  values of both ER fluids at  $65^\circ\text{C}$ , the fluid based on S1 possesses shorter relaxation times than S2 (by one order of a magnitude – see Table 1). The shift to higher frequencies, which also represents increase in conductivity (Davis, 1997; Hao, 1998), can thus be one of the significant phenomena responsible for the increase in the ER effect of the fluids (Belza et al., 2008; Kim et al., 2007; Yin et al., 2011). Therefore, the increased ER effect of both ER fluids should be attributed mainly to the shift of  $\tau_{rel}$  to higher frequencies rather than to changes in the  $\Delta\epsilon$ .

The values of the Cole–Cole exponent, which are far from 1.0, show that the relaxation process is not represented by a unique relaxation, that is, the Debye model is not useful to characterize these materials. A distribution of  $\tau_{rel}$  is then observed (Chihaoui et al., 2013; Macdonald, 1987).

In accordance with Mrlik et al.’s (2014) work, which describes a temperature dependence of the



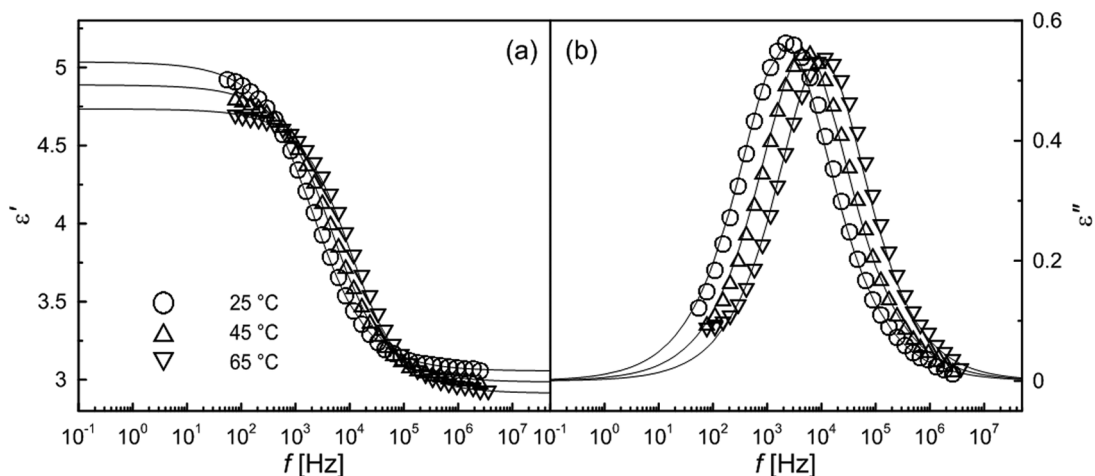


**Figure 6.** Dielectric spectra of (a) relative permittivity and (b) dielectric loss factor for the prepared ER fluid based on S1 particles at various temperatures.

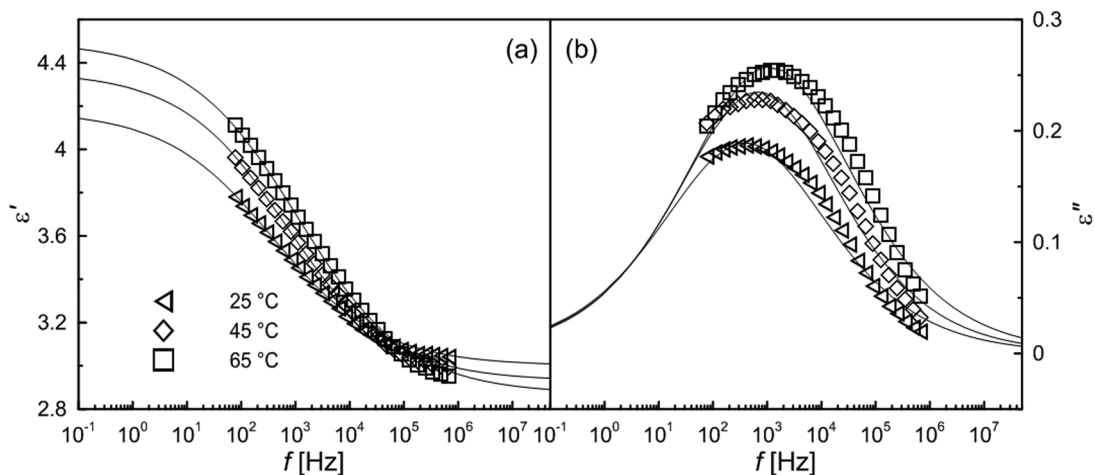


**Figure 7.** Dielectric spectra of (a) relative permittivity and (b) dielectric loss factor for the prepared ER fluid based on S2 particles at various temperatures.

**Table 1.** Dielectric parameters of prepared ER fluids obtained from Cole–Cole model at various temperatures.

Parameter	Fluid based on S1			Fluid based on S2		
	25°C	45°C	65°C	25°C	45°C	65°C
$\epsilon_S$	5.04	4.89	4.73	4.18	4.36	4.50
$\epsilon_\infty$	3.06	2.99	2.92	3.00	2.93	2.89
$\Delta\epsilon$	1.98	1.90	1.81	1.18	1.43	1.61
$\tau_{rel}$ ( $\mu s$ )	72.8	32.9	15.6	411.0	233.0	144.0
$\alpha$	0.65	0.66	0.68	0.39	0.40	0.39

dielectric spectra of particles based on aniline oligomers, the activation energy of the relaxation process was then calculated from the relaxation times of the ER fluids (Table 1) according to the Arrhenius type of equation

$$\tau_{rel} = \tau_a \exp\left(\frac{E_a}{\kappa T}\right) \quad (2)$$

where  $\tau_{rel}$  represents relaxation time and  $\tau_a$  is a pre-exponential factor,  $E_a$  is the activation energy of the relaxation process, and  $\kappa$  and  $T$  stand for Boltzmann

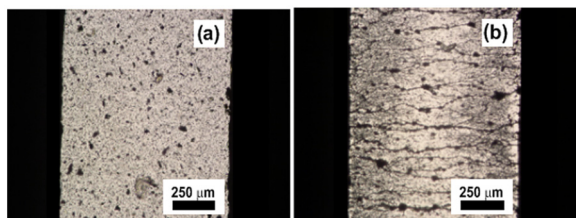


**Figure 8.** Optical microscopy of ER fluid based on the S1 particles (0.3 vol%) under various electric field strengths,  $E$ : (a)  $0 \text{ kV mm}^{-1}$  and (b)  $1 \text{ kV mm}^{-1}$ .

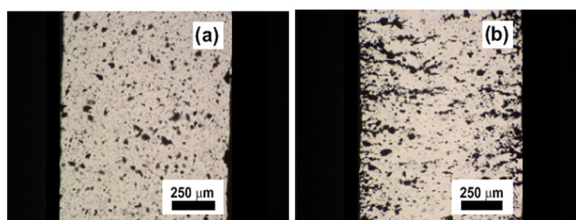


**Figure 9.** Optical microscopy of ER fluid based on the S2 particles (0.3 vol%) under various electric field strengths,  $E$ : (a)  $0 \text{ kV mm}^{-1}$  and (b)  $1 \text{ kV mm}^{-1}$ .

constant and thermodynamic temperature, respectively. The values of  $E_a$  calculated from the slope of the dependence of  $\ln \tau_{rel}$  on  $1/T$  are 0.28 and 0.19 eV ( $4.49 \times 10^{-20}$  and  $3.04 \times 10^{-20}$  J, respectively) for the ER fluid based on S1 and S2, respectively. The lower activation energy of the relaxation process can then lead to more significant changes with the increasing temperature for the ER fluid based on S2 representing its bigger changes in the ER effect at elevated temperature.

### Optical microscopy

Figures 8 and 9 show the optical microscopy images of the prepared ER fluids in the absence and in the presence of electric field of strength  $1 \text{ kV mm}^{-1}$ . In the case of the ER fluid based on S1, the transition in distribution of the particles from random (Figure 8(a)) to highly organized structures after the application of the electric field is clearly observed (Figure 8(b)). On the other hand, the particles of the fluid based on the S2 were not able to properly form strands after the application of the electric field (Figure 9), probably due to the low mobility of those particles, which is not high enough, that is, the external field magnitude is not higher than the friction forces between the particles and the silicone oil. The high viscosity of the liquid medium hinders the particles from movement. The viscosity decreases with increasing temperature, which significantly helps the particles to form highly organized structures under the application of an external electric field leading to higher ER effects.

### Conclusion

The study describes the temperature-dependent rheological behaviour of prepared ER fluids based on carbonized aniline oligomers in the absence and in the presence of an external electric field. The ER effect increased with increasing temperature, while the increase was more significant in the case of the ER fluid based on the larger particles. Dielectric spectra explain the temperature-dependent ER behaviour of prepared ER fluids. The dielectric relaxation strength decreases in the case of the ER fluid based on the smaller particles that can be disturbed through the Brownian motion; on the other side, it increases for the ER fluid based on the larger particles. Dielectric spectra confirm that the ER effect is more sensitive to the position of relaxation time than to the value of dielectric relaxation strength of the ER fluid since its position is connected with the conductivity of the dispersed particles. Also the decrease in the viscosity of the liquid medium plays an important role in the forming of chain-like structures from particles upon the application of the external electric field due to the lowering energy barrier for particles movement. This can explain the higher sensitivity of the ER fluid based on larger particles to temperature changes.

### Declaration of Conflicting Interests

The author(s) declared no potential conflicts of interest with respect to the research, authorship and/or publication of this article.

### Funding

The author(s) disclosed receipt of the following financial support for the research, authorship, and/or publication of this article: T. Plachy wishes to thank the Internal Grant Agency of Tomas Bata University (IGA/FT/2014/017) for the financial support. This article was written with support of the Operational Program Education for Competitiveness co-funded by the European Social Fund (ESF) and national budget of the Czech Republic, within the framework of project Advanced Theoretical and Experimental Studies of Polymer Systems (CZ.1.07/2.3.00/20.0104) and with support of the Operational Program Research and Development for Innovations co-funded by the European Regional Development Fund (ERDF) and national budget of the Czech Republic, within the framework of the project Centre of Polymer Systems (CZ.1.05/2.1.00/03.0111).

### References

- Belza T, Pavlinek V, Saha P, et al. (2008) Effect of field strength and temperature on viscoelastic properties of electrorheological suspensions of urea-modified silica particles. *Colloids and Surfaces A: Physicochemical and Engineering Aspects* 316: 89–94.
- Chae HS, Zhang WL, Piao SH, et al. (2015) Synthesized palygorskite/polyaniline nanocomposite particles by oxidative

- polymerization and their electrorheology. *Applied Clay Science* 107: 165–172.
- Chihaoui N, Bejar M, Dhahri E, et al. (2013) Dielectric relaxation of the  $\text{Ca}_2\text{MnO}_{4.8}$  system. *Journal of Alloys and Compounds* 577: 483–487.
- Choi WW and Oyadiji SO (2005) Characterizing the effect of temperature and magnetic field strengths on the complex shear modulus properties of magnetorheological (MR) fluids. *International Journal of Modern Physics B* 19: 1318–1324.
- Cole K and Cole R (1941) Dispersion and absorption in dielectrics I. Alternating current characteristics. *Journal of Chemical Physics* 9: 341–351.
- Davis LC (1997) Time-dependent and nonlinear effects in electrorheological fluids. *Journal of Applied Physics* 81: 1985–1991.
- Hao T (1998) The interfacial polarization-induced electrorheological effect. *Journal of Colloid and Interface Science* 206: 240–246.
- Hao T (2002) Electrorheological suspensions. *Advances in Colloid and Interface Science* 97: 1–35.
- He Y, Cheng QL, Pavlinek V, et al. (2009) Synthesis and electrorheological characteristics of titanate nanotube suspensions under oscillatory shear. *Journal of Industrial and Engineering Chemistry* 15: 550–554.
- Jang DS and Choi HJ (2015) Conducting polyaniline-wrapped sepiolite composite and its stimuli-response under applied electric fields. *Colloids and Surfaces A: Physicochemical and Engineering Aspects* 469: 20–28.
- Jiang YP, Li XG, Wang SR, et al. (2015) Preparation of titanium dioxide nano-particles modified with poly (methyl methacrylate) and its electrorheological characteristics in Isopar L. *Colloid and Polymer Science* 293: 473–479.
- Kamelreiter M, Kemmetmuller W and Kugi A (2012) Digitally controlled electrorheological valves and their application in vehicle dampers. *Mechatronics* 22: 629–638.
- Kim SG, Lim JY, Sung JH, et al. (2007) Emulsion polymerized polyaniline synthesized with dodecylbenzene-sulfonic acid and its electrorheological characteristics: temperature effect. *Polymer* 48: 6622–6631.
- Koyuncu K, Unal HI, Gumus OY, et al. (2012) Electrokinetic and electrorheological properties of poly(vinyl chloride)/polyindole conducting composites. *Polymers for Advanced Technologies* 23: 1464–1472.
- Liu Y, Liao FH, Li JR, et al. (2006) The electrorheological properties of nano-sized  $\text{SiO}_2$  particle materials doped with rare earths. *Scripta Materialia* 54: 125–130.
- Liu YD and Choi HJ (2012) Electrorheological fluids: smart soft matter and characteristics. *Soft Matter* 8: 11961–11978.
- Macdonald J (1987) *Impedance Spectroscopy*. New York: John Wiley & Sons.
- Machovsky M, Mrlik M, Kuritka I, et al. (2014) Novel synthesis of core-shell urchin-like ZnO coated carbonyl iron microparticles and their magnetorheological activity. *RSC Advances* 4: 996–1003.
- Morávková Z, Trchová M, Tomšík E, et al. (2013) Transformation of oligoaniline microspheres to platelike nitrogen-containing carbon. *Journal of Physical Chemistry C* 117: 2289–2299.
- Mrlik M, Moucka R, Ilcikova M, et al. (2014) Charge transport and dielectric relaxation processes in aniline-based oligomers. *Synthetic Metals* 192: 37–42.
- Mrlik M, Sedlacik M, Pavlinek V, et al. (2013a) Electrorheology of aniline oligomers. *Colloid and Polymer Science* 291: 2079–2086.
- Mrlik M, Sedlacik M, Pavlinek V, et al. (2013b) Magnetorheology of carbonyl iron particles coated with polypyrrole ribbons: the steady shear study. In: *Proceedings of the 13th international conference on electrorheological fluids and magnetorheological suspensions (ERMR 2012)*, Ankara, 2–6 July, vol. 412, p. 7. Bristol: IOP Publishing.
- Negita K, Misono Y, Yamaguchi T, et al. (2008) Dielectric and electrical properties of electrorheological carbon suspensions. *Journal of Colloid and Interface Science* 321: 452–458.
- Niu CG, Dong XF, Zhao H, et al. (2014) Properties of aniline-modified strontium titanate-based electrorheological suspension. *Smart Materials and Structures* 23: 075018.
- Ocalan M and McKinley GH (2013) High-flux magnetorheology at elevated temperatures. *Rheologica Acta* 52: 623–641.
- Oh JS, Han YM, Lee SR, et al. (2013) A 4-DOF haptic master using ER fluid for minimally invasive surgery system application. *Smart Materials and Structures* 22: 045004.
- Plachy T, Mrlik M, Kozakova Z, et al. (2015) The electrorheological behavior of suspensions based on molten-salt synthesized lithium titanate nanoparticles and their core-shell titanate/urea analogues. *ACS Applied Materials & Interfaces* 7: 3725–3731.
- Plachy T, Sedlacik M, Pavlinek V, et al. (2014) Carbonization of aniline oligomers to electrically polarizable particles and their use in electrorheology. *Chemical Engineering Journal* 256: 398–406.
- Sim B, Zhang WL and Choi HJ (2015) Graphene oxide/poly(2-methylaniline) composite particle suspension and its electro-response. *Materials Chemistry and Physics* 153: 443–449.
- Trendler AM and Bose H (2007) Experimental studies on magnetorheological model suspensions. *International Journal of Modern Physics B* 21: 4967–4973.
- Wang DM, Zi B, Zeng YS, et al. (2014) Temperature-dependent material properties of the components of magnetorheological fluids. *Journal of Materials Science* 49: 8459–8470.
- Yan RJ, Wu JH, Li C, et al. (2013) Temperature effects of electrorheological fluids based on one-dimensional calcium and titanium precipitate. *Chinese Physics Letters* 30: 016202.
- Yilmaz H, Zengin H and Unal HI (2012) Synthesis and electrorheological properties of polyaniline/silicon dioxide composites. *Journal of Materials Science* 47: 5276–5286.
- Yin JB and Zhao XP (2004) Preparation and enhanced electrorheological activity of  $\text{TiO}_2$  doped with chromium ion. *Chemistry of Materials* 16: 321–328.
- Yin JB, Xia XA, Xiang LQ, et al. (2011) Temperature effect of electrorheological fluids based on polyaniline derived carbonaceous nanotubes. *Smart Materials and Structures* 20: 015002.

## **Paper IV**

CrossMark  
click for updatesCite this: *J. Mater. Chem. C*, 2015,  
3, 9973

## The observation of a conductivity threshold on the electrorheological effect of *p*-phenylenediamine oxidized with *p*-benzoquinone

Tomas Plachy,<sup>ab</sup> Michal Sedlacik,<sup>\*a</sup> Vladimir Pavlinek<sup>a</sup> and Jaroslav Stejskal<sup>c</sup>

*p*-Phenylenediamine was oxidized with *p*-benzoquinone in the presence of 0.1–5 M methanesulfonic acid (MSA) solutions. The resulting methanesulfonate salts of 2,5-(di-*p*-phenylenediamine)-1,4-benzoquinone are semiconducting and the particles were further suspended in silicone oil in a weight ratio of 1:9 in order to create novel electrorheological fluids. Conductivity measurements using the two-point method along with dielectric spectroscopy were carried out in order to investigate their electrical and dielectric properties, including their silicone-oil suspensions. The higher the concentration of MSA was present during the synthesis, the higher the conductivity was observed. Nevertheless, a certain threshold of the ER effect has been found and a further significant increase in conductivity causes only a slight ER effect enhancement. At an electric field strength of 1.5 kV mm<sup>-1</sup>, the observed yield stresses read at the low shear rate values were 11.5 Pa, 20.3 Pa, 24.5 Pa, and 28.2 Pa for particles with conductivities 1.5 × 10<sup>-12</sup>, 8.5 × 10<sup>-11</sup>, 1.0 × 10<sup>-8</sup>, and 1.5 × 10<sup>-7</sup> S cm<sup>-1</sup>, respectively. From dielectric spectra, it was observed that the conductivity of the particles determines the relaxation times of their silicone-oil suspensions.

Received 14th July 2015,  
Accepted 3rd September 2015

DOI: 10.1039/c5tc02119g

www.rsc.org/MaterialsC

### 1. Introduction

Electrorheological (ER) fluids are known as liquids whose rheological properties can be controlled by means of an external electric field. Generally, dry-based ER fluids are suspensions consisting of electrically polarizable particles dispersed in a non-conducting liquid medium. In the absence of electric field, particles are randomly distributed within ER fluids; however, the application of electric field leads to a creation of electric field-induced chain-like structures along the electric field strength direction spanning a gap between the electrodes due to dipole-dipole interactions.<sup>1–3</sup> This formation of internal structures is fast and reversible,<sup>4</sup> and leads to a steep increase in the viscosity<sup>5</sup> of ER fluids. This phenomenon is called the ER effect.

It was proposed that the main factors responsible for the ER effect of ER fluids are the optimal conductivity of dispersed particles and the high dielectric relaxation strength of the ER fluids.<sup>3,6,7</sup> The role of conductivity is major mainly in the presence of a DC electric field and at low frequencies of an AC electric field.<sup>8</sup>

Conductivity of the particles also determines the response time of ER fluids to an applied electric field.<sup>9</sup> It has been demonstrated that the local electric field,  $E_L$ , between two aligned polar particles is much higher than the overall applied electric field,  $E$ .<sup>10,11</sup> For a strong  $E_L$  ( $E_L \gg E$ ) leading to the formation of stiff chain-like structures, the ratio  $\epsilon_p/\epsilon_{lm}$ , where  $\epsilon_p$  represents the relative permittivity of dispersed particles and  $\epsilon_{lm}$  is the relative permittivity of a liquid medium, is crucial. Thus, a high mismatch between the dielectric constants of a dispersed phase and a liquid medium is required for high ER effects. Introducing of polar groups into the particles can then lead to high ER effects due to their increased polarizability.<sup>11,12</sup> The other important factors influencing the ER effect are the size and morphology of the dispersed particles.<sup>13</sup> It has been shown that ER fluids based on polypyrrole nanofibers<sup>14</sup> or polyaniline nanofibers<sup>15</sup> exhibit a higher ER effect than ER fluids based on their globular analogues with similar conductivities. Also the higher aspect ratio of the fibers contributes to higher ER effects.<sup>14</sup> In general, in the case of the particles with plate-like or fibrous morphology, these exhibit higher ER response also due to the higher interparticle friction.<sup>7</sup> On the other hand, Cheng *et al.* in their work have shown that in the case of dielectric particles the smaller particle-based ER fluid exhibited higher ER effects probably due to an increased content of polar molecules together with their increased surface area.<sup>16</sup>

Various ER fluids have been introduced so far, where a continuous phase was mainly represented by mineral or silicone oils,

<sup>a</sup> Centre of Polymer Systems, University Institute, Tomas Bata University in Zlin, T. Bata Ave. 5678, 760 01 Zlin, Czech Republic. E-mail: msedlacik@cps.utb.cz

<sup>b</sup> Polymer Centre, Faculty of Technology, Tomas Bata University in Zlin, T. G. Masaryk Sq. 275, 762 72 Zlin, Czech Republic

<sup>c</sup> Institute of Macromolecular Chemistry, Academy of Sciences of the Czech Republic, Heyrovsky Sq. 2, 162 06 Prague 6, Czech Republic

owing to their low relative permittivity. As a dispersed phase, both organic and inorganic electrically polarizable particles have been used. The latter are represented by clays, various titanium oxides,<sup>17,18</sup> silica particles,<sup>19</sup> *etc.* Organic particles are primarily represented by various carbon materials<sup>20–23</sup> and conducting polymers such as polyaniline,<sup>24–26</sup> polypyrrole,<sup>27,28</sup> and their derivatives.<sup>29</sup> Polyphenylenediamine, a derivative of polyaniline, can form three isomers, *i.e.* poly(*ortho*-, *meta*-, and *para*-phenylenediamine). All of them have been used in ER fluids as a dispersed phase, and the *para* isomer has exhibited the highest ER effect among them due to its highest conductivity.<sup>29</sup> Conductivity of these materials is provided by the presence of a conjugated system containing sp<sup>2</sup> hybridized carbon atoms possessing delocalized electrons. The movement of these electrons is even enhanced by a doping process. While the conductivity of deprotonated conducting polymers is low (approximately 10<sup>-12</sup>–10<sup>-9</sup> S cm<sup>-1</sup>),<sup>29,30</sup> by doping process it increases even over units of S cm<sup>-1</sup>.<sup>31</sup> This controllable conductivity makes these materials favorable for use in ER fluids. However, oligomers of conducting polymers prepared in the presence of *p*-benzoquinone forming trimers do not contain the conjugated system. Thus, the conductivity of oligomers can be then understood as a result of an inter-molecular charge transport,<sup>32,33</sup> where the delocalized electrons are responsible for the hole transport and hydrogen bonding interactions influencing the electron transport.<sup>34</sup> The doping process is then crucial for the conductivity of such oligomers.

Aniline oligomers have been recently introduced in electro-rheology exhibiting high ER effects<sup>35</sup> that can be even increased by their carbonization in an inert atmosphere.<sup>22</sup> Their ER effects increase with the amount of polar groups presented in the structure of aniline oligomers. Therefore, this study deals with the synthesis of analogous “trimers” obtained by the oxidation of *p*-phenylenediamine (*p*PDA) with *p*-benzoquinone in the solutions of methanesulfonic acid (MSA) along with their utilization as a dispersed phase in novel ER fluids. It is known that high concentrations of MSA presented during the synthesis should provide particles with high conductivity and polarizability<sup>36</sup> suitable for their use in electrorheology.

## 2. Experimental

### 2.1. Preparation of solids

*p*PDA (0.2 M, Sigma-Aldrich) was oxidized with *p*-benzoquinone (0.5 M, Sigma-Aldrich) in MSA (Sigma-Aldrich) aqueous solutions of various concentrations of MSA (0.1–5 M).<sup>36</sup> Both reactants were dissolved separately in MSA solutions, the solutions were mixed, and left at room temperature for 24 h. The solids were then isolated by filtration, rinsed with corresponding acid solution, then with ethanol, dried in the air at room temperature, and then over the silica gel in a desiccator. For more detailed characterization of the particles the reader is referred to ref. 36.

### 2.2. Characterization of the particles

Morphology and dimensions of the particles were observed using scanning electron microscopy (SEM; Vega II LMU, Tescan,

Czech Republic). Conductivity of the particles was measured by the two-point method at ambient temperature using an electrometer (Keithley 6517B, USA). For the measurement of conductivity the particles were pressed into pellets of diameter 13 mm. Thermal stability of the prepared particles was studied using thermogravimetric analysis (TGA; TA Q500, TA Instruments, USA). Thermogravimetric measurements were carried out in a nitrogen atmosphere at a heating rate of 10 °C min<sup>-1</sup> in the temperature range 25–900 °C. In the case of SEM images and the ER fluid preparation, the particles were firstly ground using a ball mill Lab Wizz 320 (Laarmann, The Netherlands), and further sieved on a sieve with a mesh diameter of 45 μm. The particles were subsequently dried in a vacuum oven at 60 °C for 24 h and stored in a desiccator for further analyses.

### 2.3. Preparation of ER fluids

Each batch of the dry particles was mixed separately with silicone oil (Fluid 200, Dow Corning, UK, viscosity  $\eta_c = 108$  mPa s, density  $\rho_c \approx 0.965$  g cm<sup>-3</sup>) in a mass ratio of 1:9 in order to create ER fluids of particle concentration 10 wt%. Before each measurement, the prepared ER fluids were manually stirred with a glass stick and sonicated for 1 min to ensure homogenous distribution of the particles within the suspension.

### 2.4. Rheological measurements

Rheological parameters of the ER fluids in the absence and in the presence of electric field were investigated using a rotational rheometer Bohlin Gemini (Malvern Instruments, UK) with a parallel-plate geometry (a gap of 0.5 mm and a diameter of 40 mm). Experiments were carried out at 25 °C, and electric field strengths of 0.5–3 kV mm<sup>-1</sup> were supplied by a DC high voltage supplier TREK 668B (TREK, USA). The rheological measurements were performed in both the steady shear and oscillatory mode at shear rates 0.1–200 s<sup>-1</sup> and at the frequencies 0.1–10 Hz, respectively. To ensure that the measurements in a frequency sweep mode are carried out in a linear viscoelastic region, the amplitude sweep mode experiment at the fixed frequency 1 Hz was firstly carried out. Before each measurement in the presence of electric field, the electric field was applied for 1 min prior the shearing in order to provide sufficient time for the creation of oriented chain-like structures. After each measurement, the ER fluids were sheared for 60 s at a constant shear rate of 50 s<sup>-1</sup> to destroy the residual structures.

### 2.5. Dielectric measurements

Dielectric spectra of the prepared ER fluids were studied using a Broadband Dielectric Impedance Analyzer Concept 40 (Novocontrol, Germany) in the frequency range 0.1–10<sup>7</sup> Hz. The dielectric parameters were obtained by application of the Havriliak–Negami model (eqn (1)) to the obtained data.<sup>37</sup>

$$\varepsilon^* = \varepsilon_{\infty}' + \frac{(\varepsilon_0' - \varepsilon_{\infty}')}{(1 + (i\omega \cdot \tau_{rel})^a)^b} \quad (1)$$

In eqn (1),  $\varepsilon^*$  stays for complex permittivity,  $\varepsilon_0'$  and  $\varepsilon_{\infty}'$  for their real part at “static” and “infinite” frequency, respectively.

Their algebraic difference,  $\Delta\varepsilon$ , represents the dielectric relaxation strength, and a parameter  $\omega$  represents angular frequency. The relaxation time is expressed as  $\tau_{\text{rel}}$ . Parameters  $a$  and  $b$  describe a width and skewness of the relaxation time distribution, respectively.<sup>37</sup>

### 3. Results and discussion

#### 3.1. Particle characterization

It has been demonstrated,<sup>36</sup> that the oxidation of *p*-PDA with *p*-benzoquinone produced a “trimer”, 2,5(di-*p*-phenylenediamine)-1,4-benzoquinone (DPB; Fig. 1 (1)). *p*-Benzoquinone is thus not a mere oxidant, as it is included in the final structure of oligomers.<sup>33,38,39</sup> When the reaction is carried out in the solutions of MSA the corresponding methanesulfonate salts are produced (Fig. 1 (2)). The degree of incorporation of MSA counter-ions into the salts depends obviously on the concentration of MSA in the reaction mixtures. Such salts are semiconducting, as discussed below.

Morphology of the DPB particles is not affected by the concentration of MSA during their synthesis (Fig. 2). These particles possess irregular shape and create agglomerates (Fig. 2a–c), whose sizes increase with higher MSA concentration (Fig. 2d–f). The higher amount of MSA introduced in the DPB oligomer trimers increases their polarity and also provides oxygen atoms that can form hydrogen bonds with hydrogens from the trimers leading to a creation of agglomerates. Thus, with increasing of MSA concentration, the size of the particles increases.

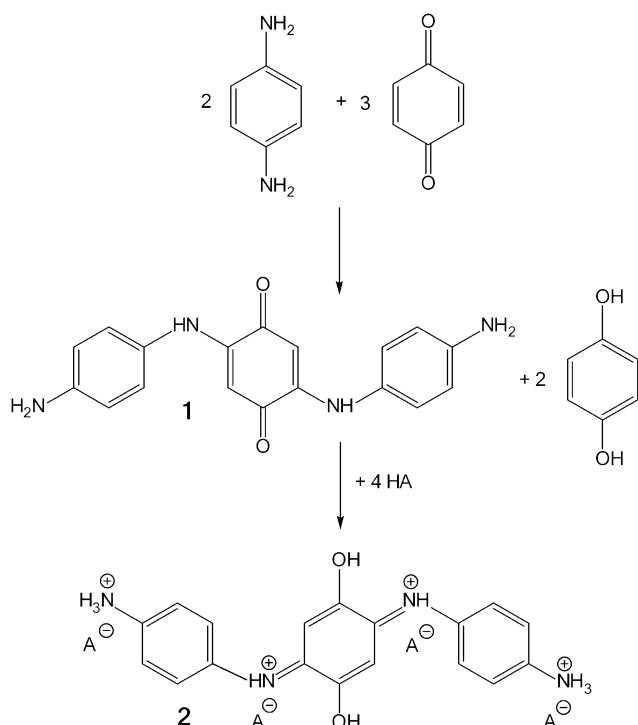


Fig. 1 *p*-Phenylenediamine is oxidized with *p*-benzoquinone to 2,5(di-*p*-phenylenediamine)-1,4-benzoquinone (1). After the “keto–enol” rearrangement, the resulting imine nitrogen atoms may become protonated with (methanesulfonate) acid (HA) to corresponding salt (2).

Thermal decomposition of DPB salts can be divided into three main steps. The first step between 25 and 100 °C represents the loss of adsorbed humidity. The amount of adsorbed water increases with increasing concentration of MSA present during the synthesis of DPB (Fig. 3a). While for particles prepared at low concentrations of MSA the loss was 4–6%, for the particles prepared in the presence of 2 M and 5 M MSA the losses were 9.2 and 14.3%, respectively. The higher amount of MSA salts incorporated into DPB increases their polar character; thus, they then adsorb more humidity. The second step was found at approximately 100–260 °C. This can be associated with decomposition of *p*-PDA<sup>40</sup> or, more likely, with the release of MSA constituting the DPB salt. The further losses up to ~370 °C can be among others ascribed mainly to leaving of sulfur dioxide.<sup>41</sup> This trend considerably increased with the increasing concentration of MSA presented during the synthesis (Fig. 3b) due to higher amount of MSA salts linked to DPB. The decomposition at higher temperatures represents the transformation of DPB into a nitrogen-enriched carbonaceous structure involving probable leaving of carbon monoxide, carbon dioxide, aromatic amines and organic groups containing oxygen (*p*-benzoquinone).<sup>41</sup>

The low conductivity of DPB salts prepared at low concentration of the MSA (Table 1) can be explained by neutralization of the MSA with the monomer *p*PDA.<sup>33</sup> The steep increase in conductivity of about three orders of magnitude between the particles prepared in the presence of 0.2 M and 0.5 M MSA resembles a certain percolation threshold. With a further increase in concentration of MSA, the conductivity increased up to the  $\approx 10^{-4}$  S cm<sup>-1</sup> (Table 1). The MSA serves as a dopant; thus, the higher concentration of MSA leads to higher conductivity of DPB obtained also due to the formation of a higher amount of hydrogen bonds.<sup>34</sup>

#### 3.2. Electrorheological behavior

The ER fluids based on DPB prepared in the presence of 2 M and 5 M MSA caused a short-circuit of the measuring apparatus due to too high conductivity of these particles (the limit for passing current was 5 mA). Therefore, properties of these ER fluids are no longer discussed. The conductivity of DPB prepared in the presence of 0.5 M and 1 M MSA enabled the measurements of their ER fluids only at the electric field strengths up to 1.5 kV mm<sup>-1</sup>.

The prepared ER fluids exhibited Newtonian behavior in the absence of external electric field, which is expressed as a linear increase in shear stress with the slope = 1 (Fig. 4a–c). Only the ER fluid based on *p*PDA particles prepared in 1 M MSA showed slightly pseudoplastic fluid character (Fig. 4d). After the application of an external electric field, the ER fluids started to behave as Bingham fluids. The ER effect of the prepared ER fluids increased with the increasing concentration of MSA presented during the synthesis, thus, with the higher conductivity of the particles the higher ER effect was observed for their ER fluid, which fits well with the theory that the stiffness of the induced chain-like structures is mainly directed by the conductivity of the particles in the presence of a DC electric field.<sup>8</sup> The higher conductivity of the particles leads to

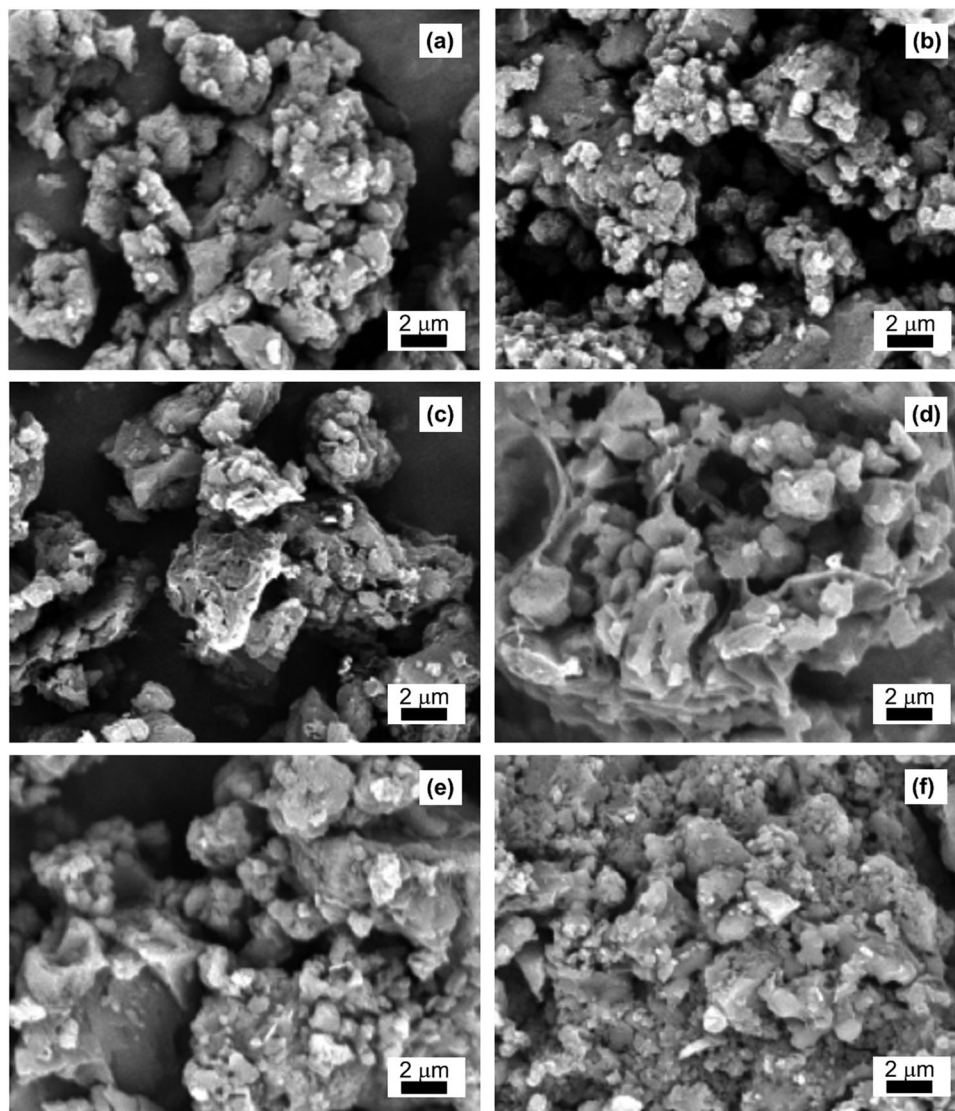


Fig. 2 SEM images of DPB trimers prepared in the presence of 0.1 M (a), 0.2 M (b), 0.5 M (c), 1 M (d), 2 M (e), and 5 M (f) MSA.

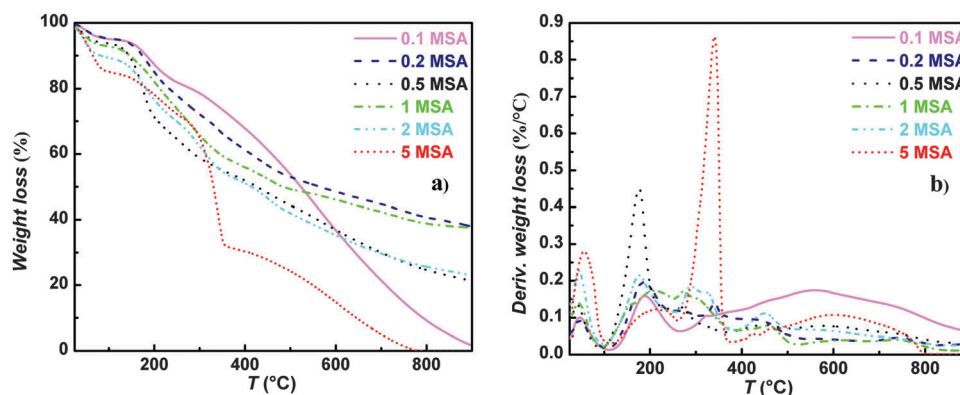


Fig. 3 TGA (a) and DTGA (b) curves of DPB prepared at various concentrations of MSA. Atmosphere:  $N_2$ ; heating rate:  $10\text{ }^\circ\text{C min}^{-1}$ .

higher electrostatic interactions between them. Such chain-like structures can then withstand higher hydrodynamic forces before the flow begins. The increasing size of the particles

could also positively contribute to higher ER effects of ER fluids based on particles prepared in a higher amount of MSA concentrations.<sup>42,43</sup>



**Table 1** Conductivity of DPB prepared at various molar concentrations of MSA

[MSA] (mol L <sup>-1</sup> )	Conductivity, $\sigma$ , (S cm <sup>-1</sup> )
0.1	$1.5 \times 10^{-12}$
0.2	$8.5 \times 10^{-11}$
0.5	$1.0 \times 10^{-8}$
1	$1.4 \times 10^{-7}$
2	$5.8 \times 10^{-5}$
5	$3.4 \times 10^{-4}$

The double-logarithmic plot of the yield stress of the ER fluids on the electric field strength conforms the power law trend

$$\tau_y = q \times E^\alpha \quad (2)$$

where  $\tau_y$  represents a yield stress,  $q$  and  $E$  stand for rigidity of the system and electric field strength, respectively, and an exponent  $\alpha$  is the slope of the exponential equation.<sup>35</sup> Since it is complicated to exactly determine a yield stress, the values of shear stress at a very low shear rate of  $0.15 \text{ s}^{-1}$ ,  $\tau_{0.15}$ , were used for this evaluation. For well-developed internal structures within the ER fluids upon an application of an external electric field, the values of exponent  $\alpha$  should be within 1.5–2. The slope of an exponent for all prepared ER fluids is within this border and the power law fits very well the  $\tau$  value dependence on  $E$  (Fig. 5). In addition, it is evident that with an increasing amount of MSA presented during the synthesis (increasing conductivity) the ER effect increases. A further increase in the conductivity of the particles

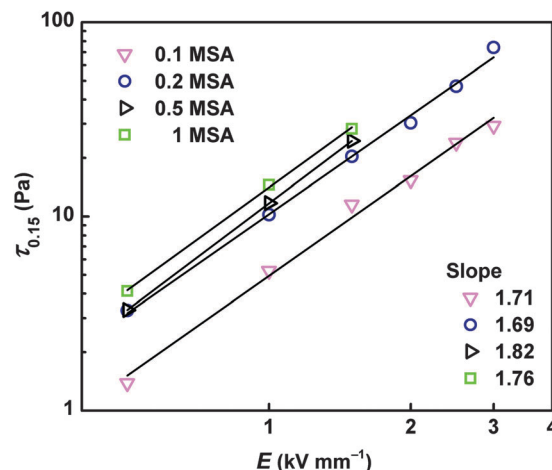


**Fig. 5** The double-logarithmic plot of shear stress values obtained at a shear rate of  $0.15 \text{ s}^{-1}$ ,  $\tau_{0.15}$ , vs. electric field strength,  $E$ , for the prepared ER fluids. The lines represent the exponential fit and their slope values involved in the graph.

would probably lead to higher ER effects, however, also to higher current density passing through the ER fluid, which was represented by the short-circuits in a measuring device for the more conducting particle-based ER fluids.

Nevertheless, from the dependence of the yield stress on the MSA concentration, it can be seen that the increment in the ER effect is not exactly proportional to the increment in conductivity

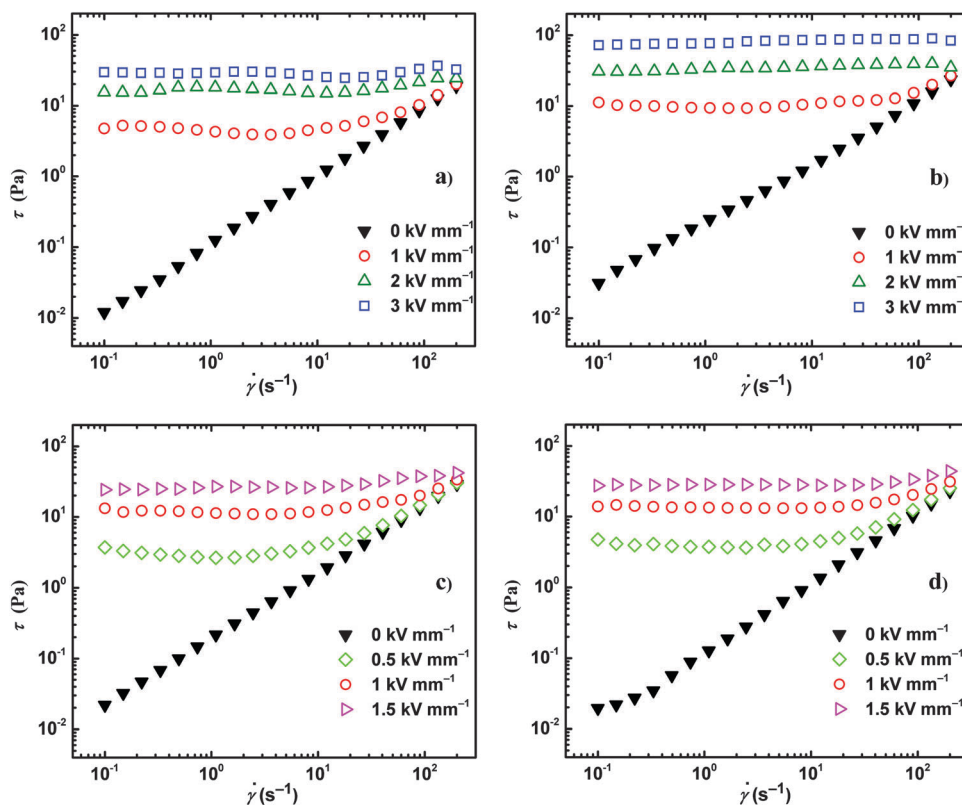


**Fig. 4** The double-logarithmic plot of the shear stress,  $\tau$ , on the shear rate,  $\dot{\gamma}$ , for the ER fluids based on DPB prepared in the presence of 0.1 M (a), 0.2 M (b), 0.5 M (c), and 1 M (d) MSA at various electric field strengths.

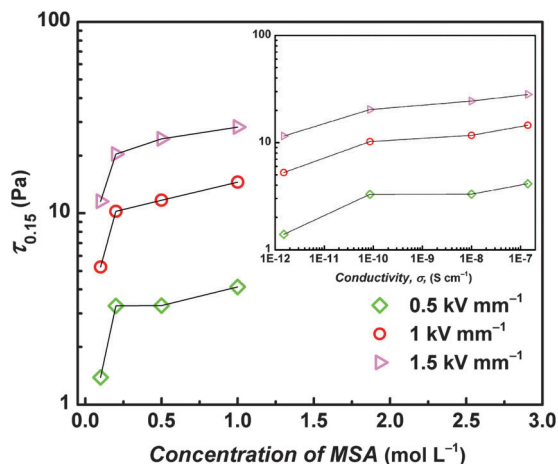


Fig. 6 The plot of shear stress values obtained at a shear rate of  $0.15 \text{ s}^{-1}$  vs. concentration of MSA presented during the synthesis of DPB for their 10 wt% ER fluids. The inset depicts shear stress values obtained at a shear rate of  $0.15 \text{ s}^{-1}$ ,  $\tau_{0.15}$ , vs. conductivity of the suspended particles.

of the particles. While a certain threshold in the conductivity of DPB salts was observed between the concentrations 0.2 and 0.5 MSA, the sort of threshold in the ER effect can be observed between 0.1 and 0.2 MSA concentrations (Fig. 6). In other words, although the DPB prepared at 0.5 MSA solution possesses conductivity of about 3 orders magnitude higher than those prepared at 0.2 MSA, the change in the ER effect of ER fluids based on 0.2 and 0.5 MSA particles is not so significant, as between ER fluids of 0.1 and 0.2 MSA-based particles, where the conductivity difference was only one order of magnitude (Fig. 6, inset). This indicates that a certain threshold of formation of the particles exists, under which a further increment of conductivity does not provide a proportional increase in the ER effect.

Behavior closer to the real applications is described by dynamic loadings of the prepared ER fluids presented by frequency sweep measurements with a fixed strain inside the linear viscoelastic region giving information about viscoelastic behavior of prepared ER fluids. The prepared ER fluids based on DPB behave like liquid materials, which is represented by the values of the viscous

modulus higher than the storage modulus ( $G'' > G'$ ) (Fig. 7a). However, after the application of an electric field, the ER fluids underwent a transition from liquid-like to a solid-like state leading to a steep increase in both moduli; nevertheless, the increase in the storage modulus is much more significant and starts to dominate over the viscous modulus ( $G'' < G'$ ). First things first, the ER fluids based on DPB prepared in 1 M, 0.5 M, 0.2 M, and 0.1 M MSA solution exhibit the highest ER effect (the storage modulus) in oscillatory measurements at an electric field strength of  $1.5 \text{ kV mm}^{-1}$  (Fig. 7b). These findings correlate well with the steady shear measurements, the conductivity of the particles, and also with dielectric properties of the prepared ER fluids. Thus, the higher conductivity and dielectric relaxation strength of the particles lead to stiffer created chain-like structures induced by an electric field.

### 3.3. Impedance spectroscopy

Values of dielectric relaxation strengths of 0.1 M and 0.2 M MSA-based ER fluids are almost the same (Table 2); however, the relaxation process of the latter ER fluid occurs at higher frequencies than the former one, which is represented by its faster relaxation time (Fig. 8a). The faster relaxation time positively contributes to the higher ER effect. The conductivity of DPB salts dramatically increased at concentration 0.5 MSA (Table 1). Dielectric spectra of their ER fluids are then distorted at low frequencies probably due to the electrode polarization, which is observed in conducting suspensions at low frequencies.

Table 2 Dielectric parameters of prepared ER fluids obtained from the Havriliak–Negami model

Parameter	Concentration of MSA			
	0.1 M	0.2 M	0.5 M	1 M
$\epsilon_0'$	4.86	4.89	6.55	6.14
$\epsilon_\infty'$	3.02	3.04	3.00	3.00
$\Delta\epsilon$	1.84	1.85	3.55	3.14
$\tau_{\text{rel}}$ [s]	1.80	$1.34 \times 10^{-1}$	$5.01 \times 10^{-2}$	$7.54 \times 10^{-3}$
$a$	0.80	0.67	0.89	0.39
$b$	0.62	0.96	0.42	0.99

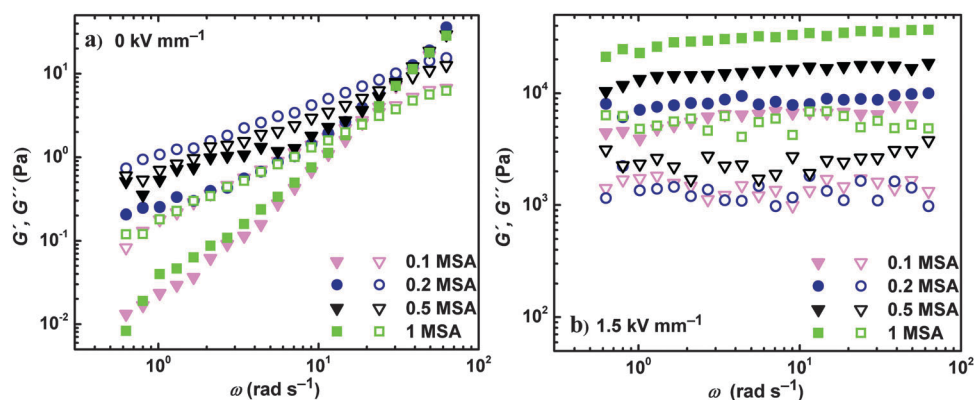


Fig. 7 The double-logarithmic plot of the storage,  $G'$  (solid symbols), and viscous,  $G''$  (open symbols), moduli vs. the angular frequency,  $\omega$ , for ER fluids based on DPB prepared in the presence of various MSA solutions in the absence (a) and in the presence of an electric field strength of  $1.5 \text{ kV mm}^{-1}$  (b).

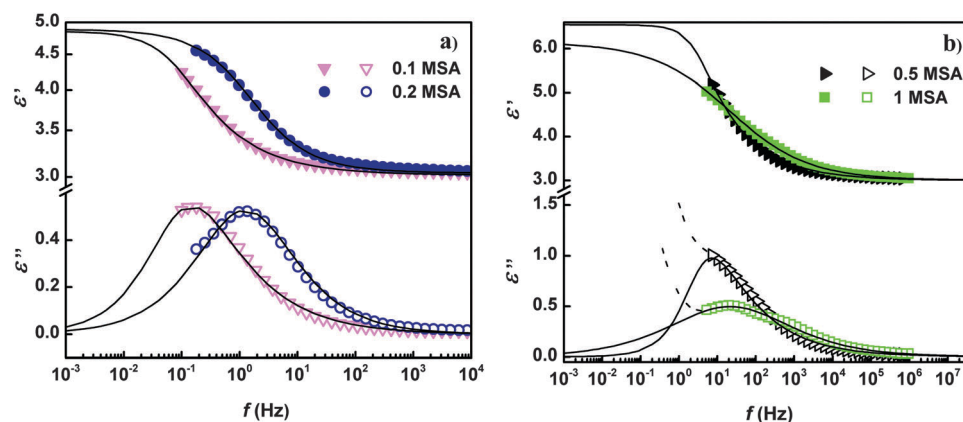


Fig. 8 Real,  $\epsilon'$ , (solid symbols) and imaginary,  $\epsilon''$ , (open symbols) parts of complex permittivity for the ER fluids based on DPB prepared in the presence of 0.1 M and 0.2 M MSA (a), and 0.5 M and 1 M MSA (b). The full lines represent the Havriliak–Negami model fits. The dashed lines represent original data indicating the electrode polarization that were excluded from fitting.

In an alternating electric field, the free ions start to migrate to electrodes,<sup>44</sup> which leads to development of ionic double layers on the electrodes implying a huge polarization of the double layer. Nevertheless, the relaxation times of the ER fluids and their polarizability can be read from undistorted data (Fig. 8b). Although, the polarizability is higher for the ER fluids based on DPB prepared in 0.5 MSA, the faster relaxation time is observed for the ER fluids based on DPB prepared in 1 MSA, corresponding to the higher conductivity of the latter particles. With increasing concentration of MSA presented during the synthesis of DPB, the higher polarizability and faster relaxation times are observed, which is in accordance with findings in the dielectric spectra of aniline oligomers by Mrlik *et al.*<sup>35</sup>

## 4. Conclusions

Oxidation of *p*-phenylenediamine with *p*-benzoquinone in the presence of methanesulfonic acid leads to the formation of “trimers”, 2,5(di-*p*-phenylenediamine)-1,4-benzoquinone methanesulfonate salts. Their conductivity increases with concentration of methanesulfonic acid present during the synthesis. The difference of about three orders of magnitude between conductivity of particles prepared in 0.2 M and 0.5 M methanesulfonic acid represents a certain percolation threshold, which prompts that the conductivity of trimer salts is directed by inter-molecular charge transport. Electrorheological fluids based on the suspension of these salts in silicone oil exhibited a considerable electrorheological effect directed by conductivity and polarizability of the particles. The higher the conductivity the higher and more stable electrorheological effect was observed. On the other hand, a certain threshold at which a further increase of conductivity only slightly contributes to the ER effect was found.

## Acknowledgements

The author T. P. would like to thank the Internal Grant Agency of Tomas Bata University (IGA/CPS/2015/007) for financial support. This work was supported by the Ministry of Education,

Youth and Sports of the Czech Republic – Program NPU I (LO1504). The support of the Czech Science Foundation (P205/12/0911) is also gratefully acknowledged.

## References

- 1 H. S. Chae, W. L. Zhang, S. H. Piao and H. J. Choi, *Appl. Clay Sci.*, 2015, **107**, 165–172.
- 2 D. S. Jang and H. J. Choi, *Colloids Surf., A*, 2015, **469**, 20–28.
- 3 Y. Z. Dong, J. B. Yin and X. P. Zhao, *J. Mater. Chem. A*, 2014, **2**, 9812–9819.
- 4 M. Sedlacik, M. Mrlik, Z. Kozakova, V. Pavlinek and I. Kuritka, *Colloid Polym. Sci.*, 2013, **291**, 1105–1111.
- 5 M. Mrlik, V. Pavlinek, Q. L. Cheng and P. Saha, *Int. J. Mod. Phys. B*, 2012, **26**, 1250007.
- 6 T. Hao, *Adv. Colloid Interface Sci.*, 2002, **97**, 1–35.
- 7 J. B. Yin, X. X. Wang, R. T. Chang and X. P. Zhao, *Soft Matter*, 2012, **8**, 294–297.
- 8 L. C. Davis, *J. Appl. Phys.*, 1992, **72**, 1334–1340.
- 9 T. Hao, *J. Colloid Interface Sci.*, 1998, **206**, 240–246.
- 10 L. C. Davis, *J. Appl. Phys.*, 1997, **81**, 1985–1991.
- 11 R. Shen, X. Z. Wang, Y. Lu, D. Wang, G. Sun, Z. X. Cao and K. Q. Lu, *Adv. Mater.*, 2009, **21**, 4631–4635.
- 12 T. Plachy, M. Mrlik, Z. Kozakova, P. Suly, M. Sedlacik, V. Pavlinek and I. Kuritka, *ACS Appl. Mater. Interfaces*, 2015, **7**, 3725–3731.
- 13 A. Lengalova, V. Pavlinek, P. Saha, O. Quadrat and J. Stejskal, *Colloids Surf., A*, 2003, **227**, 1–8.
- 14 X. A. Xia, J. B. Yin, P. F. Qiang and X. P. Zhao, *Polymer*, 2011, **52**, 786–792.
- 15 J. B. Yin, X. P. Zhao, X. Xia, L. Q. Xiang and Y. P. Qiao, *Polymer*, 2008, **49**, 4413–4419.
- 16 Y. C. Cheng, J. J. Guo, X. H. Liu, A. H. Sun, G. J. Xu and P. Cui, *J. Mater. Chem.*, 2011, **21**, 5051–5056.
- 17 Y. He, Q. L. Cheng, V. Pavlinek, C. Z. Li and P. Saha, *J. Ind. Eng. Chem.*, 2009, **15**, 550–554.
- 18 W. Q. Jiang, C. X. Jiang, X. L. Gong and Z. Zhang, *J. Sol-Gel Sci. Technol.*, 2009, **52**, 8–14.

- 19 Q. L. Cheng, V. Pavlinek, Y. He, A. Lengalova, C. Z. Li and P. Saha, *Colloids Surf., A*, 2008, **318**, 169–174.
- 20 B. Sim, W. L. Zhang and H. J. Choi, *Mater. Chem. Phys.*, 2015, **153**, 443–449.
- 21 W. L. Zhang and H. J. Choi, *Soft Matter*, 2014, **10**, 6601–6608.
- 22 T. Plachy, M. Sedlacik, V. Pavlinek, M. Trchová, Z. Morávková and J. Stejskal, *Chem. Eng. J.*, 2014, **256**, 398–406.
- 23 J. Y. Hong, E. Lee and J. Jang, *J. Mater. Chem. A*, 2013, **1**, 117–121.
- 24 H. J. Choi, T. W. Kim, M. S. Cho, S. G. Kim and M. S. Jhon, *Eur. Polym. J.*, 1997, **33**, 699–703.
- 25 M. Stenicka, V. Pavlinek, P. Saha, N. V. Blinova, J. Stejskal and O. Quadrat, *Colloid Polym. Sci.*, 2011, **289**, 409–414.
- 26 Y. D. Liu, F. F. Fang and H. J. Choi, *Mater. Lett.*, 2010, **64**, 154–156.
- 27 J. W. Goodwin, G. M. Markham and B. Vincent, *J. Phys. Chem. B*, 1997, **101**, 1961–1967.
- 28 Y. D. Kim and I. C. Song, *J. Mater. Sci.*, 2002, **37**, 5051–5055.
- 29 J. Trlica, P. Saha, O. Quadrat and J. Stejskal, *Physica A*, 2000, **283**, 337–348.
- 30 M. Stenicka, V. Pavlinek, P. Saha, N. V. Blinova, J. Stejskal and O. Quadrat, *Colloid Polym. Sci.*, 2009, **287**, 403–412.
- 31 T. Abdiryim, R. Jamal and I. Nurulla, *J. Appl. Polym. Sci.*, 2007, **105**, 576–584.
- 32 M. Mrlik, R. Moucka, M. Ilcikova, P. Bober, N. Kazantseva, Z. Spitalsky, M. Trchova and J. Stejskal, *Synth. Met.*, 2014, **192**, 37–42.
- 33 J. Stejskal, P. Bober, M. Trchová, J. Horský, J. Pilař and Z. Walterová, *Synth. Met.*, 2014, **192**, 66–73.
- 34 L. Liu, G. C. Yang, X. D. Tang, Y. Geng, Y. Wu and Z. M. Su, *J. Mol. Graphics*, 2014, **51**, 79–85.
- 35 M. Mrlik, M. Sedlacik, V. Pavlinek, P. Bober, M. Trchová, J. Stejskal and P. Saha, *Colloid Polym. Sci.*, 2013, **291**, 2079–2086.
- 36 J. Stejskal, M. Trchová, Z. Morávková, P. Bober, M. Bláha, J. Pflieger, P. Magdziarz, J. Prokeš, M. Havlicek, N. Sariciftci, A. Sperlich, V. Dyakonov and Z. Zujovic, *J. Solid State Electrochem.*, 2015, DOI: 10.1007/s10008-015-2838-3.
- 37 S. Havriliak and S. Negami, *Polymer*, 1967, **8**, 161–210.
- 38 C. H. B. Silva, D. C. Ferreira, V. R. L. Constantino and M. L. A. Temperini, *J. Raman Spectrosc.*, 2011, **42**, 1653–1659.
- 39 S. R. Surwade, V. Dua, N. Manohar, S. K. Manohar, E. Beck and J. P. Ferraris, *Synth. Met.*, 2009, **159**, 445–455.
- 40 I. M. Khan and A. Ahmad, *J. Mol. Struct.*, 2010, **975**, 381–388.
- 41 Z. Morávková, M. Trchová, E. Tomšík, A. Zhigunov and J. Stejskal, *J. Phys. Chem. C*, 2013, **117**, 2289–2299.
- 42 A. Kawai, K. Uchida and F. Ikazaki, *Int. J. Mod. Phys. B*, 2002, **16**, 2548–2554.
- 43 Y. G. Ko, U. S. Choi and Y. J. Chun, *J. Colloid Interface Sci.*, 2009, **335**, 183–188.
- 44 P. Ben Ishai, M. S. Talary, A. Caduff, E. Levy and Y. Feldman, *Meas. Sci. Technol.*, 2013, **24**, 102001.

# CURRICULUM VITAE

## Personal information

Surname / First name **Plachý Tomáš**  
Address Husova 1314, 763 61 Napajedla, Česká republika  
Telephone +420 727 877 097  
E-mail [plachy@ft.utb.cz](mailto:plachy@ft.utb.cz)  
  
Nationality Czech  
  
Date of birth 27/05/1988

## Work experience

Dates 2012–present  
Occupation or position held Junior researcher – Centre of Polymer Systems  
Name of employer Tomas Bata University in Zlín, University Institute,  
Centre of Polymer Systems

## Education

Dates 2012–present  
Title of qualification awarded Doctoral study – planned finish in 08/2016 and receiving the  
title Ph.D.  
Principal branch Technology of Macromolecular Substances  
Organization providing education Tomas Bata University in Zlín, Faculty of Technology  
  
Dates 2010–2012  
Title of qualification awarded Ing.  
Principal branch Polymer Engineering  
Organization providing education Tomas Bata University in Zlín, Faculty of Technology  
  
Dates 2007–2010  
Title of qualification awarded Bc.  
Principal branch Polymer Engineering  
Organization providing education Tomas Bata University in Zlín, Faculty of Technology

## Training Abroad

Dates	August – December 2010 (4 months) Student internship at the Chalmers University of Technology, Göteborg (Sweden)
Field of study	Material engineering
Dates	October – December 2013 (2.5 months) Study stage at the University of Aveiro, Aveiro (Portugal)
Field of study	Dielectric spectroscopy
Dates	September – November (3 months) Study stage at Norwegian University of Science and Technology, Trondheim (Norway)
Field of study	Clays and anionic clays

## Expertise

Fields electrorheology, magnetorheology, rheology, polymer processing

## Other languages

	Level
English	C1
German	A2

## LIST OF PUBLICATIONS

### Publications in the journals with impact factor:

**PLACHÝ, Tomáš; SEDLAČÍK, Michal; PAVLÍNEK, Vladimír; STEJSKAL, Jaroslav; GRAÇA, Manuel Pedro, COSTA, Luis Cadillon.** Temperature-dependent electrorheological effect and its description with respect to dielectric spectra. *Journal of Intelligent Material Systems and Structures*. 2016, vol.27(7); p. 880-886. ISSN 1045-389X.

**MRLÍK, Miroslav; ILČÍKOVÁ, Markéta; PLACHÝ, Tomáš; PAVLÍNEK, Vladimír; ŠPITALSKÝ, Zdenko; MOSNÁČEK, Jaroslav.** Graphene oxide reduction during surface-initiated atom transfer radical polymerization of glycidyl methacrylate: Controlling electro-responsive properties. *Chemical Engineering Journal*. 2016, vol. 283, p. 717-720. ISSN 1385-8947.

**PLACHÝ, Tomáš; SEDLAČÍK, Michal; PAVLÍNEK, Vladimír; STEJSKAL, Jaroslav.** The observation of a conductivity threshold on the electrorheological effect of p-phenylenediamine oxidized with p-benzoquinone. *Journal of Materials Chemistry C*. 2015, vol. 3(38); p. 9973-9980. ISSN 2050-7526.

**ILČÍKOVÁ, Markéta; FILIP, Jaroslav; MRLÍK, Miroslav; PLACHÝ, Tomáš; TKÁČ, Jan; KASÁK, Petr.** Polypyrrole nanotubes decorated with gold particles applied for construction of enzymatic bioanodes and biocathodes. *International Journal of Electrochemical Science*. 2015, vol. 10(8); p. 6558-6571. ISSN 1452-3981.

**CVEK, Martin; MRLÍK, Miroslav; ILČÍKOVÁ, Markéta; PLACHÝ, Tomáš; SEDLAČÍK, Michal; MOSNAČEK, Jaroslav; PAVLÍNEK, Vladimír.** A facile controllable coating of carbonyl iron particles with poly(glycidyl methacrylate): a tool for adjusting MR response and stability properties. *Journal of Materials Chemistry C*. 2015, vol. 3(18); p. 4646-4656. ISSN 2050-7526.

**MACHOVSKÝ, Michal; MRLÍK, Miroslav; PLACHÝ, Tomáš; KUŘITKA, Ivo; PAVLÍNEK, Vladimír; KOŽÁKOVÁ, Zuzana; KITANO, Takeshi.** The Enhanced Magnetorheological Performance of Carbonyl Iron Suspensions Using Magnetic Fe<sub>3</sub>O<sub>4</sub>/ZHS Hybrid Composite Sheets. *RSC Advances*. 2015, vol. 5; p. 19213-19219. ISSN 2046-2069.

**PLACHÝ, Tomáš; MRLÍK, Miroslav; KOŽÁKOVÁ, Zuzana; ŠULY, Pavol; SEDLAČÍK, Michal; PAVLÍNEK, Vladimír; KUŘITKA, Ivo.** The electrorheological behavior of suspensions based on molten-salt synthesized lithium titanate nanoparticles and their core-shell titanate/urea analogues. *ACS Applied Materials & Interfaces*. 2015, vol. 7; p. 3725-3731. ISSN 1944-8244.

**PLACHÝ, Tomáš; SEDLAČÍK, Michal; PAVLÍNEK, Vladimír; TRCHOVÁ, Miroslava; MORÁVKOVÁ, Zuzana; STEJSKAL, Jaroslav.** Carbonization of aniline oligomers to electrically polarizable particles and their use in electrorheology. *Chemical Engineering Journal*. 2014, vol. 256, p. 398-406. ISSN 1385-8947.

**PLACHÝ, Tomáš; SEDLAČÍK, Michal; PAVLÍNEK, Vladimír; MORÁVKOVÁ, Zuzana; HAJNA, Milena; STEJSKAL, Jaroslav.** An effect of carbonization on the electrorheology of poly(p-phenylenediamine). *Carbon*. 2013, vol. 63, p. 187-195. ISSN 0008-6223.

#### **Conference contributions:**

**PLACHÝ, Tomáš; MÜNSTER, Lukáš; KUŘITKA, Ivo; PAVLÍNEK, Vladimír.** Electrorheology of barium titanates – The role of the particle size. In: Annual Transactions – The Nordic Rheology Society. 24th Nordic Rheology Conference, Karlstad (Sweden). 2015, 23, p. 215-220. ISBN: 978-91-637-9104-8.

**SEDLAČÍK, Michal; PAVLÍNEK, Vladimír; PLACHÝ, Tomáš.** On the improvement of magnetorheological elastomer oxidation stability. In: Annual Transactions – The Nordic Rheology Society. 24th Nordic Rheology Conference, Karlstad (Sweden). 2015, 23, p. 191-194. ISBN: 978-91-637-9104-8.

**PLACHÝ, Tomáš; ROHRER, Patrik; PAVLÍNEK, Vladimír.** Core-shell magnetic biocompatible particles and their magnetorheological performance. In: Book of Abstracts. The 2nd International Conference on Rheology and Modeling of Materials. Miskolc (Hungary). 2015, p. 116. ISBN: 978-963-12-3463-3.

**PLACHÝ, Tomáš; SEDLAČÍK, Michal; PAVLÍNEK, Vladimír.** Influence of temperature on the electrorheological effect. In: Book of Abstracts: Nordic Workshop on Soft Matter Physics. Nordic Workshop on Soft Matter Physics. 2014. Oslo (Norway). www.dnva.no [online] p. 17.

**PLACHÝ, Tomáš; SEDLAČÍK, Michal; PAVLÍNEK, Vladimír; STEJSKAL, Jaroslav; GRAÇA, Manuel Pedro; COSTA, Luis Cadillon.** Temperature dependent electrorheological effect and its description with respect to dielectric spectra. In: Book of Abstracts. 14th International Conference on Electrorheological Fluids and

Magnetorheological Suspensions, Granada (Spain). 2014., www.ermr2014.com [online], p. 170.

**CVEK, Martin; MRLIK, Miroslav; ILCIKOVA, Marketa; PLACHY, Tomas; SEDLACIK, Michal; MOSNACEK Jaroslav; PAVLINEK, Vladimír.** Magnetorheology of suspensions based on carbonyl iron particles coated with poly(glycidyl methacrylate). In: Book of Abstracts. 14th International Conference on Electrorheological Fluids and Magnetorheological Suspensions, Granada (Spain). 2014. www.ermr2014.com [online], s. 152.

**PLACHÝ, Tomáš; SEDLAČÍK, Michal; PAVLÍNEK, Vladimír; STEJSKAL, Jaroslav.** Electrorheology of suspensions based on carbonized poly(p-phenylenediamine) particles. In: Book of Abstracts. 14th International Conference on Electrorheological Fluids and Magnetorheological Suspensions, Granada (Spain). 2014. www.ermr2014.com [online], p. 71.

**PLACHÝ, Tomáš; MÜNSTER, Lukáš; PAVLÍNEK, Vladimír; KUŘITKA, Ivo; GRAÇA, Manuel Pedro; COSTA, Luis Cadillon.** Preparation of strontium titanate and its use in electrorheological fluid. In: Konference PLASTKO 2014. PLASTKO 2014. 2014. Zlín, p. 248-257, ISBN 978-80-7454-335-7.

**SEDLAČÍK, Michal; ANNAPANDIYAN, Subbu; PLACHÝ, Tomáš; PAVLÍNEK, Vladimír.** Electrorheological Properties of Polypyrrole–Silver Composite Particles. In: Advances in Modern Mechanical Engineering Proceedings of the 4th International Conference on Fluid Mechanics and Heat & Mass Transfer (FLUIDSHEAT '13). Dubrovnik (Croatia). WSEAS World Science and Engineering Academy and Science, 2013. 2013. p. 105-110. ISSN 2227-4596. ISBN 978-960-474-307-0.

**PLACHÝ, Tomáš; KOŽÁKOVÁ, Zuzana; PAVLÍNEK, Vladimír; KUŘITKA, Ivo.** Sodium and potassium titanates prepared via microwave-assisted molten-salt synthesis and their use in electrorheological fluids. In: Advances in Modern Mechanical Engineering Proceedings of the 4th International Conference on Fluid Mechanics and Heat & Mass Transfer (FLUIDSHEAT '13). Dubrovnik (Croatia). WSEAS World Science and Engineering Academy and Science, 2013. 2013. p. 134-139. ISBN 978-960-474-307-0.

### Work on projects

Project	Dates	Position
TAČR, “project Centre of advanced polymeric and composite materials”; TE01020216	2014-present	Member of research team
MŠMT, “Centre of polymer systems”, ED2.1.00/03.0111	2012-2015	Member of research team
IGA UTB, “Electrorheological fluids with enhanced sedimentation stability and dimorphic magnetorheological suspensions”, IGA/FT/2015/007	2015	Project leader
TAČR, “Research and development of functional properties of passive automobile safety travelers agents by using innovative technological polymer manufacturing processing”, TA01011211	2012-2014	Member of research team



IGA UTB, “ Modification of particles for intelligent systems with higher efficiency and enhanced stability”, IGA/FT/2014/017	2014	Project leader
IGA UTB, „A new trend in preparation of particles for intelligent systems“,IGA/FT/2013/014	2013	Project leader